Trade-offs between extended TESS missions

Luke Bouma, Joshua Winn, Jacobi Kosiarek, Peter McCollough

September 2, 2016

The Transiting Exoplanet Survey Satellite (*TESS*) will observe the southern and then the northern ecliptic hemispheres beginning in early 2018 and ending in 2020. What then? Performing Monte Carlo simulations of the planets that *TESS* detects in hypothetical extended missions, we begin to explore the trade-offs between select observing strategies. Notable results include that *(1)* over a third year's extended mission, varying where *TESS* looks on the sky changes the number of newly detected planets by $\lesssim 30\%$ and that *(2)* it will be possible to detect about as many new $P > 20$ day planets in one year of *TESS*'s extended mission as in both years of the primary mission. We also catalog many of the desires and opportunities which go beyond detecting small planets around bright stars, and recommend the next steps in defining *TESS*'s extended mission.

Contents

1 *Executive Summary*

TESS is scheduled to launch in December of 2017. The primary mission will run for two years, and the *TESS* Science Office will submit a proposal for an extended mission to NASA's senior review of operating missions in early 2020. In this report we lay out technical requirements, science goals, opportunities, and risks that will impact the decision of how *TESS* should observe after completing its primary mission.

Building on Sullivan et al. [2015], we perform Monte Carlo simulations of the population of planets that *TESS* will detect for the Year-3 observing strategies shown in Fig. 1. None of our proposed strategies entail observing the ecliptic for an entire year. For ~ 4 months of such a scenario, the Earth and Moon cross *TESS*'s field of view at a drastically higher rate than during the rest of the year (Fig. 9). We circumvent this issue by proposing `elong` and `eshort`. We also note in passing that `hemis14d` spends a single spacecraft orbit ($\sim$14 days) per field, 'zig-zagging' across the sky.

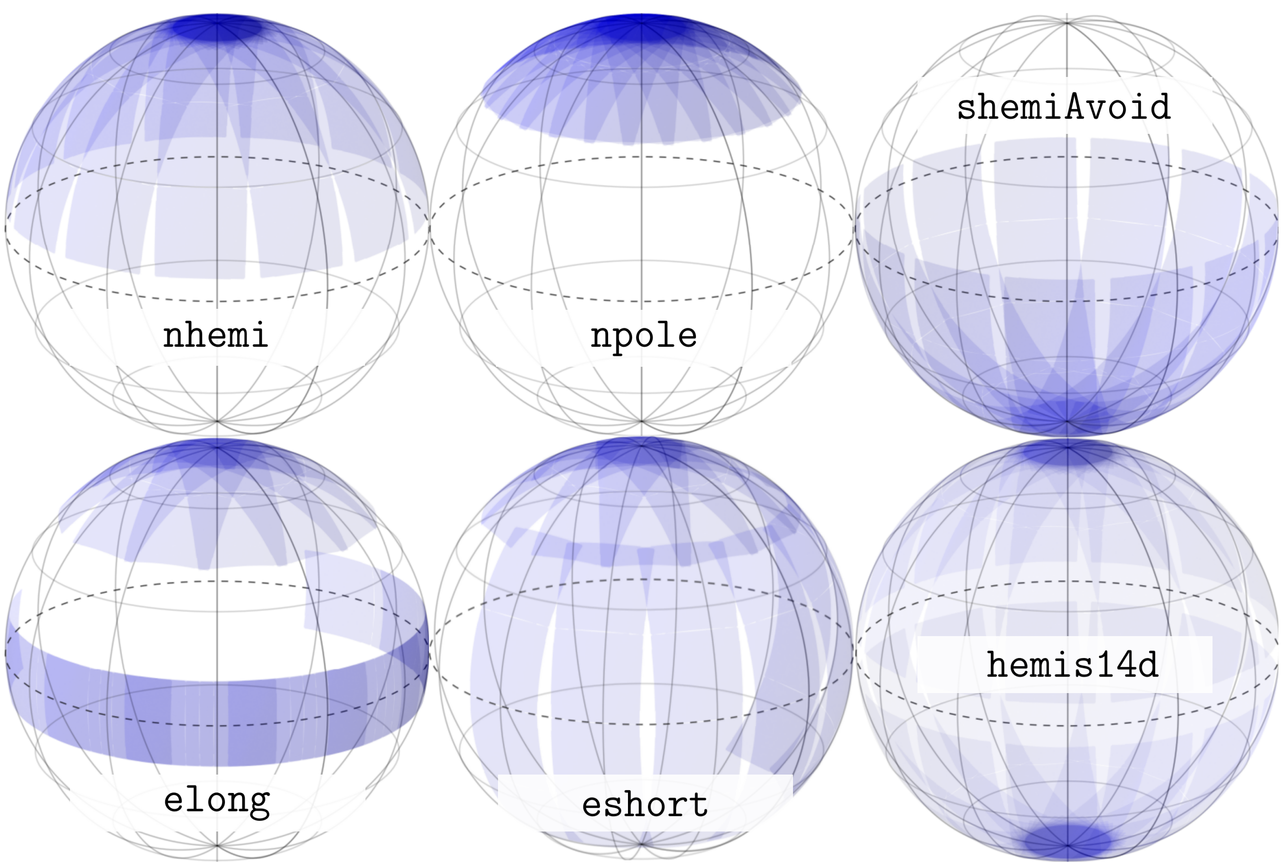

Figure 1: Six proposed pointing strategies for a *TESS* extended mission, visualized in ecliptic coordinates. Earth and moon crossings make looking at the ecliptic for an entire year impractical (see Fig. 9).

The most notable result from this study is that a third year's extended mission will yield as many new sub-Neptune radius planets as either Years 1 or 2 – roughly 1250. This holds irregardless of where on the sky observe, with the newly detected planet yields varying by $\lesssim 30\%$ between our six proposed scenarios.

Another notable result is that it will be possible to detect about as many new $P > 20$ day planets in one year of *TESS*'s extended mission as in both years of the primary mission.

Assessing pointing strategies based on yield statistics Different strategies perform better and worse by different metrics. We focus only on detected planets with $R_p < 4R_\oplus$ (Fig. 14). In terms of absolute sub-Neptune radius planet yield, `hemis14d`, `npole`, and `shemiAvoid` offer the most new planets (1300-1400, compared to the primary mission's 2500). `hemis14d`, `npole`, and `nhemi` offer the most new long period planets (250-300, compared to the primary mission's 290). `hemis14d`, `shemiAvoid`, and `eshort` offer the most new planets orbiting $I_c < 10$ hosts ($\sim$190, compared to the primary's 385; see Table 2). They all offer similar numbers of new habitable zone planets (about 120, to the primary's 210)[1]. `npole` is the worst at detecting new planets with atmospheres that are amenable for atmospheric follow-up, but extended missions only yield $10 - 25$ such planets, compared to the primary mission's $\sim$110.[2]

An important assumption behind these statistics is that we assume 2 transits and a phase-folded SNR of 7.3 are sufficient for detection. `hemis14d` is more dependent on this assumption than any other scenario: it detects the most new planets and the most new $P > 20$ day planets, but if we were to modify our detection requirement to $N_{\rm tra} \geq 3$, roughly half of the long period planets that `hemis14d` detects would be lost (Fig. 16). By way of comparison, `npole` detects most of its long-period planets with ≥ 4 transits.

Desires in exoplanet science: Planet yield statistics are useful, but they are blind to other important considerations.

1.) Ephemeris times: Our uncertainty on the mid-transit times of *TESS* objects of interest, σ_{t_c}, propagate to be roughly

$$\sigma_{t_c}\ [\mathrm{hr}] \approx 2 \times (\text{number of years after detection})\,.$$

This problem is reduced by an order of magnitude if we capture just one transit with a year's baseline after the initial detection (Figs. 23, 24). This argues strongly for an extended mission which, whether over 1 or 2 years, re-observes many of the targets that *TESS* detects in its primary mission. The smallest-radius Earths and super-Earths may otherwise be irrecoverable.

[1] We let 'habitable zone' mean that the planet insolation S is within $0.2S_\oplus - 2S_\oplus$. The physically-motivated Kopparapu et al. [2013] HZ gives roughly a third of our quoted numbers (Fig. 19).

[2] We let 'amenable for atmospheric follow-up' mean $\mathrm{SNR_{atm}} > \mathrm{SNR_{GJ\ 1214b}}/4$, where $\mathrm{SNR_{atm}}$ refers to the signal-to-noise of the planet in transmission over 4 transits observed by *JWST*'s NIRISS instrument, and the normalization is $\mathrm{SNR_{atm}}$ for GJ 1214b. Dividing by a factor of four helps avoid small-number fluctuations. Note for *JWST* follow-up the ecliptic latitude of the detections also matters (see following footnote).

2.) Follow-up of TESS objects

2.1) JWST: TESS should detect the most promising planets for *JWST* follow-up[3] after only a year's observation (Table 5). This means that *TESS* is not 'bound' to the ecliptic poles in an extended mission to support *JWST*'s target selection. More important for ensuring *JWST*–*TESS* overlap will be the efficient spectroscopic and photometric follow-up of *TESS*'s planets from the ground; by *JWST*'s launch in October 2018, only a few verified *TESS* planets will be known.

[3] We let 'promising planets for *JWST* follow-up' mean those that have $R_p < 4R_\oplus$, $\mathrm{SNR}_{\mathrm{atm}} > \mathrm{SNR}_{\mathrm{GJ\ 1214b}}/5$, and absolute ecliptic latitude $|\beta| > 80°$ so that they can be observed for more than two-thirds of the year by *JWST*.

2.2) CHEOPSs' visibility is best near the ecliptic, and non-existent near the ecliptic poles. Extended missions that focus exclusively on the ecliptic poles neglect *TESS* and *CHEOPS*s' complementarity [Berta-Thompson et al., 2016]. Those that focus on the ecliptic, including `elong` and `eshort`, provide the largest amount of overlapping coverage, with `nhemi` providing a middle-ground.

2.3) The primary mission will clarify whether the availability of *ground-based follow-up resources* will need to constrain *TESS*'s extended observing. Ideally, it will not.

3.) TESS as a follow-up mission: TESS's target list in the primary mission will include known planet-hosts from transit and RV surveys. Summarizing those that are most strategically important for an extended mission:

3.1) The Kepler field receives ∼52 days of coverage from *TESS* in 2019 (Fig. 4). An extended mission like `npole` could observe the field for 104 days per year – twice as long as say repeating `nhemi`. The main reasons to allocate extra importance to *Kepler*'s field include: *(a)* measuring transit timing variations over a long baseline; *(b)* confirming few-transit KOI candidates, *(c)* calibrating *TESS* against well-studied candidates, *(d)* continuing observations of circumbinary planets, and *(e)* characterizing stellar cycles over long timescales. Sullivan [2013] studied *TESS*'s performance on the field in detail, and found that *TESS* should detect ∼5% of KOIs at $\geq 3\sigma$ significance per transit. A few dozen of these planets have $R_p < 4R_\oplus$, and ∼50 reside in multi-planet systems and are likely to give valuable TTV measurements. We note that Sullivan [2013] used October 2013's KOI catalog, which now lists ∼7000 objects of interest.

3.2) K2's fields will have covered $\gtrsim$ 60% of the area in the $|\beta| < 6°$ band about the ecliptic by the beginning of *TESS*'s extended mission. Our simulated planet populations for both `elong` and `eshort` assumed no knowledge from *K2*. This is unrealistic. A large fraction of the planets that *TESS* will be capable of detecting near the ecliptic will already either exist as candidates in *K2*'s data or have been discovered[4]. Summarizing then what we find to be the most compelling reasons to observe the ecliptic in an extended *TESS* mission: *(a)* combine *TESS* and *K2* data, doubling the *K2* observing baseline for most

[4] Our coarse estimate is that ∼175 of *TESS*'s 500 new $|\beta < 12°|$, $R_p < 4R_\oplus$ detections from `elong` would already be detected by *K2* (see Sec. 6)

targets. In turn, confirm low-SNR candidates, and detect extra transits for a relatively large number of $20 < P < 40$ day planets; *(b)* catch 'holes' in the $|\beta| < 12^\circ$ band that *K2* missed, completing the all-sky search for small planets transiting the brightest stars; *(c)* observe targets in *K2* fields that simply were not selected in *K2*'s $\sim 2 \times 10^4$ per campaign. For instance, *TESS*'s bandpass allows probing down to cooler M dwarfs; *(d)* measure TTVs for targets over baselines up to 5-years. *(e)* confirm a small but significant number of $P > 40$ day planets.

Given the central role that combining *TESS* and *K2* data would play if *TESS* were to observe the ecliptic, and given our non-treatment of this question in our yield simulations, we recommend that a detailed study of *K2* and *TESS*'s combined potential be carried out before ruling for or against `elong` or `eshort`.

3.3) TESS following up ground-based surveys: The north and south skies have similar numbers of known ground-detected transiting and RV planets, so the desire to follow up ground-based surveys probably will not impact *TESS*'s extended mission on a 1-year timescale. Over 2-year timescales, if an extended mission were to focus on a single hemisphere it would neglect half of the known transiting/RV planets, no longer *(a)* discovering additional small transiting companions (à la WASP 47) or *(b)* improving uncertainties in the physical and orbital parameters of known planets.

Desires outside of exoplanet science: We motivate cases for using *TESS* data in asteroseismology, variable-star astronomy (pulsating stars, eruptive stars, supernovae), and solar system astronomy (main belt asteroids) in Sec. 5.2. To our understanding an extended mission can observe anywhere on the sky without neglecting these sub-fields. Observational cadence is a more important free-parameter – asteroseismology in particular benefits greatly from short cadence data.

Results summary:

1 year extension: None of the pointing options that we propose are obviously bad (Fig. 14). `hemis14d` does well under idealized assumptions, but is risky because of aliasing and low $N_{\rm tra}$ issues. That said, it would be the fastest way to deal with the ephemeris issue. The biggest qualitative difference between looking at and away from the ecliptic is *K2*. *K2* does mean fewer 'new *TESS* planets', but combining the two datasets might lead to many long period planet detections (see recommendations – we did not deal with this quantitatively).

2 year extension: Knowing when *TESS* planets transit is incredibly important for follow-up efforts, and needs to be addressed either through `hemis14d` or by going 'all-sky' over two years. We did not study 2-year extensions in depth, but we know that doing the opposite-hemisphere complements of `nhemi`, `npole`, and `shemiAvoid` would yield the same large number of new planets as from Year 3. Another reason to observe both hemispheres is to be sure that we have really detected all of the best super-Earths for transmission spectroscopy (Table 5).

The main reason to repeat one-hemisphere observations indefinitely is to detect long period planets. Our opinion is that the reasons to observe all-sky are more compelling.

Recommendations (expanded in Sec. 7.1):

Analyze target prioritization problem and decide whether or not to optimize target selection based on results.

Optimize cadence: 200k at 2min vs. 400k at 4min, & related trade-offs.

Take steps to address the 'upgrading cadence' problem: if there is a likely transiting planet in full frame image data, upgrading the planet to short cadence in future observing sectors improves the probability and quality of detection.

Guest Investigator Office / TESS Science Office: solicit advice More broadly, solicit community feedback during the process of defining the extended mission. This may entail a call for white papers, comments on this report, or direct proposals to the GI office.

Decide (explicitly or implicitly) on weights between our proposed metrics. Sec. 3.3 gives a summarized list.

Simulate combining TESS and K2 data from `elong` *and* `eshort`. This is perhaps the most important qualitative difference between observing towards and away from the ecliptic.

2 *Statement of problem*

Once *TESS*'s primary survey is complete, what should the spacecraft do next? Different observing strategies may benefit different science goals. As a preliminary example, observing a given region of sky for as long as possible allows *TESS* to detect planets with the longest possible orbital periods. However, if we want to discover new small planets around the brightest possible stars, it may behoove us to target new sky, perhaps near the ecliptic.

This memo is a trade study of a non-exhaustive set of plausible extended mission scenarios. Our main aim is to quantify how different spacecraft-pointings will affect *TESS*'s planet yield. We also discuss different opportunities that may become available by observing different regions of sky.

Some important free parameters that will define *TESS*'s extended mission include:

- Where to point the cameras on the sky.
- The duration of proposed observations.
- With a fixed data mass, the relative allocations between short (2 minute) and long (30 minute) cadence images[5].
- The cadence of full frame images; for instance keeping full-frames at 15 minute cadence at the cost of observing fewer short-cadence targets.
- The cadence of postage stamps; for instance stacking them at 4 minute cadence instead of 2 minute cadence, and observing twice as many target stars.
- The target allocation strategy. This includes how to prioritize target stars from the *TESS* Input Catalog. It also involves the question of how to use knowledge obtained from full frame images in the primary mission when re-observing the same fields in an extended mission.

[5] Respectively referred to as 'postage stamps' because the aperture centered on any given star resembles a small-area postage-stamp, and as 'full frame images' since they are the entire CCD readout. The 'postage stamp' target stars are a subset, nominally 2×10^5 stars, of the *TESS* Input Catalog.

In this report, we evaluate how well a set of extended mission spacecraft pointings (for 1 year of extra observing) satisfies different technical requirements and science goals. We also discuss unique opportunities that may be available through each option. The other parameters outlined above, notably the relative allocations between different data products at a fixed data mass, will also impact the primary and extended missions. We recommend that they be studied separately.

2.1 Outline of report

We begin in Sec. 3 by discussing how we select and compare different pointing strategies, as well as how we model *TESS*'s observations and planet detections. We then compare the newly detected planet populations from some plausible one-year extended missions in Sec. 4. Critically, newly detected planets are not the only valuable outcome of an extended mission. In Sec. 5, we thus highlight some of the broader science that *TESS* could and perhaps should perform beyond new planet detections. We go on to discuss opportunities, notably for ground and space-based follow-up, as well as risks that could come from each observing strategy in Sec. 6. We conclude in Sec. 7 with recommendations for what comes next in defining *TESS*'s extended mission.

3 Approach

3.1 Constraints on possible pointing strategies

The main constraint on *TESS*'s spatial orientation is that its cameras must oppose the sun. Specifically, the camera center must point within $\sim 30^\circ$ of immediately antisolar, with $\lesssim 15^\circ$ preferred. This is necessary for the sunshade and spacecraft to block solar photons. It also enables the solar panels (which are free to rotate about the $+Y$ axis in Fig. 2) to collect sunlight. Given the spacecraft's orbit [Gangestad et al., 2013], this means that *TESS* should advance $\sim 28^\circ$ east in ecliptic longitude every lunar month, as it does during the primary mission. Focusing on a fixed field for say, 3 spacecraft orbits ($\sim$ 42 days), would be in tension with this requirement. In practice, another technical restriction is whether the Earth or Moon passes through *TESS*'s camera fields during a proposed pointing (see Sec. 3.6). For purposes of exploring possible science in extended missions, the spacecraft's finite fuel reserves can be ignored.

3.2 Our proposed pointing strategies

Given the constraints outlined in Sec. 3.1 and the additional (non-physical) constraint of a single year's observing time, we select the following options for further study:

Option 1. Focus on the North Ecliptic Pole (hereafter, `npole`). Note that the geometry of *TESS*'s lens hood still suppresses incoming sunlight in this scenario. *Justification:* maximizes average observing baseline per star; longest period coverage.

Option 2. Repeat observations of the northern hemisphere (`nhemi`).

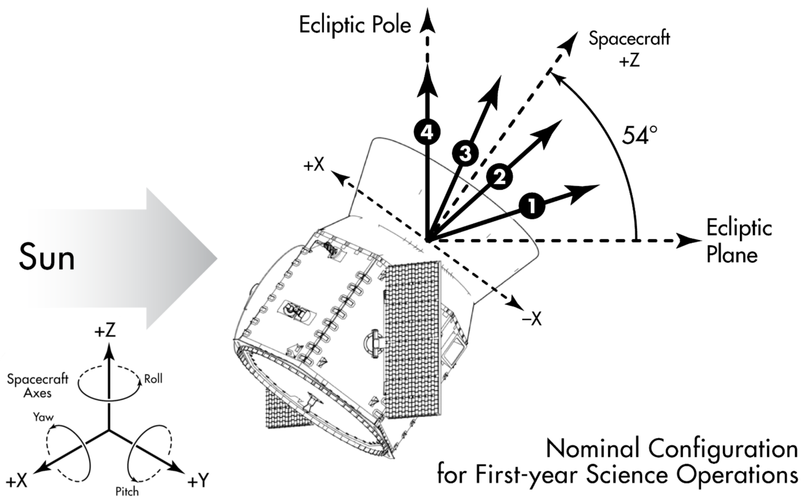

Figure 2: *TESS*'s solar panels pitch about the $+Y$ axis. The spacecraft must point so that incident sunlight is collected by the solar panels, and not the cameras. (Adapted from Orbital ATK design document)

Justification: 'two-survey' strategy used for primary mission – long survey at the North Ecliptic Pole; also gets fresh ephemerides at low ecliptic latitudes. Can phase in longitude to cover 'gaps' from primary.

Option 3. Repeat year 1 in the southern hemisphere, but with all fields 6 degrees further north in ecliptic latitude (`shemiAvoid`). *Justification:* covers most of sky missed in primary survey, freshens ephemerides & avoids Earth-Moon crossings that would happen with this same strategy inverted in the North.

Option 4. 7 sectors (14 orbits) with *TESS*'s long axis along the ecliptic, 6 sectors focused at the North Ecliptic Pole (`elong`). *Justification:* covers sky missed in primary survey with $\sim$ 3 orbits of observing time per star on the ecliptic, opportunity of K2 follow-up, can be extended for longer period coverage, avoids Earth-Moon crossings.

Option 5. 7 sectors with *TESS*'s short axis along the ecliptic, 6 sectors focused at the North Ecliptic Pole (`eshort`). *Justification:* similar to `elong`, with slightly better ability to follow-up on *TESS* objects of interest (TOIs).

Option 6. Cover both northern and southern ecliptic hemispheres in a year, by switching between northern and southern hemisphere sectors every $\sim$ 13.7 day orbit (`hemis14d`). *Justification:* freshen ephemeris times for most TOIs, faster than any other scenario.

In selecting these options for further study, we omitted other possible scenarios that will remain of interest, for instance in a fourth year of observing. We comment on these options and justify their omission from detailed calculations below:

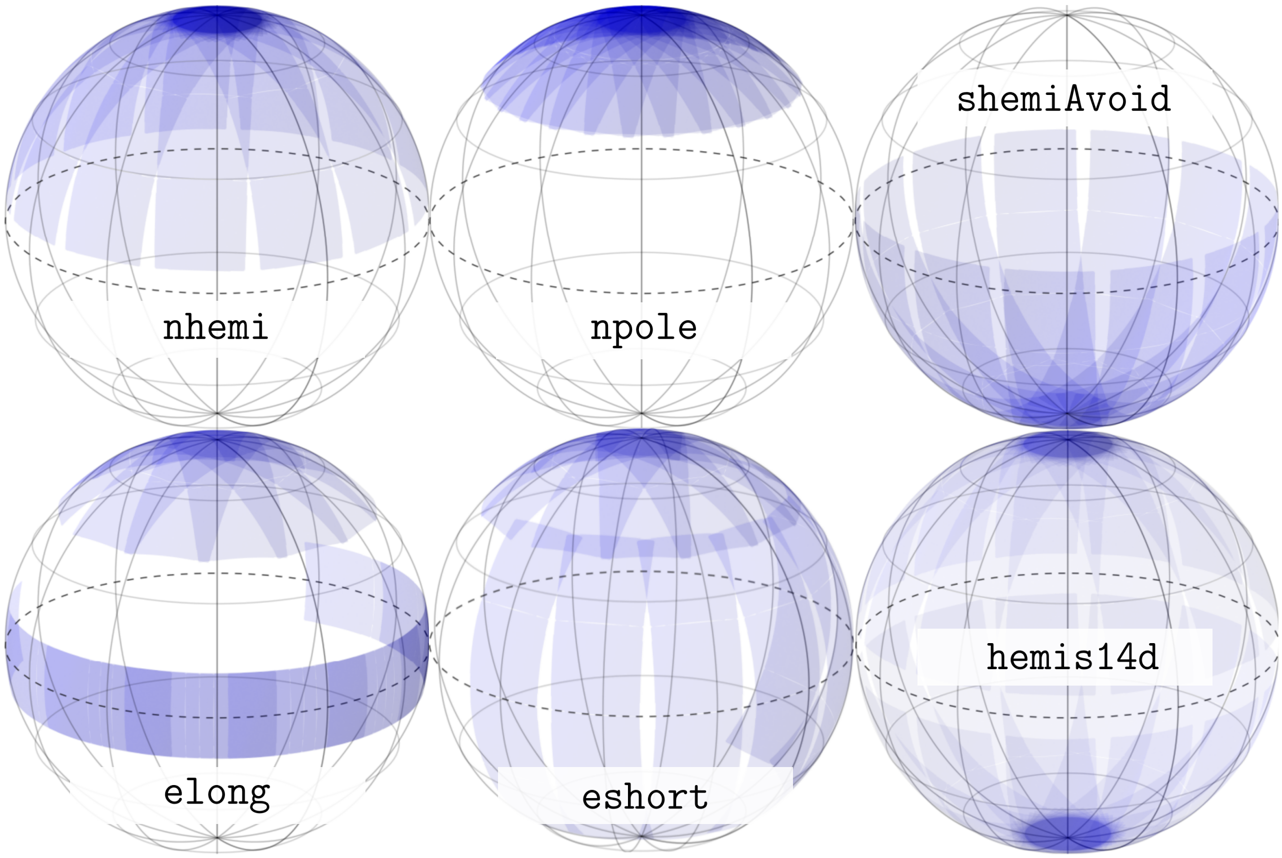

Figure 3: Proposed pointing strategies for a *TESS* extended mission, visualized in ecliptic coordinates. `nhemi`, `npole`, `shemiAvoid`, `elong`, `eshort`, and `hemis14d`. Note for `elong` and `eshort` that Earth and moon crossings likely make an entire year looking at the ecliptic impractical (see Fig. 9).

- Focus on the South Ecliptic Pole: omitted for simplicity (complement of `npole`).
- Repeat observations of the southern hemisphere: omitted for simplicity (complement of `nhemi`).
- Repeat year 2 in the northern hemisphere, but 6 degrees further south in ecliptic latitude: omitted for simplicity (complement of `shemiAvoid`), and also due to Earth/Moon crossings (see Sec. 3.6).
- 1 year with *TESS*'s long axis along the ecliptic. Omitted due to Earth/Moon crossings, which prevent detailed photometry for ~ 6 months/year. We show the outage as a function of time in Fig. 9.
- 1 year with *TESS*'s short axis along the ecliptic. Omitted due to Earth/Moon crossings, which prevent detailed photometry for ~ 6 months/year.
- Cover both northern and southern ecliptic poles over a year, by switching between hemispheres every spacecraft orbit. Omit-

ted because an important justification for this scenario – refined ephemeris times, described in Sec. 5.1 – suffers compared to `hemis14d`.

- Monthly-specific scenarios. For instance, in the `nhemi` scenario, during a month when the Earth or Moon crosses through the field of a camera pointed close to the ecliptic, tilt all the cameras away from the ecliptic as in the `npole` scenario. Omitted for simplicity.

All of these potential spacecraft pointings, both selected and omitted, meet the constraint of having *TESS*'s cameras point anti-Sun throughout the year, while also allowing the solar panels to collect sunlight.

3.3 Metrics by which we compare pointing strategies

We assess extended missions based on the risks and opportunities they present, as well as through their performance on select technical and science-based criteria. These criteria are organized following an approach originally outlined in Kepner and Tregoe [1965]. Summarizing them in list-form:

Technical musts: Cameras anti-sun? Solar panels collecting sunlight?

Technical wants: Duration of each sector $<$ 28 days? Earth/Moon crossings? Zodiacal background? Scattered sunlight off lens hood?

Exoplanet science wants:

- *New planet detection statistics:* number of newly detected planets (considering postage stamps and full frame images, independently and combined); number of new long-period planets (which may be detected through long period coverage, or by follow-up on single-transit events); number of new habitable zone planets; number of new planets with characterizable atmospheres; number of newly detected planets with bright host stars; number of systems with extra detectable planets (usually long-P companions to short-P transiting planets); number of newly detected planets with bright host stars.
- *Broader TESS science:* better ephemeris times on known TOIs; observe more transits over a long baseline to enable TTV searches; ability to alter target allocation weights between {white dwarfs, known planet-hosts, candidate planet-hosts, circumbinary & circumprimary planets, open clusters, evolved stars (notably to detect asteroseismic oscillations), dwarf stars later than M7, stars with well-measured properties, . . .}.

Broader science wants: Make observations relevant to stellar astrophysics, many of which may overlap with 'exoplanet science wants'. For instance, observe many stars to measure stellar rotation periods, or allocate a larger fraction of the data mass for short-cadence asteroseismic targets. May also wish to observe optical/near-IR variable targets across the sky, in particular pulsating stars (Cepheids, RR Lyrae, Delta Scuti, slowly pulsating B stars), eruptive stars (protostars, giants, eruptive binaries, flare stars), cataclysmic variables (dwarf novae, novae, supernovae), rotating variable stars (deformed by ellipsoidal variations, showing variability from stellar spots or magnetic fields), and eclipsing binaries. In particular, star spots can be used as indicators for magnetic activity to characterize long timescale stellar activity. In solar system science, may wish to observe main belt asteroids and the brightest near Earth asteroids. In galactic astronomy and high energy astrophysics, may wish to gather light curves for variable active galactic nuclei.

Opportunities:

- What's best on a > 1 year horizon for planet detections? For instance, if *TESS* were to continue for 5, or even 10 years, would any strategy be optimal?
- Ability to move targets detected in FFIs to PSs in extended mission
- Shorten the cadence of FFIs & lengthen the cadence of 'target' stars.
- *TESS as follow-up mission:* ability to observe *CoRoT* objects; ability to observe *Kepler* field (key benefits in broader science wants above); ability to observe *K2* fields (follow-up *K2* few-transit objects); ability to observe targets previously monitored by ground-based surveys.
- *Follow-up for TESS :* potential for *JWST* follow-up? Potential for *CHEOPS* follow-up? Ability to get *TESS* photometry contemporaneously with ground-based observations? Ability to observe from both North and South hemispheres on Earth?
- Impact on Guest Investigator program?

Risks: Risk of spacecraft damage? Risk of not meeting threshold science (to be defined)? Risk of excessive false positives, for instance from crowding? Would partial instrument failure in primary mission make this scenario infeasible? Would reduced precision (from aged CCDs, worse pointing accuracy, or other mechanical sources) invalidate this scenario? Risk of planet detection simulation over or under-estimating planet yield?

The specific weights between all of these desires will be allocated, explicitly or implicitly, in the process of defining an extended mission. This report is structured to address technical musts and wants in Sec. 3, new exoplanet detection statistics in Sec. 4, broader science *TESS* could perform beyond planet detection, whether or exoplanet-related or not, in Sec. 5, and the remaining opportunities and risks in Sec. 6.

3.4 *Description of planet detection model*

Sullivan et al. [2015] (hereafter, S+15) developed a direct simulation of *TESS*'s planet and false positive detections based on the spacecraft and payload design specified in Ricker et al. [2014]. We adapt this simulation for extended mission planning. With our additions, we can change where *TESS* looks in additional years of observing while keeping all other mission-defining parameters constant. Our approach is then to run our planet detection simulation for each plausible pointing strategy, and to compare the relative yields of detected planets. This lets us contrast extended mission planet yields with those of the primary survey, and also lets us compare extended missions in bulk.

Background on synthetic catalogs: *TESS* is sensitive to sub-Neptune sized transiting planets orbiting M dwarfs out to $\sim$ 200pc and KFG dwarfs out to $\sim$ 1kpc. It is sensitive to giant planets and eclipsing binaries across a significant fraction of the galactic disk. With this sensitivity in mind, the stellar catalog we 'observe' in our planet detection simulation is drawn from the output of TRILEGAL, a population synthesis code for the Milky Way [Girardi et al., 2005]. S+15 made select modifications to the catalog, notably in the M dwarf radius-luminosity relation, to better approximate interferometric stellar radii measurements. We keep these modifications; the modified TRILEGAL stellar catalog shows acceptable agreement with observations[6], specifically the Hipparcos sample [Perryman et al., 1997, van Leeuwen and Leeuwen, 2007] and the 10pc RECONS sample [Henry et al., 2006].

[6] Looking closely at the radius-luminosity relations, we do see non-physical interpolation artifacts. These outliers are visible in Figs. 5 and 3.5 below, but are a small enough subset of the population that we ignore them for this work.

With a stellar catalog defined, we populate the stars in the catalog with planets based on occurrence rates derived from the *Kepler* sample. We use rates Fressin et al. [2013] found for planets orbiting stars with $T_{\rm eff} > 4000$K and those that Dressing and Charbonneau [2015] found for the remaining M and late K dwarfs.

Detection process: We then simulate transits of these planets. Assuming the transit depth and number of transits are known, we use a model of *TESS*'s point spread function (PSF) to determine optimal photometric aperture sizes for each postage stamp star (*i.e.*, we compute the noise for all plausible aperture sizes, and find the number of pixels that minimizes this noise). With the aperture sizes and noise corresponding to a given integration time known, we compute a signal to noise ratio for each transiting object. Our model for planet detectability is a simple step function in SNR: if we have two or more transits and SNR > 7.3, we rule it as 'detected', otherwise it is not detected[7]. Our model for *TESS*'s photometric precision is described in S+15 and shown in Fig. 7.

[7] The value of this threshold is chosen to ensure that no more than 1 statistical false positive is present in the 'detections' from 2×10^5 target stars. Observing a greater number of stars, for instance in full frame images, should require a higher threshold value to maintain the same condition. We discuss this in Sec. 6.2.

Assumptions of SNR calculation: Our approach to computing SNRs for each transiting object is not time-resolved. In other words, we are not simulating every 2 second CCD readout, stacking those hypothetical readouts into 2 minute cadence postage stamps and 30 minute full frames, and then reducing simulated light curves.

Our calculation is simpler. We assume perfect period-recovery, phase folding, and identical conditions between transits. We also assume that we observe a constant transit depth, which is diluted by binary companions and background stars in the same manner between transits. Our approach is then to simply tally the number of *TESS* fields a given host star falls within, which corresponds to a known total observing baseline. Assuming random orbital phasing, we then compute the number of transits *TESS* observes for planets of any given host. With a model PSF, we determine ideal aperture sizes (see two paragraphs above), and then obtain an accurate noise per transit (since the transit durations are known, and we assume our noise, computed first over a single hour, then bins like white-noise, *i.e.*, proportionate to the inverse square root of the time in-transit).

Coupled with the known transit signal, this gives us the SNR per transit, and then to 'phase-fold our light-curves' (light-curves which are never explicitly computed point-by-point) we just[8] multiply the SNR per transit by the square root of the number of transits observed.

[8] We actually take a quadrature sum of both transit and occultation signals, but this is negligible for planets. It only matters for the case of eclipsing binaries, which we ignore in this work.

We have changed other aspects of this simulation since S+15 was published, and describe these changes in Sec. B of the appendix.

3.5 Selecting target stars (and full frame images)

In the actual mission, *TESS*'s short cadence (2 min) targets will be drawn from a subset of the *TESS* Input Catalog. The prioritization statistic that the mission will use in this selection has yet to be explicitly defined.

Regardless, we know that for *TESS* to detect small transiting planets it should observe stars that are small and bright. For this work, we define a simple statistic, `Merit`, proportional to the SNR we should expect from an arbitrarily sized planet orbiting any star:

$$\texttt{Merit} \equiv \frac{1/R_\star^2}{\sigma_{\text{1-hr}}(I_c)/\sqrt{N_{\text{obs}}}}\,, \tag{1}$$

where $R_\star$ is the radius of the star in question, $\sigma_{\text{1-hr}}$ is the relative precision in flux measurements over one hour of integration time, taken from an empirical fit to Fig 7, I_c is the Cousins band I magnitude *TESS* observes for the star (or more precisely, the star system) and N_{obs} is the number of observations the star receives over the course of the mission. For multiple systems, we use the radius of the planet host for $R_\star$, and the combined flux from all companion stars to compute the system's I_c magnitude.

We evaluate `Merit` for all the star systems in our modified TRILEGAL catalog, and then choose the best 2×10^5 as target stars to be observed at 2 minute cadence. Target stars selected in this manner are shown in Fig. 4. We take the next-best 3.8×10^6 stars and observe them at 30 minute cadence to simulate full frame image detections. This statistic is simpler than the procedure outlined in Section 6.7 of S+15 and it produces a nearly identical population of target stars (shown in Fig 5). Our approach for full frame image simulation is different from that of S+15, and we justify it further below.

This statistic also generalizes to extended missions. Over an entire mission, the total number of observations a star receives is the sum of its observations in the primary and extended missions: $N_{\text{obs}} = N_{\text{primary}} + N_{\text{extended}}$. Our selection criterion then remains identical, with the added condition that if $N_{\text{extended}} = 0$ for a given star, then we do not select that star as a target star for the extended mission.

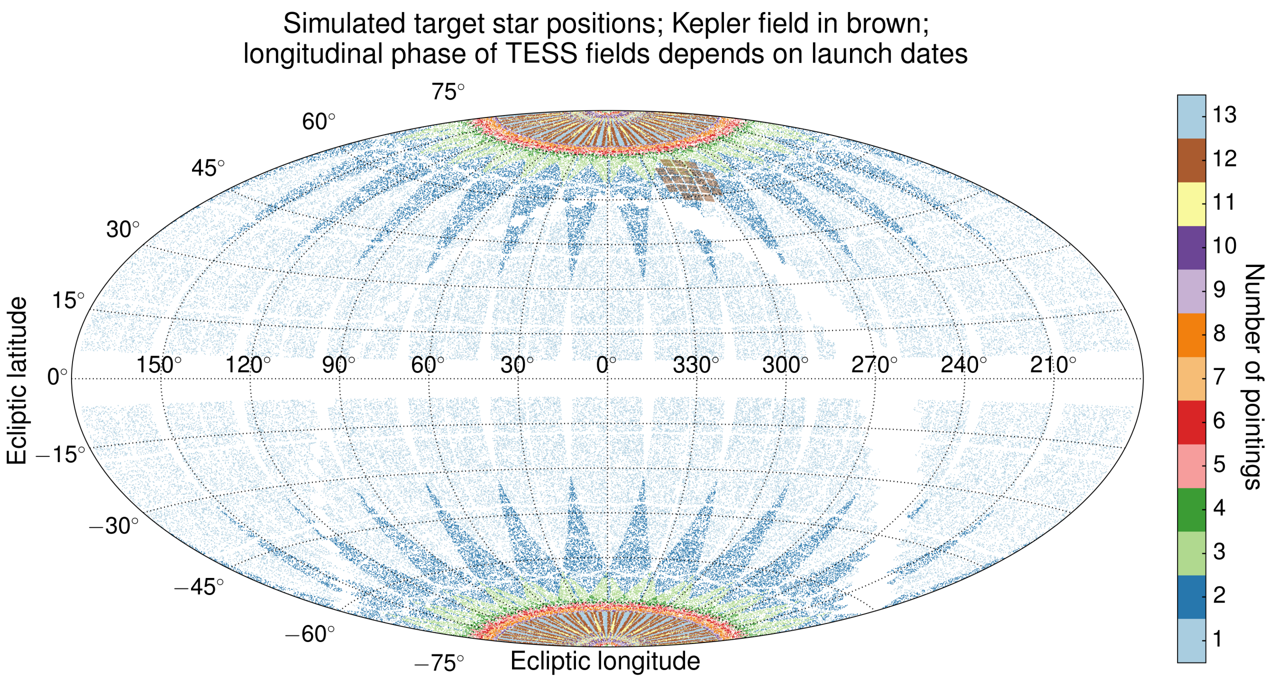

Figure 4: Selected target stars in the primary mission. Their density increases towards the poles because of the $\sqrt{N_{\rm obs}}$ weight in selection. Dead space on the CCDs creates 'gaps' in the continuous viewing zones.

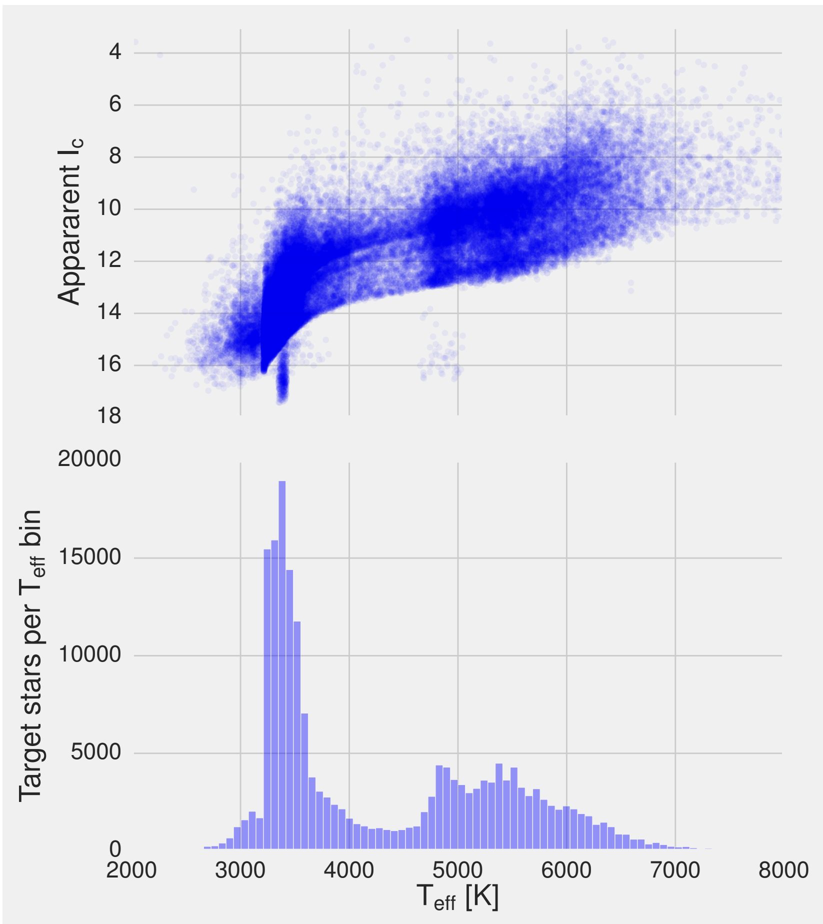

Figure 5: Replica of Figure 17 from S+15. Target stars are selected as the best 2×10^5 stars according to `Merit` $\equiv \sqrt{N_{\rm obs}}(1/R_\star^2)/\sigma_{1\text{-hr}}(I_c)$. The top subplot shows 1 in 10 stars. This simple model could inform the target selection to be performed on the *TESS* Input Catalog.

The lower histogram is bimodal, selecting heavily for M dwarfs, and selecting more F and G dwarfs than K dwarfs. This shape arises from the combined $1/R_\star^2$ and $1/\sigma_{1\text{-hr}}(I_c)$ weights: the fact that the minimum falls around K dwarfs occurs because of both a Malmquist bias (there are more F than K stars of comparable brightness in our catalog from which to select) as well as a corresponding dip in the TRILEGAL (& observed) V-band luminosity functions (see S+15 Figure 5).

Outliers visible in the upper scatter-plot are non-physical, possibly artifacts from S+15's Padova-to-Dartmouth interpolation as they tend to have greater masses than all other stars on the main sequence. They are less than 1% of the target stars, so we ignore them in order to proceed.

Alternative prioritization approaches: The procedure of simply applying Eq. 1 attempts to select a stellar sample that will yield the most small transiting planets around the brightest stars. An alternative approach would be to select stars that will give the most relative benefit in 2 minute postage stamps over 30 minute cadence observations. This 'relative benefit' could be a function of improved transit detectability, or perhaps improved capacity to resolve ingresses and egresses.

For transit detectability, the difference between 2 and 30 minute cadence matters most for short transit durations – in other words for small stars, and for close-in planets. Switching to this alternative approach would consequently bias us even more strongly towards selecting M dwarfs. We already select almost every M dwarf with $I_c < 14$. Referencing Winn [2013], these are M dwarfs for which we can only detect $R_p > 2R_\oplus$ planets. The limiting I_c magnitude for detecting $R_p > 4R_\oplus$ planets with *TESS* is ~ 16, which is where we see the dimmest stars in Fig. 5.

Additionally, the procedure of applying Eq. 1 and assuming that it will maximize the number of small planets that *TESS* will detect about bright stars ignores the functional dependence of planet occurrence rates on stellar properties. A more robust approach might be to take that probability into account, as in Kipping and Lam [2016].

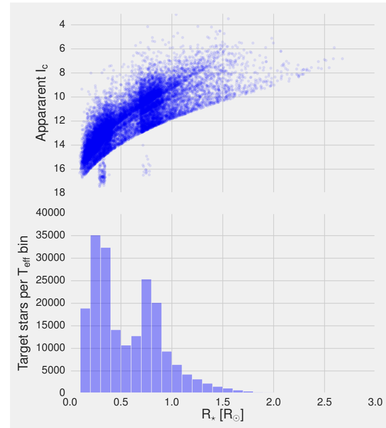

Figure 6: Same as Fig. 5, but as a function of stellar radius. $1/R_\star^2$ selection weight clearly visible, along with the same outliers.

Alternative prioritization approaches in extended missions: Our `Merit` statistic also neglects the option of an extended mission which only observes stars with known planets or planet candidates (*TESS*'s objects of interest, or those from other transit and RV surveys) at short cadence. This approach would free up a considerable portion of *TESS*'s data mass for full frame images at *e.g.*, 15 minutes rather than the current nominal 30 minutes.

Approach to full-frame images: To make simulating the full frame image detections computationally tractable, instead of considering every potentially transiting object about each of the $\sim 1.6 \times 10^8$ stars in our synthetic catalog (as S+15 did), most of which are too dim or too large for *TESS* to detect a $R_p < 4R_\oplus$ transiting planet about, we only simulate full frame image detections for the 3.8×10^6 next-highest `Merit` stars, after the 2×10^5 highest `Merit` stars observed as 'postage stamps'. This number (3.8×10^6) was initially estimated based on the number of searchable stars about which we expect *TESS* to be able to detect sub-Neptune radius planets [Winn, 2013]. The detection process is then identical to that for postage stamps,

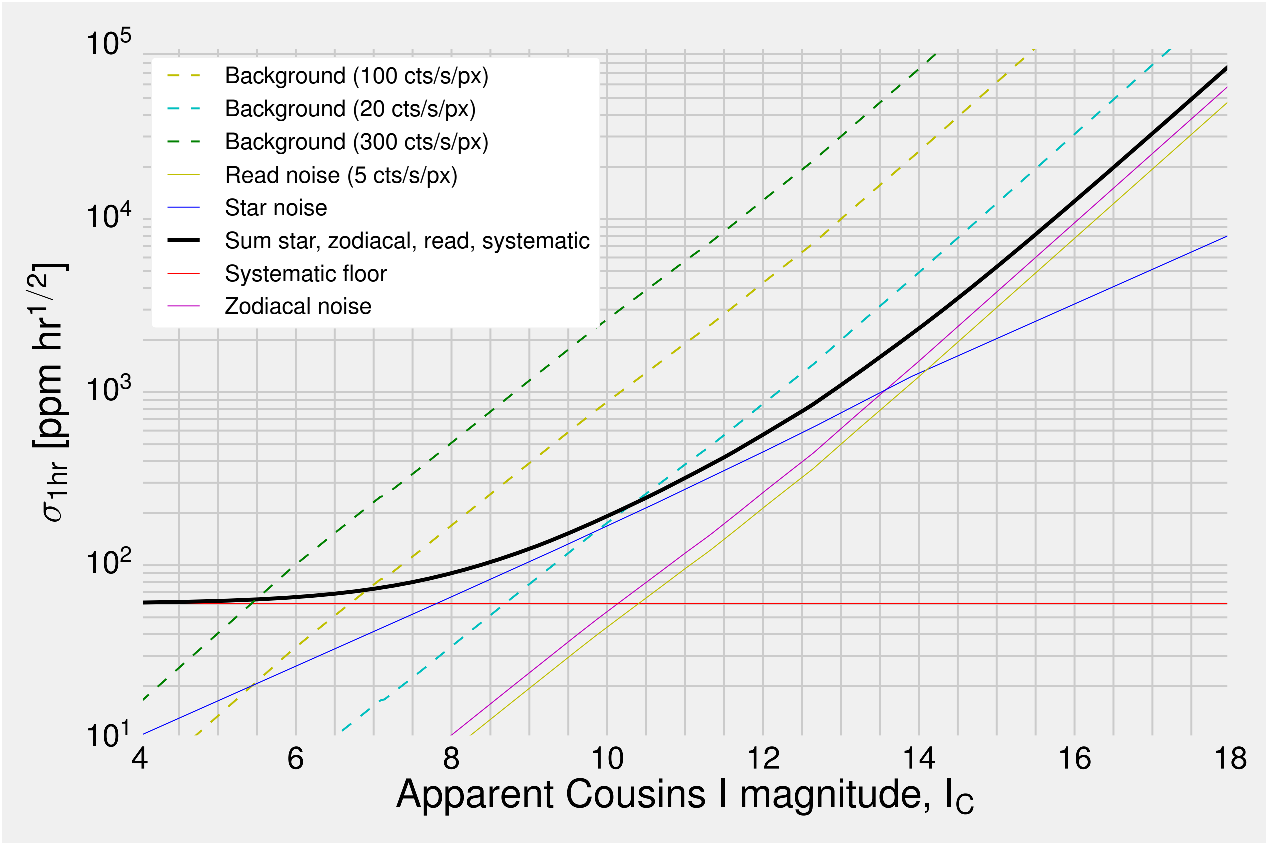

Figure 7: Relative precision in measured flux over a one hour integration time (scatter from contaminating background stars and PRF centroid offsets ignored). The noise sources described in Sullivan et al. [2015] are solid thin lines. The dashed lines exemplify noise from contaminating background flux, for instance from the Moon or Earth outside the *TESS* field, but still scattering light off the *TESS* lens hood. A dynamical 3-body simulation lets us estimate the impact lunar and Earth backgrounds have on *TESS*'s photometry. The photometric precision with which we simulate observations has additional scatter about the thick black line owing to randomly-assigned contaminating stars.

except with 30 minute instead of 2 minute exposures, which will extend the effective durations and shrink the apparent depths for transits with durations of $\lesssim$1 hour. To ensure that 3.8×10^6 stars is sufficient to include all stars about which *TESS* might detect sub-Neptune radius planets, we repeated this process for the primary mission using 5.8×10^6, 9.8×10^6 and 19.8×10^6 'full frame image' stars, and confirmed that there was no significant difference in the planet yields at $R_p \leq 4R_\oplus$ between any of the cases. There are still many stars that are dimmer or larger for which *TESS* detects planets with $R_p > 4R_\oplus$. Increasing the number of FFI stars, the runs yield increasing numbers of giant planets (particularly near the galactic disk, where contamination is also highest). We argue that knowledge that there will be thousands of giant planet candidates is a sufficient level of accuracy, and focus our attention on $R_p < 4R_\oplus$.

3.6 Earth/Moon crossings

When the Earth or Moon passes through *TESS*'s camera fields they flood the CCD pixels to their full well capacity ($\sim 2 \times 10^5$ photoelectrons). Precision differential photometry becomes impossible during these direct crossings. Even when the body (the Earth or Moon) is not directly in the camera's field of view, its light can scatter off the interior of the lens hood and act as a background source of contaminating flux. The Poissonian scatter in the number of photons arriving from the Earth or the Moon in such a scenario degrades *TESS*'s photometric performance. This can be important for field-center to body angles of $\theta \lesssim 34^\circ$ (see Fig. 26 in Sec. A of the appendix). We show a few representative background fluxes in Fig. 7.

Separately from our planet detection simulation, we study the impact of these crossings in a dynamical simulation based on JPL NAIF's standard SPICE toolkit. Given a nominal launch date, this code determines *TESS*'s orbital phasing throughout its entire mission. At every time step of the three-body orbit, we calculate the distance between *TESS* and the other two bodies of interest, and the separation angles among each of the four cameras and each of the two bodies (eight angles in total). The gravitational dynamics behind this calculation treat the Earth, Moon, and Sun as point masses, and the *TESS* spacecraft as a massless test particle. The spacecraft's inclination oscillates in the simulation as it will in reality.

Taking the Earth and Moon's integrated disk brightnesses as fixed values[9] we use a model for scattered light suppression from the *TESS* lens hoods (Fig. 26), to tabulate the photon flux from each of these bodies onto each of the cameras throughout the orbit.

[9] $I_{☽} = -13.5$, so the full moon delivers 1.5×10^6ct/s/px, and the Earth delivers approximately $80\times$ that amount.

To determine the cumulative impact of these crossings on *TESS*'s observing, we ask: for each camera, what fraction of the total observing time is *TESS* unable to operate at desired photometric precision because of Earth and Moon crossings? An upper limit for what we mean by 'unable to operate at desired photometric precision' is when terrestrial or lunar flux make it impossible to observe any star in our selected target star catalog with photometric precision < 1mmag over one hour of integration time. This limit, $F_{\rm max}$, is roughly

$$F_{\rm max} \approx 1000 \text{ cts/s/px} = 200 F_{\rm readout\ noise}.$$

Considering *TESS*'s precision (Fig. 7), as well as the target star catalog's apparent magnitude distribution (Fig. 5), even a background of 100 ct/s/px would be a problem, since it would hinder sub-mmag photometry for all stars with $I > 10$ ($\sim 75\%$ of the target star catalog). We plot the percentage of target stars that are 'lost' as a function of background counts (*i.e.*, those that could be observed at sub-mmag precision over an hour, but no longer can) in Fig. 27.

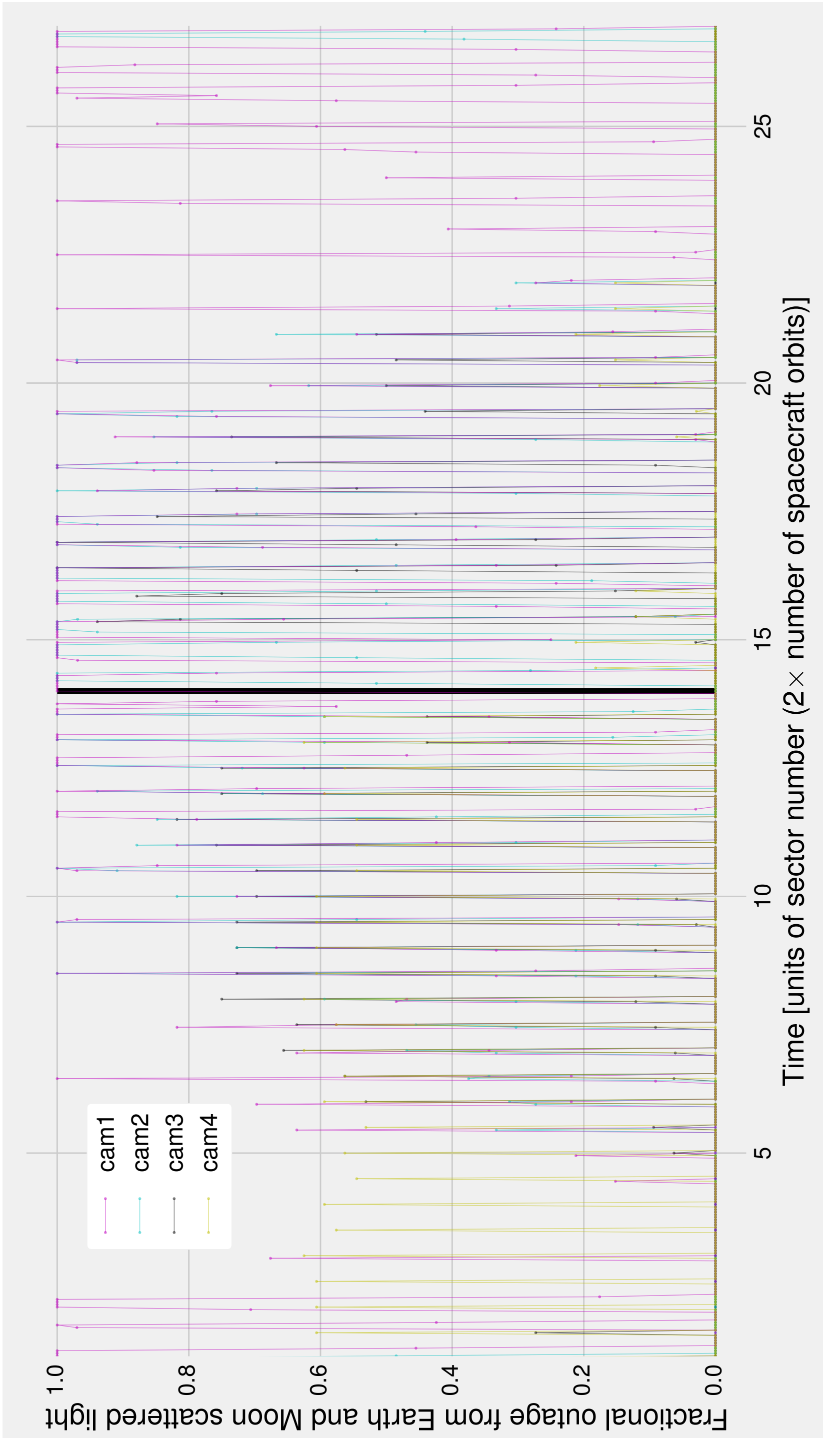

Figure 8: Fractional outage caused by Earth and Moon light either falling directly onto *TESS*'s cameras or scattering off of their lens hoods and into the lenses, as a function of time in the orbit. The first year of observations are in the southern ecliptic hemisphere. The black dividing line indicates the beginning of 'Year 2' of northern hemisphere observations. Note that the worst fractional outage per orbit is in Camera 1 (which points towards the ecliptic) over the first ~ 5 orbits of the second year. By 'fractional outage' in these plots, we mean the fraction of target stars that could be observed with $\sigma_{1\mathrm{hr}} < 10^3$ppm precision that no longer can because of Earth or Moon light. The time-step is 1/20th$^{\mathrm{th}}$ of an orbit. The plot has 'spikes' because outage typically only occurs over a small fraction of the orbit.

A detailed model of how these crossings impact *TESS* photometry is outside the scope of this work. That said, to account at least

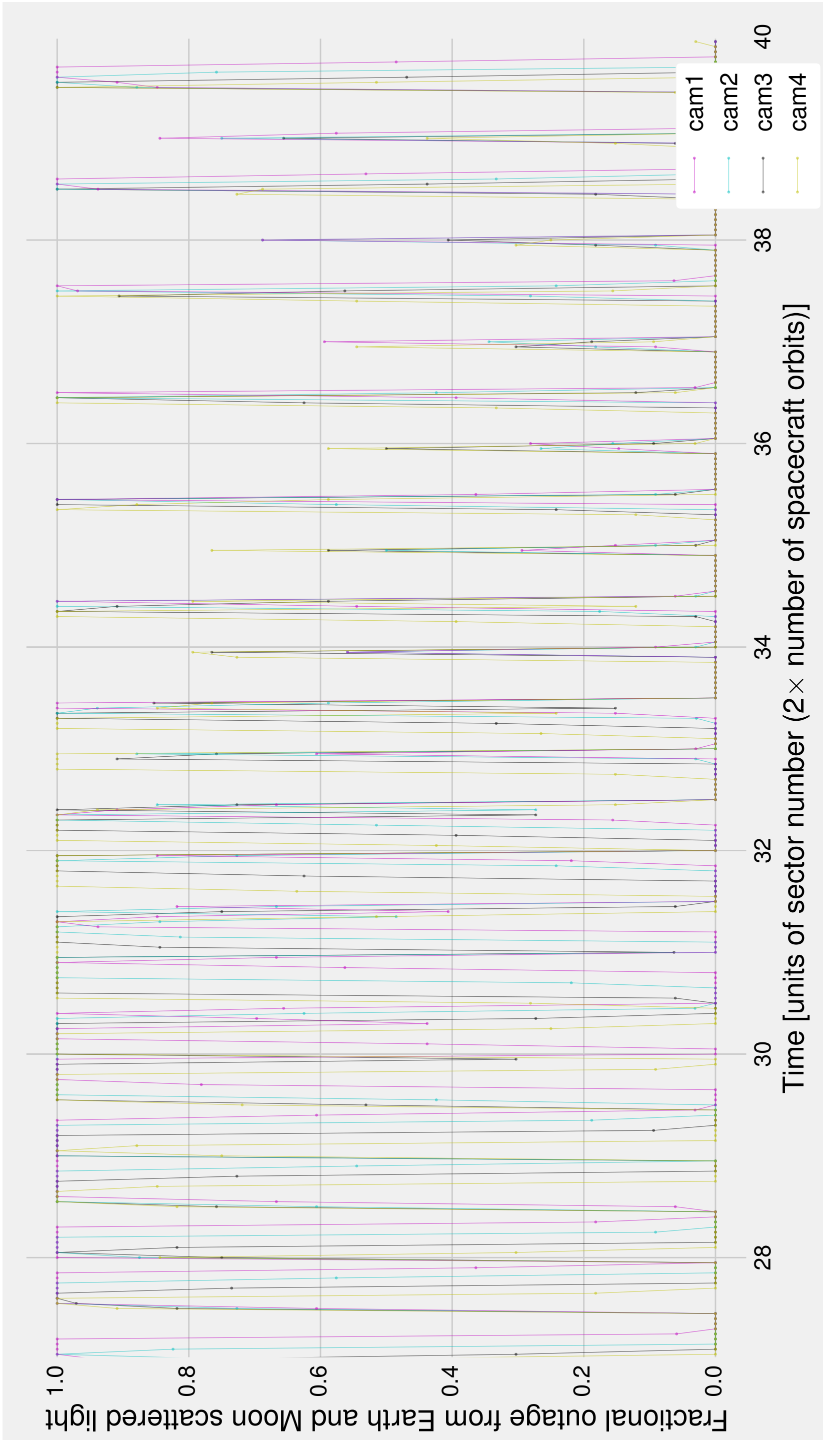

Figure 9: Same as Fig. 8, except for a hypothetical third year in which *TESS* observes the ecliptic with the cameras' long axis along the ecliptic plane. The latter half of the year experiences far less Earth and Moon interference than the first half. Considering it implausible that we would opt to sacrifice such a large fraction of our observing time ($\sim$ 50% over the first 6 months), we study the `elong` and `eshort` scenarios instead, as they make useful observations during the first ~ 5 months (shown in Fig. 3).

qualitatively for this effect in our planet detection simulation we use a simple approximation: we impose that a camera has an 'outage'

	Camera 1	Camera 2	Camera 3	Camera 4
Year 3 selected				
`npole`	0	0	0	0
`nhemi`	2	1	0	0
`shemiAvoid`	2	0	0	0
`elong`	1	1	1	1
`eshort`	0	1	1	0
`hemis14d`	1	1	0	0
Year 3 omitted				
`spole`	0	0	0	0
`shemi`	1	0	0	0
`nhemiAvoid`	4	3	0	0
`elong1yr`	4	4	4	4
`eshort1yr`	1	3	4	2
`poles14d`	0	0	0	0
Primary mission				
`shemi (year 1)`	2	1	0	0
`nhemi (year 2)`	4	2	0	0

Table 1: Number of sectors (of 13 per year) 'dropped' due to the Earth and Moon crossings in both selected and omitted pointings, with those of the primary mission for reference. The method of 'dropping' fields (which omits the temporal nature of the crossings, discussed in the text) gives a representative sense of the cumulative impact of Earth/Moon crossings. `elong1yr` corresponds to a full year with the *TESS* field's long axis along the ecliptic, and `eshort1yr` corresponds to the same, but with the long axis perpendicular to the ecliptic. These scenarios are neglected because their outages are time-correlated. (see Fig. 9)

if there are over $F_{\rm thresh} \equiv 300$ cts/s/px arriving from the Earth and Moon during a given exposure. We then compute the average outage time per observing sector that *TESS* suffers in each of its cameras. For instance, a given sector might have 660 hours of observing time over two spacecraft orbits, of which 220 hours might either have the Earth, the Moon, or both shining with a background $F > F_{\rm thresh}$. This would correspond to a fractional outage of 1/3. We proceed by computing the mean of this fractional outage across all 13 sectors of a given year to derive a 'mean camera outage' for each proposed pointing scenario.

As we mentioned in Sec. 3.4, our planet detection simulation is not explicitly time-resolved; it takes the ecliptic coordinates of camera fields for each orbit to compute the number of observations a given star receives over a specified mission. In a somewhat ad-hoc manner, we decide to approximate the effect of Earth and Moon crossings by selectively omitting the closest integer number of observing sectors corresponding to the 'mean camera outage' described above. For instance, if the 'mean camera outage' was 17% of *TESS*'s observing time over a given year, we would omit the 2 (of 13) observing sectors that suffer the greatest number of lost hours, for that given camera. The relevant number of omitted sectors is shown in Table 1. While this procedure ignores the temporal nature of the 'outages' (which is shown resolved over time-steps of $1/20^{\rm th}$ of an orbit in Figs. 8 and 9), it gives a representative sense of the cumulative impact of Earth and

Moon crossings over the course of a year. We discuss the impact of this approximation for the primary mission in Sec. 4.1, and for extended missions in 4.3. The summarized version is that modeling Earth/Moon crossings in this manner causes a drop of $< 10\%$ of $R_p < 4R_\oplus$ planet detections compared to the case of not accounting for the crossings at all. Given that Earth/Moon crossings typically last for a small fraction of an orbit (Fig. 8), if the timescales required for the cameras to 're-settle' after the crossings are small compared to orbital timescales, then our approach may in fact over-estimate the effect's importance.

3.7 *Summarized input assumptions to planet detection simulation*

- The TRILEGAL catalog (modified to match interferometric radii, as described in S+15) is an accurate representation of the stellar neighborhood to $\lesssim$ 2kpc.
- *TESS*'s large pixel size ($21 \times 21''$) combined with crowding near the galactic disk will cause substantial source confusion and a large astrophysical false positive rate. We thus omit the 5% of the sky closest to the galactic disk (see Fig. 4), and focus on planet detection statistics for $R_p < 4R_\oplus$.
- We know the radii and apparent magnitudes of TRILEGAL's synthetic stars, so we can prescribe a simple prioritization statistic (Eq. 1) that we expect (but have not verified) maximizes the number of small planets we discover about bright stars[10].
- The only 'imperfection' in our (simulated) knowledge of a given host star's parameters is its apparent magnitude, which in reality could be dimmer than the value we use for prioritization owing to dilution from companion and background stars (whose presence will not be known a priori, but which we account for when computing 'observed' SNRs).
- Planet distributions derived from the *Kepler* mission in Fressin et al. [2013] and Dressing and Charbonneau [2015] are accurate for the $P \lesssim 180$ day planets to which *TESS* is sensitive.
- Multiple planet system distributions can approximated as repeated draws from the above distributions (with independent probability) with added impositions of co-planarity and orbital stability.
- For our instrument and noise models, we assume:
  - A point-spread function (PSF) derived from ray-tracing simulations, similar to that described in S+15, Sec 6.1.
  - All stars are observed at the *center* of the *TESS* CCDs. This ignores off-axis and chromatic aberrations within the *TESS*

[10] Although it is difficult to determine accurate photometric radii, we expect that by the time *TESS* launches *Gaia* will provide accurate proper motions for the majority of *TESS* targets, allowing *TESS* to discriminate between red dwarfs and red giants for purposes of target prioritization.

optics, and consequently ignores the angular dependence of the pixel response function (the fraction of light from a star that is collected by a given pixel). While S+15 took a different approach to this, we argue that the methodology used in that work was inconsistent (see appendix Sec. B). Keeping a PSF that does not depend on observed stellar field angles is better suited to our goal of comparing extended mission pointings.

  - The time/frequency structure of all noise (except for stellar variability, see below) is 'white'. This means that we ignore time-correlated instrumental effects such as spacecraft jitter, thermal fluctuations, and mechanical flexure, which will be addressed by the mission's data reduction pipeline.
  - The instruments work equally well in year 3 as in years 1 and 2.
  - Contributors to white noise include: CCD read noise, shot noise from stars, a systematic noise floor of 60 ppm $\cdot$ hr$^{1/2}$, and zodiacal background. See Fig. 7 for the relative contributions of these terms as a function of apparent magnitude.
  - Noise contributions from stellar intrinsic variability are identical to those described in S+15 Sec3.5, which uses variability statistics from the *Kepler* data computed by Basri et al. [2013]. Unlike all previously mentioned noise sources, we do not scale noise from stellar variability as $t_{\rm obs}^{-1/2}$, since the photon flux from stars may vary over time-scales similar to typical transit durations. Instead, we assume the noise contribution from stellar variability is independent across transits, and thus scales as $N_{\rm tra}^{-1/2}$, for $N_{\rm tra}$ the number of observed transits.

- For our detection model, we assume:
  - A step-function detection threshold: for SNR $\geq$ 7.3, we rule transiting planets as detected, for SNR $<$ 7.3, they are not detected.
  - The top 2×10^5 merit-ranked targets (Eq. 1) are observed at two-minute cadence, and the next 3.8×10^6 stars are observed at thirty-minute cadence. We use S+15 Sec. 6.8 approach to 'blurring' transits with durations $\lesssim$ 1hr, so that for longer cadence images shorter transits get shallower depths and longer apparent durations. As described in Sec. 3.5, we verify that under this assumption, our detections are complete for $R_p < 4R_\oplus$, and incomplete for Jupiter-sized planets.
  - $\geq$ 2 transits for detection. No uncertainties in 'derived' periods or in identifying which target stars are exhibiting the transit signals.

- We do not have any knowledge of previous observations that may have been performed on our stars. For instance, observing the ecliptic, we do not simulate the *TESS* -*K2* overlap.
- For Earth and Moon crossings, we assume we can drop a fixed number of orbits of observing time for the cameras that suffer most from the Earth, the Moon, or both being in *TESS*'s camera fields. We summarize this effect in Table 1. Although this ignores the time-correlated nature of the outages shown in Figs. 8 and 9, it is sufficient for comparing detected planet yields across missions.
- We can perfectly discriminate between astrophysical false positives (for instance background eclipsing binaries or hierarchical eclipsing binaries) and planet candidates.
- We can compute SNR with effective signal $\delta_{\rm eff} = \delta \times D$ for $\delta = (R_p/R_\star)^2$ the transit depth, and

$$D = \frac{\Gamma_N + \Gamma_T}{\Gamma_T} \tag{2}$$

  where D is the dilution factor of a target star with incident photon flux Γ_T from the target star and incident photon flux Γ_N from neighboring stars (e.g., on the sky background, or binary companions).

  The noise is computed by creating a synthetic image for every host star with a planet that transits above a 'pre-dilution' SNR threshold (this threshold is imposed for the sake of lowering our computational cost). This 16×16 pixel image is of the number of photoelectrons *TESS* sees from the star and its companions/background stars at each pixel of each CCD. We produce it through our PRF model, which in turn requires the host star's $T_{\rm eff}$ and apparent I_c. Over each image, the noise is computed for a range of possible aperture sizes about the brightest pixel (see S+15 Secs. 6.2 and 6.3), and then finally a single 'noise' for each transit is selected by choosing the aperture size that minimizes the noise.

4 *Planet detection statistics*

Using the planet detection model described in Sec. 3.4 and the target selection procedure of Sec. 3.5, we simulate three years of *TESS* observing, with for six cases for third-year extended missions: `nhemi`, `npole`, `shemiAvoid`, `elong`, `eshort`, and `hemis14d`. How many new planets do we detect, and how do their properties differ between extended missions? We give results for planets with radii $R_p < 4R_\oplus$, due to both the subtlety and computational cost of modeling full frame image recovery of giant planets near the galactic disk.

4.1 Planet yield from the primary mission

We first examine our results for just the first two years of *TESS*'s observing, before presenting an analysis of our detected planet populations from a single extended mission (Sec. 4.2) and all six of our proposed extended missions (Sec. 4.3). Here we highlight commonalities and differences between S+15 and this work.

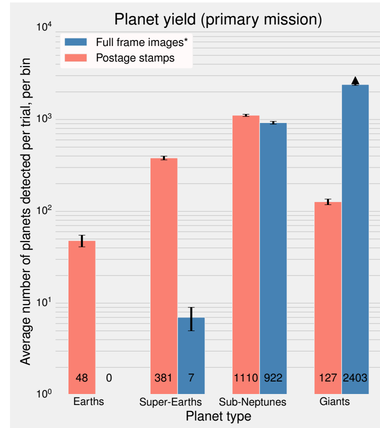

Figure 10: Mean numbers of planets detected in *TESS*'s primary mission (error bars are from Poisson fluctuations and do not account for systematic uncertainty). In postage stamp detections, the number of Earths ($R_p < 1.25R_\oplus$), super-Earths ($1.25R_\oplus \leq R_p < 2R_\oplus$), sub-Neptunes ($2R_\oplus \leq R_p < 4R_\oplus$) and giants ($R_p > 4R_\oplus$) is comparable to those quoted in Sullivan et al. [2015], despite modifications to our target selection procedure (Sec. 3.5). Our full frame images detections in are complete for $R < 4R_\oplus$, and incomplete for giant planets. Here we disagree, by for instance two orders of magnitude in the super-Earth bin, with Sullivan et al. [2015] (see text).

Detected planet yield The first point of comparison is the detected planet yield from our simulation, shown in Fig. 10. The number of Earths, super-Earths, sub-Neptunes and giants we detect in postage stamps agrees with the numbers quoted in S+15, despite our modified target selection procedure. Other changes to our simulation's inputs, for instance using an as-built model of *TESS*'s PSF informed by laboratory tests (courtesy Deborah Woods) rather than the idealized PSF described in Sec6.1 of S+15, also had little impact on this final result.

However, our yields from full frame images differ markedly from those quoted in Fig. 18 of S+15. We agree with S+15 that no Earths are detected in the full frame images. However, we detect only ~ 10 super-Earths by observing the $200,001^{\text{st}}$ to $4,000,000^{\text{th}}$ `Merit`-ranked stars at 30 minute cadence. This is two orders of magnitude less than the ~ 1000 super-Earth detections claimed from FFIs in S+15. There is also a small discrepancy in FFI-detected sub-Neptunes, for which we claim detection of ~ 1000, while S+15 claims ~ 2000.

We empirically verified that our full frame image detections are complete for $R < 4R_\oplus$ by changing the number of stars observed at 30-minute cadence and seeing that the number of detected planets with radii less than Neptune did not change. We do not understand the origin of the difference between our method and S+15's, but note that our results are in much better agreement with order-of-magnitude analytic arguments for *TESS*'s expected planet yield. Assuming an exponentially distributed stellar population in the galaxy and computing limiting magnitude thresholds, Winn [2013] predicted detections of $600 - 6000$ Neptunes, $24 - 300$ super-Earths, and $1 - 10$ Earth-sized planets, where the lower bounds correspond to planets detected with $\text{SNR} > 10$, and the upper bounds for $\text{SNR} > 7$. S+15's prediction of a total of 1500 detected super-Earths is a factor of 5 larger than these analytic estimates, while ours is in rough (< factor of 2) agreement.

We also present the following plausibility argument for our yields vs. those of S+15: consider the two adjacent bins of the relevant histogram, where one bin has width $0.75R_\oplus$ and 1400 planets fall within it, and the other has width $2R_\oplus$ and 3000 planets fall in it if we believe S+15, and 400 and 2000 do if we believe our own work. Letting 'rate' mean the number per bin width, this means that ratio of the rates of detected super-Earths to sub-Neptunes for S+15's case is $(1400/0.75R_{\oplus})/(3000/2R_{\oplus}) = 1.25$, and for our case it is $(400/0.75_{\oplus})/(2000/2R_{\oplus}) = 0.53$. The actual *input* ratio for these rates (cf. S+15, Fig 8) is about 2 for $T_{\text{eff}} < 4000$K hosts and 1.5 for $T_{\text{eff}} > 4000$K hosts. In the top 4×10^6 merit ranked stars from TRILEGAL (those that we empirically saw give all $R_p < 4R_{\oplus}$ planets), 31% of them have $T_{\text{eff}} < 4000$K. Thus the weighted input ratio is roughly $2 \times 0.31 + 1.5 \times 0.69 = 1.66$. S+15's result is that the detection bias for super-Earths (typically $R_p = 1.5R_{\oplus}$) versus sub-Neptunes (typically $R_p = 3R_{\oplus}$) is so slight that actually observing leads to a relative loss of $1.66/1.25 = 1.3\times$ fewer super-Earths than sub-Neptunes. Our result is that it's $1.66/0.53 = 3.1\times$ fewer. A naive expectation would have us believe that it's 4× fewer, given that $\delta \propto R_p^2$. This means that S+15's results imply a detection efficiency biased sub-linearly in R_p, whilst ours implies a bias between linear and quadratic in R_p.

Properties of planets detected in primary mission We show the population properties of planets detected from postage stamps and full frame images in the primary mission in Figs. 12 and 13. We agree with S+15 for all major postage stamp properties (apparent magnitude I_C, planet radius R_p, orbital period P, and insolation S), while, as discussed above, differing in full frame image yields. For instance, the dearth of $P < 5$ day Neptune-radius planets in Fig. 12 was observed by *Kepler* [Mazeh et al., 2016], and thus it is present in our input occurrence rates, rather than being an observational bias. It was also seen in S+15.

The differences between planets detected in postage stamps vs. in full frame images follow our expectation from our `Merit` statistic. Namely, Fig. 13 shows that at a fixed brightness, full frame image detections tend to occur at larger stellar effective temperature (and thus stellar radius). At a fixed host star radius, postage stamp detections occur around brighter stars.

Impact of earth and moon crossings on primary mission's detected planet yield We drop the most fields for Camera 1 in Year 2 of the primary (4 of 13 'observing sectors', see Table 1 and Fig. 8). This reduces the number of planet detections near the ecliptic at the beginning of Year 2, in some fields to zero. This is visible in the orange points of Fig. 11. In the primary mission *TESS* detects ~ 20 planets with $R_p < 4R_{\oplus}$ from both 2 minute and 30 minute data in each $24^{\circ} \times 24^{\circ}$ camera field nearest to the ecliptic (where each field is observed for 2 *TESS* orbits). As implemented in our simulation, Earth and

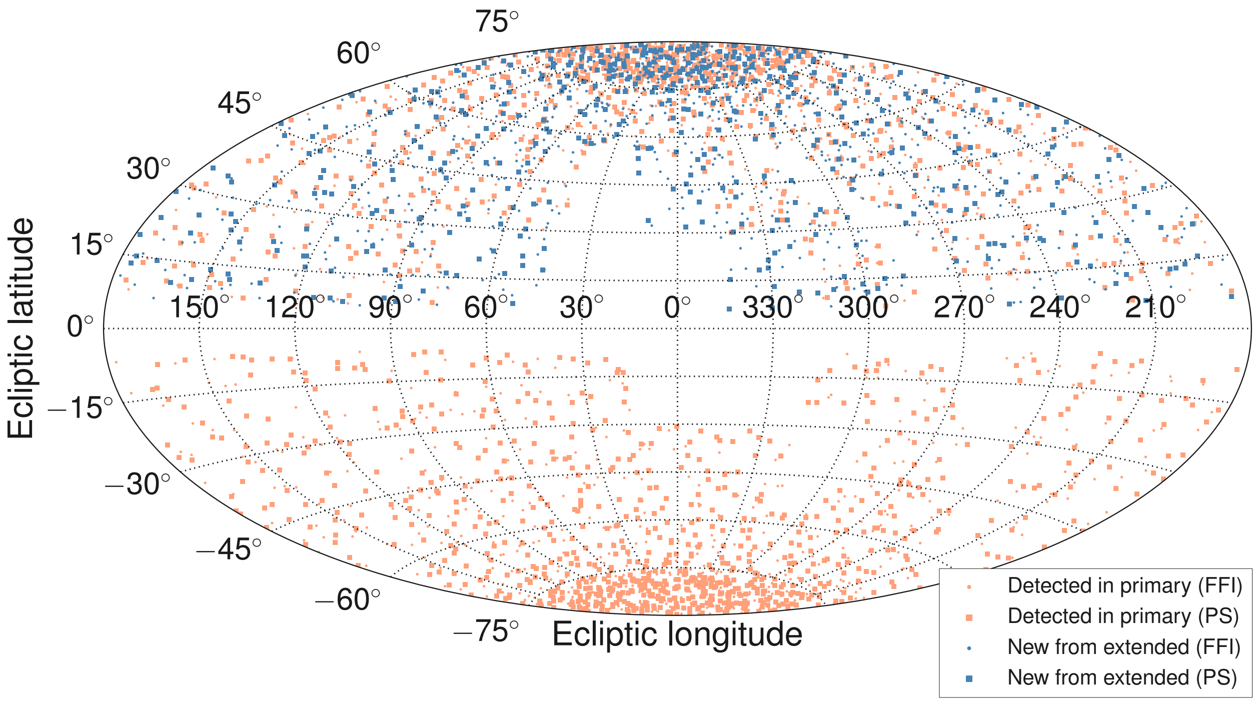

Figure 11: Positions of $R < 4R_\oplus$ planets detected in the `nhemi` scenario. Squares (postage stamps) and dots (full frame images) are observed at 2 and 30 minute cadence respectively. Orange denotes detection over the first two years of observing (the primary mission), and blue denotes newly detected planets from the extra third year. The 'gaps' in fields due to Earth and Moon crossings during the primary and extended missions are noted in Table 1. For instance, the field centered at $(\lambda = 330°, \beta = 18°)$ is observed in the extended but not the primary mission.

Moon crossings result in fields simply not being observed, so in these cases planets orbiting stars in these fields are never detected. Considering only the primary mission, we would naively expect that dropping a total of 9 fields over the two years (again, see Table 1) would result in a loss of $\sim 9 \times 20 = 180$ planets. This agrees with what our simulations actually give: running them without accounting for Earth and Moon losses returns a mean of 2678 detected planets with $R_p < 4R_\oplus$, while running them with Earth and Moon crossings gives a mean of 2482 such planets (a loss of 196 planets, or 7% of the sub-Neptune yield).

4.2 *Planet yield from an example extended mission* (`nhemi`)

Before comparing our six selected extended mission scenarios simultaneously (Sec. 4.3), we describe the detected planet populations from a single realization of an extended mission. As an example case, we choose the `nhemi` scenario.

A sky map showing the positions of detected planets for this mission is drawn in Fig. 11. Commenting on this map, we note that:

- Any planet detected in this scenario's primary mission is also de-

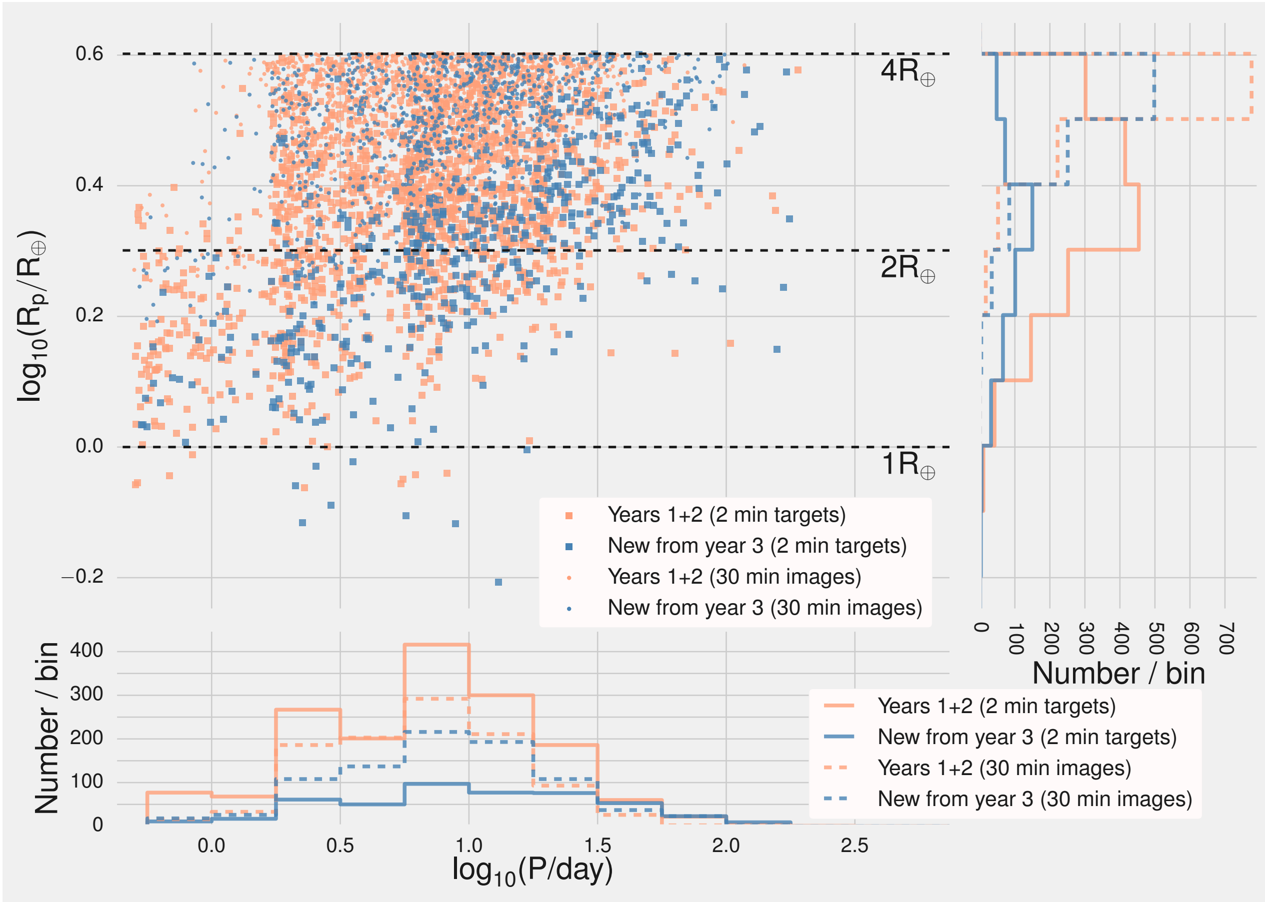

Figure 12: Radius vs period of detected $R_p < 4R_\oplus$ planets from one Monte Carlo realization of the `nhemi` scenario. At a fixed period, extended missions help us detect smaller planets; at a fixed radius, they let us probe out to longer periods. The radius histogram, and the location of all dots (rather than squares) on the scatter plot show that almost all $R < 2R_\oplus$ planets are detected in postage stamps, not full frame images (also shown in Fig. 10).

tected in its extended mission. We consequently color the detected planets depending on if they are discovered in the primary mission, or whether they are detected thanks to extra observations in the extended. In our simulation, these extra observations will lead to new detections (a) because of an increased number of observed transits leading to a higher phase-folded SNR, which causes the transiting object's SNR to clear our threshold of 7.3, and/or (b) because raising the number of observed transits clears the minimum number of transits we require for detections ($N_{\text{tra}} \geq 2$).

- The 'dropped' fields described in Sec. 3.6 owing to Earth/Moon crossings are visible for both the primary and extended missions in the $\lambda = (30°, 0°, 330°, 300°)$ fields.

Beyond the positions of the detected planets, we select and plot some of their properties, notably planet radius R_p, orbital period P, apparent magnitude I_c, and effective temperature T_{eff} in Figs. 12 and 13. Both of these figures are visualizations from a single Monte

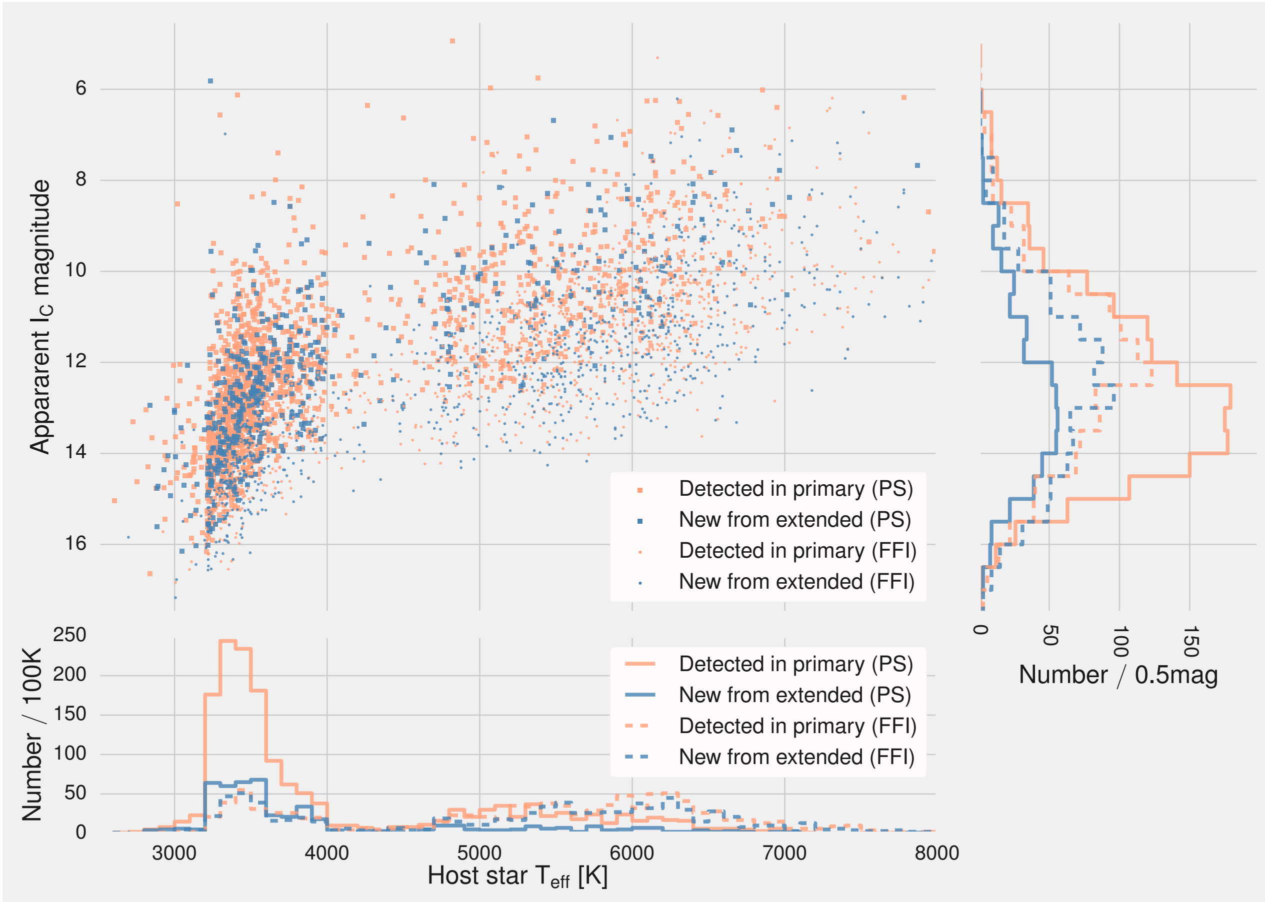

Figure 13: Apparent Cousins I magnitude plotted against effective temperature for $R_p < 4R_\oplus$ planets detected from one Monte Carlo realization of the `nhemi` scenario. Postage stamp (PS) detections are biased towards M dwarfs in part because of our selection procedure. For a given effective temperature, full frame images (FFIs) are taken of dimmer stars.

Carlo realization of the `nhemi` scenario, and only show planets with $R_p < 4R_\oplus$. These plots clarify a few points:

- At a fixed period, extended missions help us detect smaller planets; at a fixed radius, they let us probe out to longer periods. This is one of the major reasons to extend *TESS*'s observations.
- Almost all $R < 2R_\oplus$ planets are detected in postage stamps, not full frame images. This is an indication that the top 2×10^5 `Merit` stars are a sufficient sample to detect most of the $R < 2R_\oplus$ planets that *TESS* can detect.
- Postage stamp detections are biased towards M dwarfs, in part because of our selection procedure.
- For a given effective temperature, full frame images are taken of dimmer stars. Projecting the FFI detections onto apparent I_c magnitude (Fig. 13, right panel), the median brightness of planets detected from FFIs is actually greater than the median brightness

of planets detected from PSs. This is because these detections are about stars with radii that, on average, are greater than those from postage-stamp detections.

- The large number of full frame image detections between 5000K $< T_{\rm eff} <$ 7000K suggest that our proposed selection procedure (Sec. 3.5) may not be optimal, and that a robust approach towards target prioritization, for instance using expected planet occurrence rates as a function of stellar type in a Bayesian approach, could maximize *TESS*'s expected yield. For instance, Kipping and Lam [2016] note that the probability of short-period transiters having additional transiting outer companions is functionally dependent upon the properties of the short period transiters – for instance their orbital periods and radii. Target prioritization for *TESS* could benefit from a similar approach.

There are a few other statistics that interesting for purposes of characterizing the value of this extended mission – how many new planets do we detect? How many are at long orbital periods? How many are in habitable zones? We respond to these questions in Sec. 4.3, in particular showing our detected planet yields in Fig. 14.

4.3 *Comparing planet yields from all extended missions based on new planet detection metrics*

To compare extended missions in terms of planet detection statistics, we focus on the subset of all detected planets that are *newly* detected from each extended mission. These may come from stars that were not observed at all in the primary mission (notably for scenarios such as `elong`), or they may also come from transiting planets that were observed in the primary mission with SNR $<$ 7.3, or from planets that were single-transiters in the primary mission (we require $N_{\rm tra} \geq 2$) for detection. With this in mind, for each extended mission scenario we ask the following questions:

1. $N_{\rm new}$: How many new planets do we detect?

2. $N_{\rm new,P>20d}$: How many of these new planets are at long orbital periods, for instance $P > 20$ days?

3. $N_{\rm new,HZ}$: How many are in the habitable zone?

4. $N_{\rm sys,extra\ planets}$: In how many systems do we find extra planets?

5. $N_{\rm new,atm}$: How many new planets do we find that are amenable to atmospheric characterization (defined below by Eq. 3)?

	nhemi-ps	npole-ps	shemiAvoid-ps	elong-ps	eshort-ps	hemis14d-ps
$N_{\rm uniq}$	2051	2219	2051	2114	2127	2130
$N_{\rm new}$	499	616	482	530	472	584
$N_{\rm pri}$	1544	1543	1547	1557	1552	1543
$N_{\rm new,P>20d}$	137	153	119	118	108	176
$N_{\rm pri,P>20d}$	214	210	213	216	215	216
$N_{\rm new,HZ}$	102	108	101	95	94	128
$N_{\rm pri,HZ}$	196	201	200	208	202	200
$N_{\rm sys,extra\ planets}$	62	54	59	38	53	82
$N_{\rm new,atm}$	11	7	19	19	21	17
$N_{\rm pri,atm}$	97	102	100	99	104	98
$N_{\rm new,new\ stars}$	29	37	70	193	110	20
$N_{\rm new,SNR\vee N_{tra}}$	471	580	411	337	362	564

	nhemi-ffi	npole-ffi	shemiAvoid-ffi	elong-ffi	eshort-ffi	hemis14d-ffi
$N_{\rm uniq}$	1716	1682	1762	1558	1574	1776
$N_{\rm new}$	785	803	846	639	744	849
$N_{\rm pri}$	940	939	938	947	933	931
$N_{\rm new,P>20d}$	116	122	114	89	110	128
$N_{\rm pri,P>20d}$	80	82	80	80	83	80
$N_{\rm new,HZ}$	20	16	21	12	25	18
$N_{\rm pri,HZ}$	9	8	9	9	8	9
$N_{\rm sys,extra\ planets}$	9	7	9	5	7	10
$N_{\rm new,atm}$	3	1	5	2	2	5
$N_{\rm pri,atm}$	7	7	7	7	7	6
$N_{\rm new,new\ stars}$	35	56	90	173	61	22
$N_{\rm new,SNR\vee N_{tra}}$	750	747	755	466	682	827

	nhemi-both	npole-both	shemiAvoid-both	elong-both	eshort-both	hemis14d-both
$N_{\rm uniq}$	3767	3901	3813	3672	3701	3907
$N_{\rm new}$	1284	1419	1327	1169	1216	1433
$N_{\rm pri}$	2483	2482	2486	2504	2485	2474
$N_{\rm new,P>20d}$	253	275	234	207	218	304
$N_{\rm pri,P>20d}$	294	292	294	296	298	296
$N_{\rm new,HZ}$	122	124	122	107	120	146
$N_{\rm pri,HZ}$	205	210	209	217	210	208
$N_{\rm sys,extra\ planets}$	71	65	67	44	61	92
$N_{\rm new,atm}$	14	8	24	21	23	22
$N_{\rm pri,atm}$	104	108	107	106	112	104
$N_{\rm new,new\ stars}$	63	92	161	366	171	42
$N_{\rm new,SNR\vee N_{tra}}$	1220	1327	1167	803	1045	1390

Figure 14: Detected planet metrics for six possible extended missions (values are means of 50 Monte Carlo realizations of our calculation, all for $R_p < 4R_\oplus$). *Top:* postage stamp detections, *Middle:* full frame image only detections, *Bottom:* sum of both. The best two scenarios for select statistics are highlighted in green.

$N_{\rm uniq}$: number of unique planets detected over all 3 years. $N_{\rm new}$: number of planets detected in year 3 that were not detected in years 1&2 (newly detected planets). $N_{\rm pri}$: number of planets detected in the primary mission (years 1&2). $N_{\rm new,P>20d}$: number of newly detected planets with orbital periods greater than 20 days. $N_{\rm pri,P>20d}$: same as previous, but from the primary mission. $N_{\rm new,HZ}$: number of newly detected planets satisfying $0.2 < S/S_\oplus < 2.0$ (approximate habitable zone). $N_{\rm pri,HZ}$: same as previous, from the primary mission. $N_{\rm sys,extra\ planets}$: number of systems in which extra planets are detected. $N_{\rm new,atm}$: number of newly detected planets with SNR in transmission greater than (that of GJ 1214b)/2, as measured by *JWST* – see text. $N_{\rm pri,atm}$: same as previous, from primary mission. $N_{\rm new,new\ stars}$: number of newly detected planets that orbit stars that were not observed during the primary mission. $N_{\rm new,SNR\vee N_{tra}}$: number of newly detected planets that were observed during the primary mission, but either (a) which had SNR < 7.3, a non-detection and/or (b) had $N_{\rm tra} < 2$, and so would not be 'detected'.

6. $N_{\rm new,new\ stars}$: How many of the new planets come from stars that were not observed in the primary mission, vs.

7. $N_{\rm new,SNR\vee N_{tra}}$ stars that were observed, but either did not have enough transits or a high enough SNR to result in a detection.

For each extended mission, we compare these numbers to their counterparts from the primary mission as well as to all the other extended missions. We compare them to their primary mission counterparts in order to assess the overall value of a given metric: suppose that the primary mission detects 2000 planets, Extended Mission A detects 200 new planets, and Extended Mission B detects 100. Although case A gives twice as many new planets as case B, the more notable fact is that both are paltry compared to the primary mission. In that case, it would likely be sensible for *TESS* to focus on something other than detecting new planets in bulk.

We show the results of our simulations in Fig. 14. The first point to notice is that for all but one of the new planet detection metrics ($N_{\rm new}$, $N_{\rm new,P>20d}$, $N_{\rm new,HZ}$, $N_{\rm sys,extra\ planets}$, $N_{\rm new,atm}$, $N_{\rm new,SNR\vee N_{tra}}$) the yields between extended missions vary by less than a factor of two. The exception is in $N_{\rm new,new\ stars}$, in which `elong` detects roughly twice as many planets orbiting never-before-observed stars as any other proposed mission.

The second point is on the absolute yields of new planets: postage stamp observations find $\mathcal{O}(500)$ new planets, relative to the primary mission's $\mathcal{O}(1500)$. Full frame image observations find $\mathcal{O}(800)$ new planets, relative to the primary mission's $\mathcal{O}(900)$. All extended missions find $\mathcal{O}(1300)$ new planets, relative to the primary mission's $\mathcal{O}(2500)$. We discuss these results – the rough invariance of the number of new planets to different pointing scenarios, and the essential contribution of FFIs – further in point #1 below.

Skimming the bottom panel for which missions are highlighted in green when accounting for both PSs and FFIs, we see that `npole` and `hemis14d` are the 'superlative-winning' missions in terms of detected planet statistics: considering both PSs and FFIs, `npole` places top-2 in 5 of 8 relevant categories, and `hemis14d` does the same in 6 of 8. They both do well at maximizing the number of newly detected planets, while also performing well at detecting long period planets, and thus planets in their stars' habitable zones. `hemis14d` also has the largest number of systems in which extra planets are detected.

We now discuss each metric in more depth:

1. $N_{\rm new}$: we detect about as many new planets in Year 3 as we detect planets in either Years 1 or 2: roughly 1250. The worst and the best scenarios (`elong` and `hemis14d`, respectively) differ only by a factor of 1.2. The fact that there are so many new planets to be detected from extended observations, particularly from full frame images, and that the absolute number of new planets is roughly invariant to the spacecraft's pointing, can be understood from Fig. 15. This figure shows what was originally noted in S+15: *TESS*'s original survey is incomplete. There are a substantial number of planets just below the detection threshold, predominantly with $2R_\oplus < R_p < 4R_\oplus$ (cf. Fig. 10). An extended mission will enable their detection, irrespective of where on the sky we observe! This result should hold equally well for realistic detection efficiency thresholds, and it is demonstrates that extended observations will be valuable, because *TESS* will not yet be at the point of diminishing returns for longer observations (which will happen when more observations only allow pushing out to longer orbital periods). There will still be small, short-period candidates to discover after

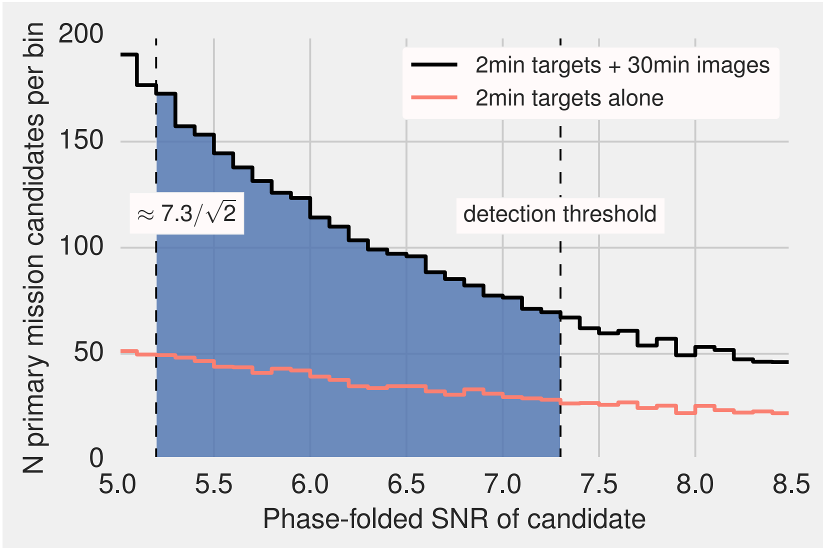

Figure 15: Histogram of phase-folded SNRs for candidate $R_p < 4R_\oplus$ planets following the primary mission (from both PS and FFI observations; values are means of 20 Monte Carlo trials). If an extended mission observes half of the sky, it roughly doubles the number of observed transits for half of the planets observed in the primary mission, enabling detection of $\approx 2316/2 = 1158$ planets (half of the blue integrated area in the plot). This coarse estimate is a similar result to our detailed calculations, and shows the value of continuing *TESS*'s observations *irrespective of where we observe.*

TESS's primary mission.

2. $N_{\mathrm{new,P>20d}}$: it will be possible to detect as many new $P > 20$ day planets in one year of *TESS*'s extended mission as in both years of the primary mission. The primary mission detects about 295 such planets; `hemis14d` and `npole` scenarios detect similar amounts. These two scenarios are achieving the goal of long-period planet detection in slightly different ways: `npole` maximizes the average observing baseline per star, while `hemis14d` observes the greatest possible number of stars for longer than 40 days. The latter approach could succeed at detecting many planets (our result is that `hemis14d` detects the most $P > 20$day planets), but it relies heavily upon the assumption that we can detect planets from only two transits over the course of the entire mission, even if this means only one transit in the primary, and one transit in the extended.

   This point – that the ability of the `hemis14d` scenario to detect many long period planets is grounded on the assumption that two transits at high enough SNR are sufficient for detection – is made explicit in the right panel of Fig. 16. About half of the long period planets that `hemis14d` finds are detected with only two transits. By way of comparison, `npole` detects most of its long-period planets with ≥ 4 transits. This means that the `npole` detections are more secure. Two-transit detections, especially those separated by a gap of a year or more in the *TESS* data, will be tenuous; *Kepler* searches showed that requiring 3 or more self-consistent transits

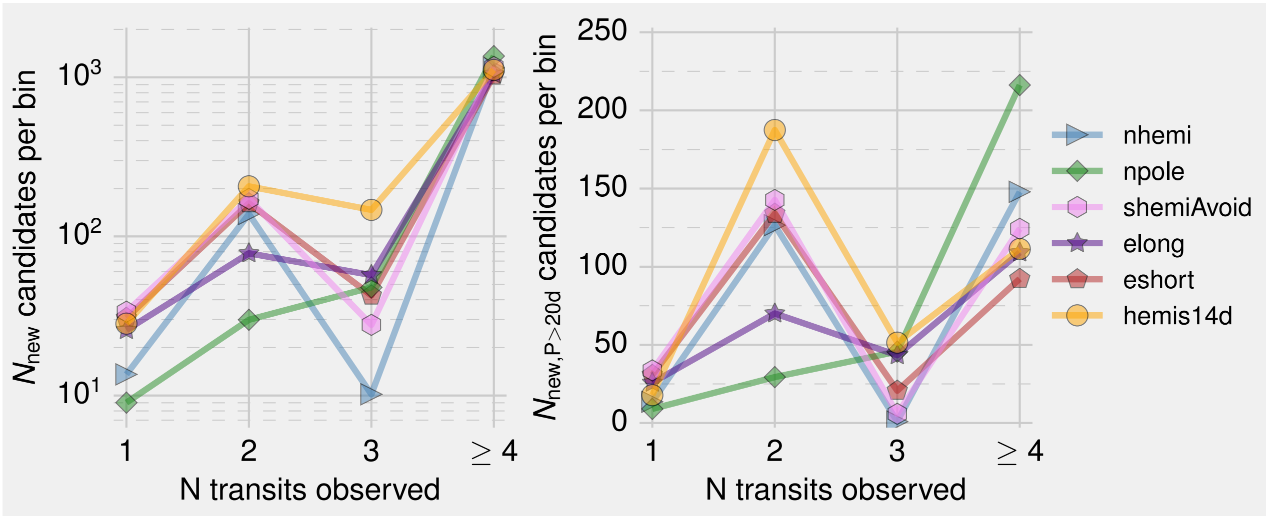

Figure 16: *Left:* Histogram of new $R_p < 4R_\oplus$ planet candidates from each extended mission as a function of the number of observed transits. Candidates are 'detected' in Fig. 14 if $N_{\mathrm{tra}} \geq 2$. *Right:* Same as left, restricted to $P > 20$ day planets. If any given scenario has a 'bump' at 2 observed transits, then that scenario depends more heavily on our assumption of being able to make detections based on only two transits. Lines between points have no physical meaning; they are intended to improve readability.

substantially lowers the fraction of false signals [Burke et al., 2014]. In cases with a relatively high SNR per transit it is possible to confirm candidates, but with less certainty than if we had more transits in the first place.

3. $N_{\mathrm{new,HZ}}$: we approximate the habitable zone as the geometric shell around a host star in which a planet's insolation satisfies $0.2 > S/S_\oplus > 2.0$ With this approximation, the `hemis14d` scenario finds the most new habitable zone planets: 146 (which is subject to the same caveats discussed above for long period planet detections). The next-best scenarios, `npole`, `nhemi` and `shemiAvoid`, all detect around 120. Relative to the primary mission's 210 detections, this means extended missions boost the number of detected habitable zone planets by a factor of ~ 1.6. For purposes of weighing the value of habitable-zone detections in deciding between missions, the result that these scenarios all detect a similar number of planets indicates that this metric will likely not 'tip the scales' in any direction.

We note in passing that $\sim$ 80% of the habitable zone planets that *TESS* detects orbit M dwarfs with spectral classes ranging from M4 - M0, and $\sim$ 15% of them orbit M dwarfs later than M4. We show this quantitatively in Fig. 18. Additionally, our values for the number of $0.2 < S/S_\oplus < 2$ planets from the primary mission are slightly revised from those of S+15: while S+15 quote 48 ± 7 $0.2 < S/S_\oplus < 2$ and $R_p < 2R_\oplus$ planets, we find 34 ± 5. Adopting the habitable zone of Kopparapu et al. [2013], S+15 quoted 14 ± 4 $R_p < 2R_\oplus$ planets. We find 11 ± 3. The rule of thumb that

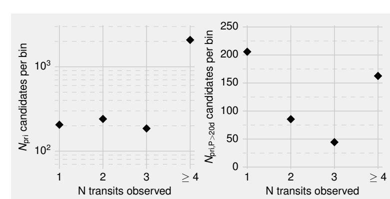

Figure 17: Similar to Fig. 16, but for the primary mission.

extended missions give roughly $1.6\times$ the number of new $0.2 < S/S_\oplus < 2$ habitable zone planets applies to the Kopparapu et al. [2013] habitable zone as well as $0.2 < S/S_\oplus < 2.0$. Another result shown in Fig. 19 is that the Kopparapu et al. [2013] habitable zone, which is physically motivated by 1-D radiative-convective cloud-free climate models with accurate absorption coefficients, results in roughly 3 times fewer 'habitable zone' planet detections than our ad-hoc criteria of $0.2 < S/S_\oplus < 2$.

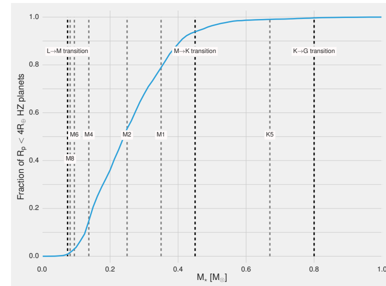

Figure 18: Cumulative distribution of $R_p < 4R_\oplus$ and $0.2 < S/S_\oplus < 2$ planet candidates from the primary mission (a proxy for the habitable zone). Boundaries of spectral classes are highly approximate, and taken from from Habets and Heintze [1981] and Baraffe and Chabrier [1996].

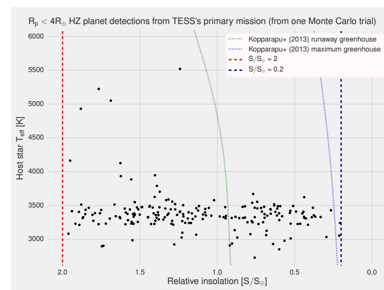

Figure 19: Scatter plot of $R_p < 4R_\oplus$ planet candidates falling in the S+15 or Kopparapu et al. [2013] habitable zones.

4. $N_{\text{sys,extra planets}}$: for how many systems do we detect extra planets? Our assumptions about multiple planet system distributions are coarse – we assume independent probability draws from single planet occurrence distributions. Thus our simulated planet population does not have systems of tightly packed inner planets. That said, we expect this statistic to be some indication of the information that we are not explicitly modeling, but which can be obtained from extended observations of planetary systems post-planet detection. This additional information includes improved precision on physical and dynamical parameters of the system. It also includes transit timing variations, which could be used to discover non-transiting planets as well as transiting outer companions. TTVs can also give dynamical hints for the formation history of planetary systems, for instance, discriminating between *in situ* formation and inward migration as Mills et al. [2016] argued for the Kepler 223 system.

   With our somewhat nebulous hopes for this metric stated, the most prominent feature in its results is that `elong` detects the fewest systems with extra planets (44, which is 39% worse than the next-best). This is reasonable because `elong` spends the most time looking at new sky, and in the process observes fewer systems that were detected in the primary mission. `nhemi`, `shemiAvoid`, `npole`, and `eshort` all perform similarly, detecting $\sim$ 65 such planets. `hemis14d` detects the most, at 92. While this is still subject to the assumption of two-transit recoverability, in this case the requirement is not too strong: only 10 of `hemis14d`'s systems with newly detected planets come from the case where the extra detected planet comes from two transits.

5. $N_{\text{new,atm}}$: We define 'planets that are amenable to atmospheric characterization' to mean planets whose SNR in transmission is greater than (that of GJ 1214b divided by 2), where the latter factor of 2 gives us a sufficiently large sample to prevent Poisson fluctuations from hindering our comparisons. The relevant signal in transit spectroscopy is the ratio of the areas of atmosphere's annulus to the star's disk on the sky plane, $\delta_{\text{atm}} = 2\pi R_p h_{\text{eff}}/(\pi R_\star^2)$,

where the effective scale height of the atmosphere $h_{\rm eff}$ is proportional to the actual scale height. Assuming that the planet is in thermal equilibrium with incident radiation from the host star, and that its atmosphere has known mean molecular weight and Bond albedo, we can compute a representative signal. The noise performance depends on the observing instrument, and could be complex if not simply dominated by shot-noise from IR photons. We circumvent such complexities via an empirical formula provided to us by Drake Deming, based on a multi-variate regression fit to detailed simulations performed by Dana Louie. This formula estimates the SNR in transmission from 4 transits observed with *JWST*'s NIRISS instrument:

$$\begin{aligned}\log_{10}\mathrm{SNR} = {} & 2.98\log_{10}\left(\frac{R_p}{R_\oplus}\right) - 1.019\log_{10}\left(\frac{M_p}{M_\oplus}\right) \\ & - 1.459\log_{10}\left(\frac{R_\star}{R_\odot}\right) - 0.249\log_{10}\left(\frac{a}{\mathrm{AU}}\right) \\ & - 0.147\,(V-5.0) + 0.193 \end{aligned} \tag{3}$$

for V the host star's apparent V-band magnitude (calibrated for $3 > V > 22$), R_p the planet radius, M_p the planet mass, $R_\star$ the star radius, and a the planet's semi-major axis.

Is this NIRISS SOSS mode? Why would you use V band and not like... I, or something redder like K?

The coefficients are physically sensible: the 2.98 coefficient of R_p minus the 1.019 coefficient of M_p implies that the SNR depends inversely as bulk density, with puffier planets giving higher SNR for transit spectroscopy. Focusing our analysis to a *JWST* -measured SNR is sensible given *TESS*'s role as a '*JWST* finder scope' [Deming et al., 2009]. We focus specifically on NIRISS given that it will likely be the workhorse *JWST* instrument for transmission spectroscopy [Beichman et al., 2014].

Reference parameters for GJ 1214b are taken from Charbonneau et al. [2009]: $R_p = 2.678R_\oplus$, $M_p = 6.55M_\oplus$, $R_\star = 0.211R_\odot$, $a = 0.0144\mathrm{AU}$, $V = 15.1$. Using Eq. 3, we compute the SNR in transmission for all detected planets, for all extended mission scenarios. Fig. 20 shows one realization of the resulting distribution for planets detected in all three years of the `nhemi` scenario.

TESS mostly detects strongly irradiated planets (most points on Fig. 20 are yellow). A very small number, $\lesssim 10$, are both in the approximate habitable zone and also 'favorable for atmospheric characterization'. Of course, a highly compelling target with lower SNR in transmission per transit might merit a more ambitious

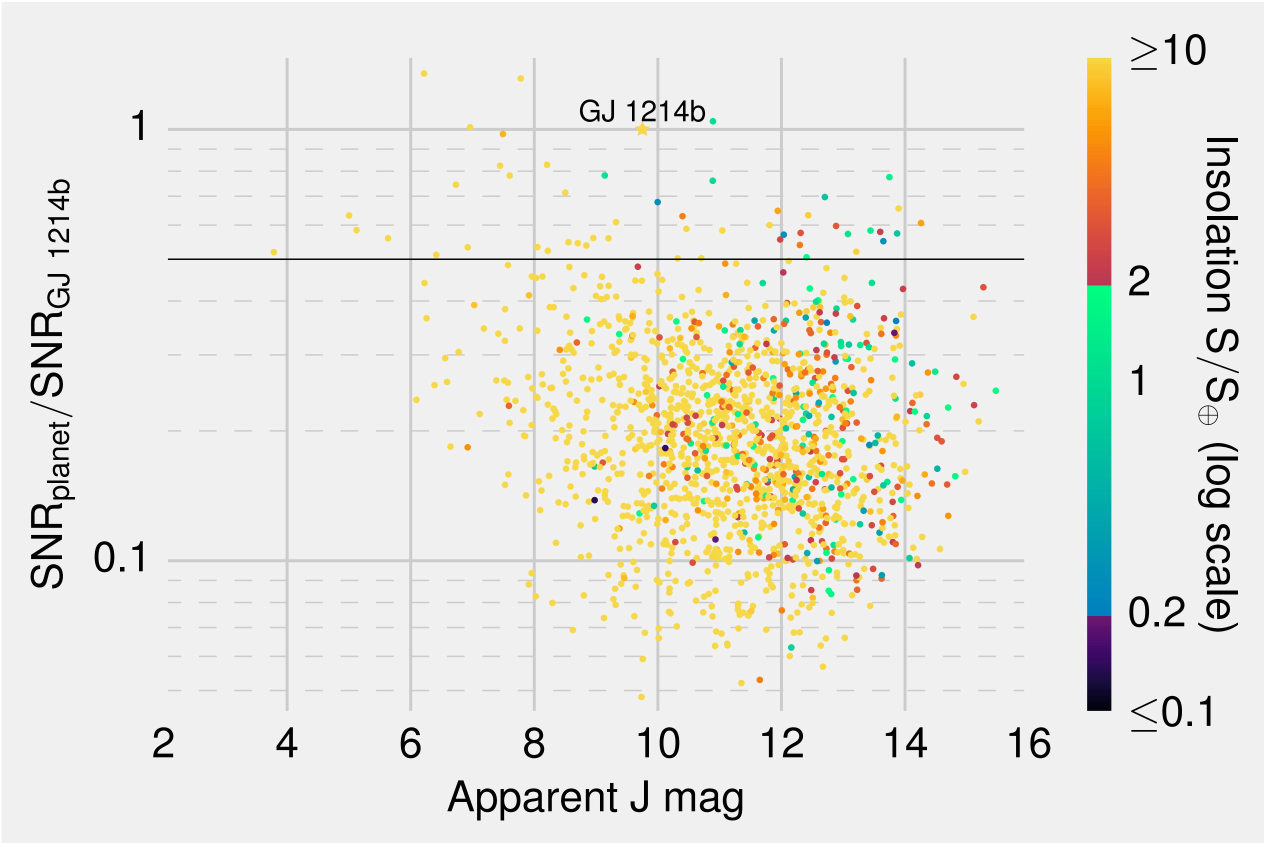

Figure 20: Scatter plot showing the SNR in transmission of detected planets with $R_p < 4R_\oplus$ from one Monte Carlo realization of all 3 years of the `nhemi` scenario. The SNR is computed from Eq. 3. Planets above the horizontal black line ($\mathrm{SNR}_{\mathrm{planet}}/\mathrm{SNR}_{\mathrm{GJ\ 1214b}} = 0.5$) are counted for Fig. 14's metric of planets with 'good' atmospheres for transmission spectroscopy. GJ 1214b is marked with a star. The coloring of planets indicates their relative insolation, as well as whether they fall our ad-hoc habitable zone ($0.2 < S/S_\oplus < 2$).

JWST observing program. We note that all of these planets are assumed to have identical mean molecular weights and cloud properties.

More importantly, Fig. 14 shows that most of the planets with 'good' atmospheres have already been discovered after two years. The best extended missions (`shemiAvoid`, `elong`, `eshort` and `hemis14d`) boost the yield of such planets from ~ 100 to ~ 125. The worst, `npole`, finds roughly 10. This best-case boost of $1.25\times$ more 'good' planets for atmospheric characterization is less than the relative boost of $1.6\times$ more newly detected long period planets. This latter point simply means that if we were to assign equal weights to both relative metrics, then $N_{\mathrm{new,atm}}$ would impact the decision of which extended mission to perform less than $N_{\mathrm{new,P<20d}}$.

6. $N_{\mathrm{new,new\ stars}}$: The observing strategy that collects the most photons from new stars should detect the most new planets about new stars. The `elong` scenario dedicates 7 of a single year's 13 observing sectors to the ecliptic (where the other 5 are spent centered at

the North Ecliptic Pole due to excessive Earth/Moon crossings). It consequently detects twice as many new planets about newly observed stars as the next-best scenarios: `eshort` and `shemiAvoid` (366 vs 171 and 161, respectively). These latter two options also spend time observing the ecliptic, but with only one camera, rather than with all four cameras simultaneously. We note that even though `elong` is the scenario most prone to detecting planets about new stars, only $\sim 30\%$ of its newly detected planets are actually from 'never-observed' hosts. [11]

[11] Dubbing these planets and hosts 'never-observed' neglects the question of overlapping fields with K2's observations (see discussion in Sec. **??**)

7. $N_{\mathrm{new,SNR} \vee \mathrm{N_{tra}}}$: This statistic is the number of newly detected planets that are detected either (a) due to their final SNR clearing our threshold (logical) or (b) their number of observed transits being greater than or equal to 2. It is the complement to $N_{\mathrm{new,new\ stars}}$: scenarios like `nhemi`, `npole`, and `hemis14d` that do not observe many new stars will detect all of their planets from a boosted SNR and/or clearing the minimum transit threshold.

Comment on meaning of 'detected in postage stamps' vs 'detected in FFIs' The invested reader may inquire "what about the cross-over case of planets that are observed as PSs during the primary (extended) mission, but as FFIs in the extended (primary) mission? These are not explicitly listed in Fig. 14". When describing the entire unique planet population detected from Years 1-3, for simplicity of language we use 'postage stamp detections' to refer to planets that are observed at any time (primary or extended missions) at 2 minute cadence. In these cases, the dominant contribution to the final signal to noise ratio tends to come from the PS observations. When describing new planet detections, we use 'postage stamp detections' to mean planets that were newly detected due to being observed as postage stamps in the extended mission. In other words, this 'cross-over' point only matters in discussions of the unique planet population from an entire mission, Years 1-3. Considering just the newly detected planet population, we can unambiguously specify whether the new detections came from full frame images or postage stamps, irrespective of their observations from the primary mission.

4.4 *On the brightness of detected stars.*

While `npole` does well by most metrics, a larger proportion of its newly detected planets orbit dim stars than the planet populations detected from alternatives like `hemis14d` or `shemiAvoid`. We demonstrate this in Fig. 21. The main point here is that if in mission selection we were to assign extra weight towards detecting planets orbiting bright host stars, then `npole` would do the worst. For instance,

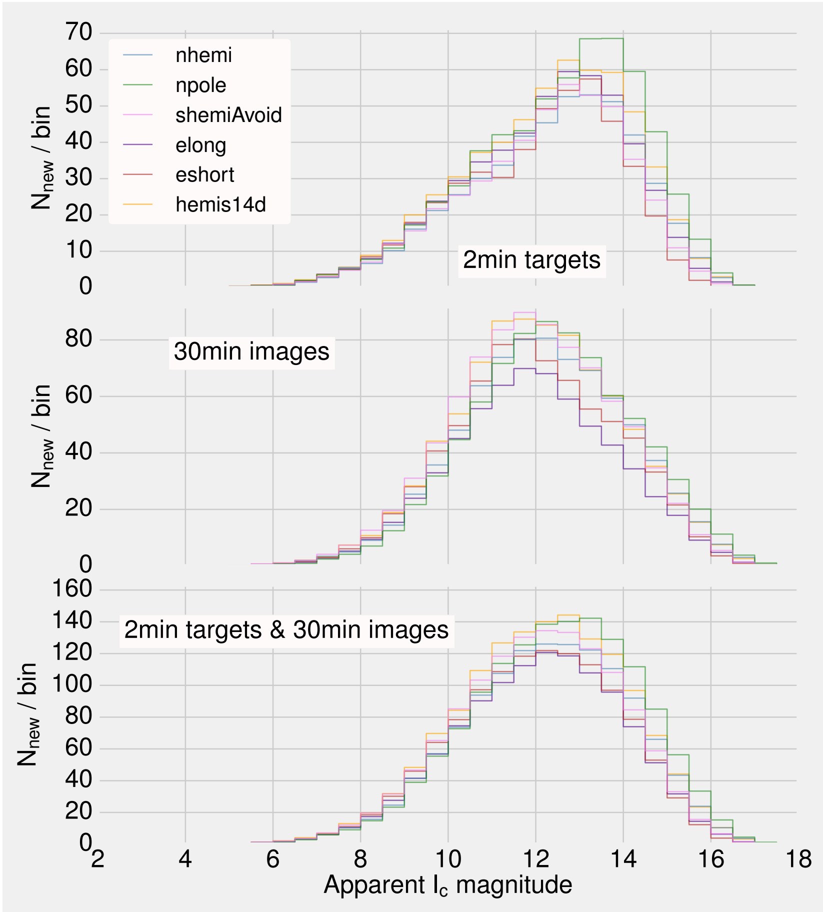

Figure 21: Histogram of apparent I_c magnitude of host star for newly detected $R_p < 4R_\oplus$ planets from all extended mission scenarios, for *top:* postage stamp detections, *middle:* full frame image detections, *bottom:* the sums thereof. While `npole` does well by most metrics, a larger proportion of the new planets it detects orbit dim stars compared to alternatives like `hemis14d` or `shemiAvoid`.

nhemi	npole	shemiAvoid	elong	eshort	hemis14d
162	154	190	167	183	198

Table 2: Number of new, $I_c < 10$, $R_p < 4R_\oplus$ planets from each extended mission (average of 50 Monte Carlo realizations of our code; showing sum of PSs & FFIs). `npole` detects the fewest new planets orbiting bright stars.

arbitrarily setting the bound at $I_c < 10$ and numerically integrating from Fig. 21's data, we see in Table. 2 that there is a $\sim 30\%$ level difference between the missions. For point of reference, the primary mission detects 386 such planets – so a single year of extended mission detects roughly as many planets orbiting bright hosts as a single year of primary mission.

5 *Broader science beyond exoplanet detection statistics*

Observing with *TESS* for more than two years could lead to more than just the new planet detections that we quantified in Sec. 4. An extended mission offers the chance to re-examine our top-level priorities. We record and in some cases provide order of magnitude estimates for desires and opportunities that do not fall under the purview of 'planet detection statistics' in what follows. In Sec. 5.1, we discuss metrics related to exoplanet science beyond *TESS*'s primary aim of finding of small planets transiting bright stars. We then highlight observations that *TESS* could perform for their implications in broader astrophysics, in particular stellar physics, solar system science, and time-domain astronomy (Sec. 5.2). The main reason to discuss these broader desires is that they may play a role in influencing *TESS*'s long term observing strategy. This section focuses entirely on observations that *TESS* can perform by itself. The next section (Sec. 6) points out opportunities in which *TESS* data could be combined with other datasets and facilities.

5.1 *Broader exoplanet science*

Ephemeris times: analytic motivation If we want to know which extended mission scenario detects the most transiting planets, our yield statistics are directly applicable. However, detection is a bare-minimum: we would also like to know when *TESS* planets transit long into the future. For a planet with a "stale" ephemeris, follow up observations are more than just inconvenient. Freshening ephemerides very probably will be a requirement before devoting significant observational resources like *JWST* to a transiting planet. Also, if the ephemeris gets very stale, we know that the star is transited but have essentially no idea when. For RV follow-up, a stale transit ephemeris will add uncertainty (or systematic bias) to the planetary mass estimate, because especially for low-mass planets, the predicted transit times are usually an important constraint of the orbital fit to the RVs.

Consider then the problem of estimating $\sigma_{t_c}(T_x)$, the uncertainty of the mid-transit time σ_{t_c} for a given planet at some time T_x following its last-observed transit. We begin analytically: assume that the planet has $N_{\rm tra} = 2$ observed transits, spaced an orbital period $P = 14$ days apart. Because that period is one half the nominal *TESS* dwell time of a given pointing, it represents the shortest period for which typically $N_{\rm tra} = 2$, and as such the worst-case scenario for predicting the times of future transits, amongst cases with $N_{\rm tra} > 1$. Given two mid-transit times, each measured with the time's uncertainty σ_0, separated by P, the uncertainty of a future mid-transit time can be derived by standard least-squares fitting and propagation of errors (*e.g.* Lyons [1991], Equation 2.18):

$$\sigma_{t_c}(T_x) = \sigma_0\sqrt{1 + 2T_x/P + 2(T_x/P)^2} \tag{4}$$

Note that for observing future transits, $E \equiv T_x/P$ is an integer, and the above equation can be re-expressed:

$$\sigma_{t_c}(E) = \sigma_0\sqrt{1+2E+2E^2}, \tag{5}$$

which is bounded by the simpler approximation:

$$\sigma_{t_c}(E) \lesssim \sigma_0\left(1+\sqrt{2}E\right), \tag{6}$$

which is exact at $E = 0$, has a maximum 8% fractional error at $E = 1$, and becomes increasingly accurate as E increases. By $E = 20$, the fractional error of the latter approximation is less than 1%.

For $T_x = 2$ years and $P = 2$ weeks, then $E \approx 50$, so $\sigma_{t_c} \approx 75\sigma_0$. At 2-minute cadence, a typical value for the per-transit timing uncertainty is $\sigma_0 = 4$ minutes, and the predicted uncertainty on its mid-transit time is 5 hours two years later or 10 hours four years later. This leads to a simple rule of thumb:

> The uncertainty of mid-transit times in hours is twice the number of years after *TESS* observes $N_{\rm tra} = 2$ transits, for a typical super-Earth detection.

If the transits are observed only at 30-minute cadence, then uncertainty will be roughly 4 times greater: $\sigma_0 \sim 16$ minutes. This claim ("4× greater") is based on Figure 9 of [Price and Rogers, 2014], a plot of the effects of finite cadence on timing precision. We compared the precisions of 2-min and 30-min cadences for their specific example of $P = 10$ days and a dwell time of 1 month.

On the other hand, Fig. 17 shows that 7 in 8 of the planets detected by *TESS*'s main mission will have $N_{\rm tra} > 3$ and so their ephemerides should be better than the example derived analytically above. Rather than generalize the analytic equations, we resort to numerical simulations in order to predict the uncertainties of mid-transit times for planets expected to be discovered by *TESS*'s main mission.

Ephemeris times: numerics We start with the analytic form Price and Rogers [2014] derive for the per-transit uncertainty on the mid-transit time σ_0:

$$\sigma_0 = \frac{1}{Q}\sqrt{\frac{\tau T}{2}}\left(1-\frac{t}{3\tau}\right)^{-1/2}$$

when $\tau \geq t$ and

$$\sigma_0 = \frac{1}{Q}\sqrt{\frac{tT}{2}}\left(1-\frac{\tau}{3t}\right)^{-1/2} \tag{7}$$

when $t > \tau$, where Q is the SNR per transit, t is the cadence, T is the transit duration, and τ is the ingress (or egress) time. We have all the later terms from our yield simulation, and show the resulting distribution of σ_0 in Fig. 22. Indeed, our suggested σ_0 of about 4 minutes for postage stamps and 16 minutes for full frame images is

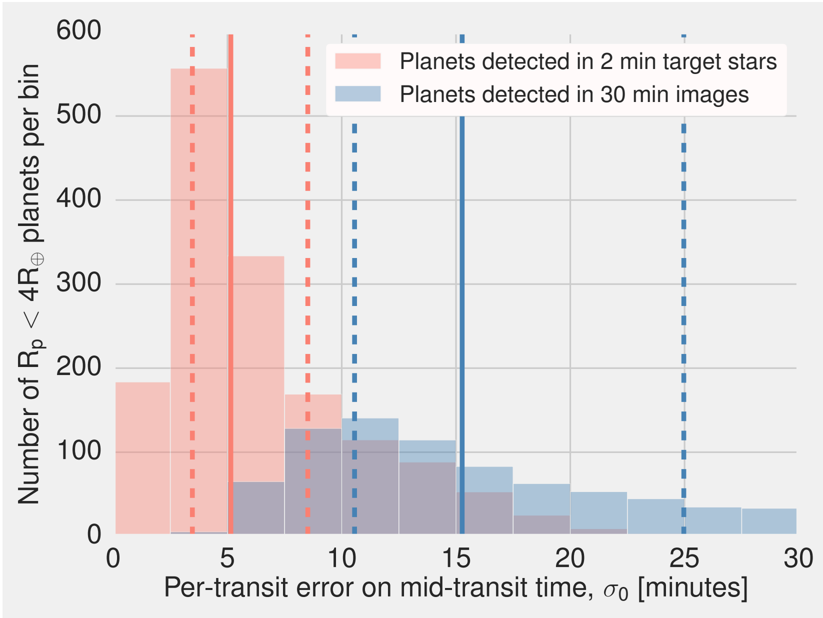

Figure 22: Uncertainty of mid-transit time on a single transit, σ_{t_c}, for all detected $R_p < 4R_\oplus$ planets from the primary mission as computed from Eq. 7. Solid lines are medians, dashed lines are 25$^{\text{th}}$ and 75$^{\text{th}}$ percentiles.

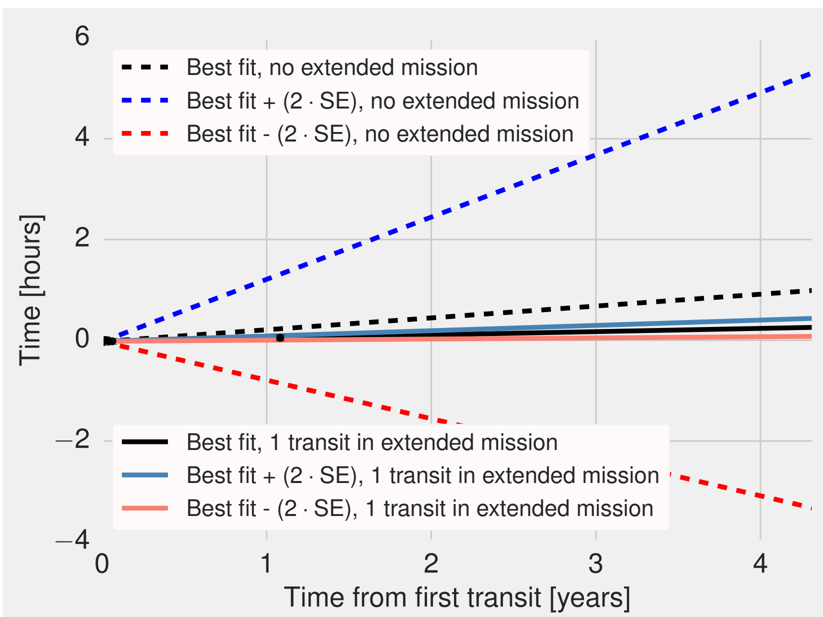

Figure 23: Observed mid-transit times (dots) and best fits to a linear ephemeris (lines). The dotted lines fit 4 data points from a nominal planet. 'SE' is the standard error on the slope which multiplied by 1.96 (rounded to 2 in the legend) gives a 95% confidence interval by subtracting blue and orange lines.

reasonable, which is good because we computed the former from the $t \to 0$ limit of Eq. 7 originally derived by Carter et al. [2008].

Given the distributions on per-transit uncertainty of t_c, we then took an example planet with 4 transits. We drew "observed" mid-transit times from a Gaussian with zero mean and standard deviation

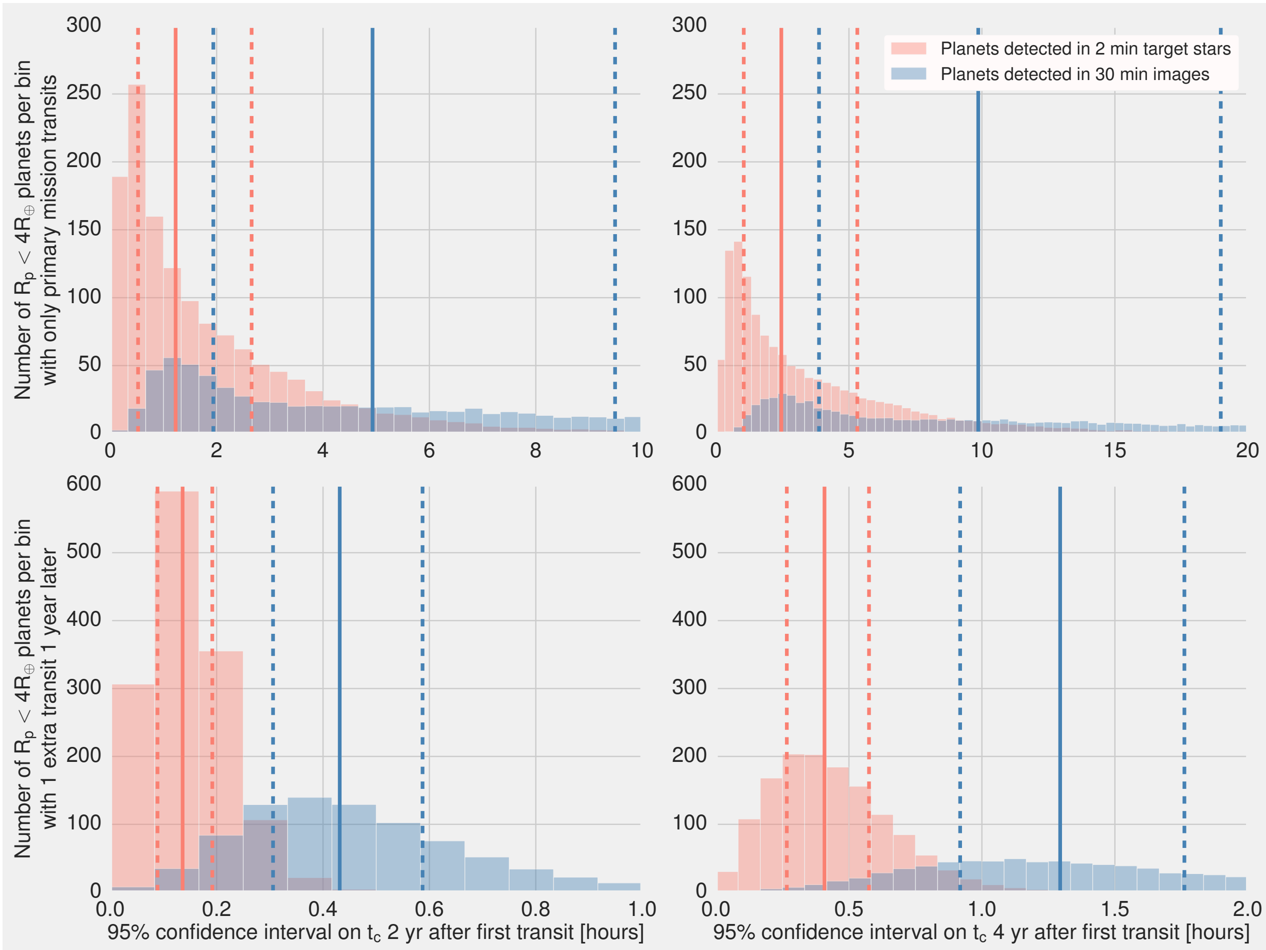

Figure 24: *Top row*: histogram of 95% confidence intervals 2 (*left*) and 4 (*right*) years following the first detected transit in the primary mission. 20 minute bins. *Bottom row*: histogram of 95% confidence intervals 2 (*left*) and 4 (*right*) years following the first detected transit in the primary mission, but with an additional data point added to the analog of Fig. 23 one year after the transit in the initial time series (5 minute bins). Note that the top row's timescale is an order of magnitude more than the bottom row. Solid lines are medians, dashed lines are 25$^{\text{th}}$ and 75$^{\text{th}}$ percentiles.

σ_0, and then ran a linear least squares regression. We then added just one data point 1 year after the final observed transit, and repeated the regression. This produces a cartoon-plot, Fig. 23, which confirms two expected points:

1. Years after the initial discovery, the uncertainty of mid-transit time is of order hours.

2. If we detect an additional transit 1 year after the final observed transit from the primary mission, the uncertainty on the mid-transit time decreases by an order of magnitude.

We proceed by repeating the above procedure for every planet, and evaluate typical 95% confidence intervals ("uncertainties", loosely) for t_c, at typical times after the first transits, for all of our detected planets. Specifically, we take them at $T_x = 2$ and 4 years, and get Fig. 24. This figure confirms (top left panel) our analytic expectation that the uncertainty of mid-transit times in hours should be somewhat less than twice the number of years after *TESS* first observes the planet at 2-min cadence, since most such planets have $N_{\mathrm{tra}} \geq 4$. It also confirms our rough expectation that the uncertainty on FFI mid-transit times is roughly 4 times that of postage stamps, although the uncertainties on FFIs have a much more uniform tail.

More importantly, Fig. 24 emphasizes the importance of refining *TESS*'s ephemerides: if we do not, the typical *TESS* planet will have many hours of uncertainty on its mid-transit time a few years following its detection. If we do follow-up, we will know when the planet transits to $\lesssim 1$ hour. This argues strongly for an extended mission which, whether over 1 or 2 years, re-observes many if not all of the targets that *TESS* detects in its primary mission. The smallest-radius Earths and super-Earths may otherwise be irrecoverable.

Observe more transits over a long baseline to enable TTV measurements
Variations in transit times away from a linear ephemeris can be combined with planetary and orbital information derived from transits *(a)* to confirm the planet-origin of transit signals and *(b)* to determine the masses and system properties, for example mutual inclinations, of transiting and non-transiting planets [Agol et al., 2005].

Our simulated dataset neglects orbital dynamics except to impose rule-of-thumb stability limits, assumes co-planarity between multiple planet systems, and assumes that multiple-planet system occurrence rates can be approximated as repeated draws from single-planet occurrence bins. In short, it is insufficient to reliably predict TTV-detectability. With that said, the best way to obtain useful TTV measurements is to observe as many high SNR transits as possible, over as long a baseline as possible. Many TTV signals have timescales greater than a few years and the information content in a TTV time series ideally scales as $t^{5/2}$ [Fabrycky et al., 2013]. Generally speaking then, the best extended mission scenario for measuring TTVs will include:

- Long baseline observations of the same field, for instance one of *TESS*'s continuous viewing zones.
- Observations of the *Kepler* field (for which measured transit times could resolve many TTV ambiguities from the 4-year dataset).

With these points in mind, `nhemi` and `npole` are likely the strongest scenarios for TTV detections over a single year's extended mission.

Targets beyond bright cool dwarf stars: *TESS*'s main targets for the purpose of detecting small planets around bright stars are F-M dwarfs.

Observing other types of objects can enable broader exoplanet science. For instance, we may wish to target:

- open cluster members,
- known hosts of circumbinary planets,
- evolved stars (notably bright subgiants and red-giants for which it will be possible to detect asteroseismic oscillations, see below),
- all stars that are known to host transiting planets,
- all stars that are suspected to host *any* planets (TOIs; KOIs from *Kepler* or *K2* ; candidates from *CoRoT* ; candidates and confirmed planets from ground-based transit and RV surveys),
- white dwarfs,
- hot bright stars (OBA class),
- cool dwarf stars with spectral classes from late-M to mid-L,
- stars with well-measured properties from existing catalogs,
- eclipsing binaries and other multiple-star systems.

Some of these categories, notably asteroseismic targets, open cluster members, cool dwarfs, and circumbinary planets, have existing working groups dedicated to selecting targets and studying the resulting data once *TESS* begins its primary mission. The *TESS* Target Star Selection team will incorporate target lists from these different working groups, while also incorporating many of the specific targets listed above[12] [Joshua Pepper, private communication]. Guest observer proposals will likely also lead to allocation of pixels for many targets beyond bright F-M dwarf stars.

[12] If the invested reader wishes to contribute to any of these lists, contact Joshua Pepper at joshua.pepper@lehigh.edu or Keivan Stassun at keivan.stassun@vanderbilt.edu

The relevance of all these objects to *TESS*'s extended mission is that 'observing time' (more precisely, data allocation) can be allotted differently between these targets in an extended mission than in the primary mission. For instance, the benefits of obtaining precise stellar parameters and probing stellar physics via asteroseismology might merit a greater share of the data mass than is being proportioned for the primary mission. The same could be argued for systems in which precise timing can greatly improve our ability to detect planets and characterize planetary systems.

We briefly highlight the cases for observing open clusters, circumbinary planets, asteroseismically-favorable targets, and stars with known or suspected planets below, and indicate which extended pointing scenarios we think will most benefit each observing program.

1. *Observing open clusters*. The main reasons to observe open clusters with *TESS* are (1) to discover planets in clusters (and then characterize them with other facilities) and (2) to perform stellar astrophysics relevant to exoplanets. Discovering planets in clusters will help determine their occurrence rate relative to field stars [Meibom et al., 2013]. This knowledge helps answer the question "how well can small planets form and survive in dense clusters?". In terms of stellar astrophysics, an open cluster surveys also enables measurements of stellar rotation periods as a function of age (gyrochronology), which can constrain age-rotation-activity relations. Such a survey could also be used to identify eclipsing binaries in order to quantify their tidal evolution as a function of age. Soren Meibom is leading *TESS*'s open cluster working group, which will construct lists of open cluster stars to be included in the *TESS* Candidate Target List.

   The majority of suitable open clusters with $V < 16$ are near the galactic disk, and they are more common in the southern ecliptic hemisphere (with a south:north ratio of $\sim 2:1$). While there are no known open clusters with $V < 16$ at the north ecliptic pole's continuous viewing zone, there are a handful in that of the south ecliptic pole. Consequently, an extended mission scenario that observes the southern hemisphere, whether through the southern-conjugates of `nhemi` and `npole`, or through a scenario like `shemiAvoid`, would be preferable for an open cluster survey. With that said, `npole` would observe ~ 70 open clusters with $V < 16$, all within $42^\circ < \beta < 68^\circ$.

2. *Circumbinary planets, circumprimary planets, and multiple star systems*. To date all ~11 known circumbinary planets (CBPs) transit and are located in the *Kepler* field. Previous work has shown a statistical dearth of CBPs orbiting short-period ($P_{\mathrm{bin}} < 3$ day) eclipsing binaries [Armstrong et al., 2014, Martin and Triaud, 2014b], and formation requirements on such circumbinary planet systems are stronger than for planets orbiting EBs in which the EB has a relatively longer orbital period [Martin et al., 2015].

   For order of magnitude purposes, consider two flavors of CBP detection from *TESS*'s primary mission: those that are detected with ≥ 3 transits, and those with ≤ 2 transits. Assume that transiting CBPs will be mostly detected about eclipsing binaries (no CBPs to date are known to orbit a non-transiting eclipsing binary, although such objects likely exist in *Kepler*'s dataset [Martin and Triaud, 2014a]). Given CBP orbital stability requirements, and the expectation that few CBPs will orbit $P_{\mathrm{bin}} < 3$ day eclipsing binaries, almost all of the $N_{\mathrm{tra}} \geq 3$ CBP detections should happen in

TESS's continuous viewing zones. Taking S+15's result that *TESS* will detect $\mathcal{O}(10^5)$ eclipsing binaries with $I < 13$, and the fact that *TESS*'s continuous viewing zones cover 2.2% of the sky (908 $\deg^2$), there will be roughly 2000 EBs observed from one year over the primary mission. To date, *Kepler*'s Eclipsing Binary Working group has identified 2878 eclipsing and ellipsoidal binary systems of the 200,000 stars observed in *Kepler*'s 115 $\deg^2$ field [Kirk et al., 2016]. This has led to ~15 CBPs that are confirmed or in the process of being verified – roughly a 0.5% detection probability. Applying the same detection probability to *TESS*'s CVZs, $\mathcal{O}(10)$ CBPs should be detected from 3 or more transits.

For purposes of detecting CBPs from ≤ 2 transits, single-conjunction two-transit events will likely contribute to a major proportion of *TESS*'s detections. Such events contain more information than single-star transits and can be used to make detections from a small number transits. For instance, they enabled the confirmation of Kepler 1647b, the CBP with the longest known orbital period [Kostov et al., 2015]. Roughly 5 out of 1000 *Kepler* EBs with $P_{\rm bin} < 30$ days had one-conjunction two-transit events [Haghighipour, private communication]. Applying the same probability to *TESS* EBs means $\sim$ 500 *TESS* EBs will have these events. Perhaps 10%-20% will lead to CBP detections – this means $\mathcal{O}(100)$ CBP detections from the *TESS* field outside of the CVZs.

How will this affect the extended mission? The relative priority of these two different detection techniques – robust CBP detections through $\geq$ 3 transits in fields observed for a long time, vs. weak detections from $\leq$ 2 transits in fields observed for shorter durations – merits further study. The former would advocate for a mission that maximizes the average observing time for all stars on a smaller sky area, for instance `npole`. If this overlapped with the *Kepler* field, this would also enable *TESS* to detect transits of a subset of the *Kepler* CBPs. However the latter approach would argue for simply repeating the primary mission (`nhemi`), or 'event catching' single-conjunction two-transit events as in `hemis14d`.

Considering circum*primary* planets, *TESS* should discover thousands of giant planets at orbital periods less than 10 days, predominantly in its full frame images, and with a heavy discovery bias towards the galactic disk (cf. Fig. 19 of S+15). Recent surveys have shown that roughly half of such hot Jupiter systems are expected to have stellar companions with semi-major axes between $50 - 2000$ AU [Ngo et al., 2016]. The population of circumprimary planets that *TESS* will detect should be dominated by these systems. There should be a sufficiently large sample of these planets for follow-up imaging with adaptive optics to obtain CPP statistics, regardless of the extended mission.

3. *Asteroseismic targets*. See 'Observing asteroseismic targets' paragraph in Sec. 5.2 below.

4. *Stars known or suspected to host transiting planets*. If we know that the geometry of an exoplanetary system allows transits, the geometric bias against transit detection is removed. We should observe these targets *(a)* to observe additional transits at precise times, enabling TTV searches, *(b)* to obtain more precise photometry and thus refined parameters on known transiters, and *(c)* in the case of ground-based detections, to observe companion transiting-planets that might not be detectable from the ground. We discuss the prospects of *TESS* observing *Kepler*'s transiting planets in Sec. 6.1. It will also be important to include the hosts of RV-detected planets in this sample. Although transit alignments are rare, combining transit and RV observables allows us to compute a planet's mean density, which is a necessary step towards detailed characterization.

   For purposes of influencing an extended mission, the main bias in the currently known population of transiting planets is the *Kepler* field. For an extended mission to follow up on the most currently-known transiting planets, it would be best target the northern ecliptic hemisphere, as in `npole` or `nhemi`.

5. *White dwarfs*. White dwarfs are scientifically interesting because of the window they offer into the long-term evolution of planetary systems. Their observational appeal for transit studies is that they have radii of $\mathcal{O}(R_\oplus)$, which means that transiting objects, whether planetary remnants (*e.g.*, [Vanderburg et al., 2015]), minor, or even major planets, produce large transit depths. However, the transit durations of major and minor planets are short ($T_{\rm dur} \sim R_\star/v_p$), and their transit probability is small ($\mathrm{prob(tra)} \sim R_\star/a$). To date, no planets are known to transit white dwarfs (Veras [2016] reviews the observational successes of the field along with this challenge).

   What this means for *TESS* is that a white dwarf survey would require short-cadence observations of many white dwarfs to overcome both the short transit durations and the low transit probability. While no group is currently advocating for this observing program, this may change by the time of an extended mission proposal.

We do not discuss the observing cases for hot bright stars, late-M to mid-L dwarf stars, eclipsing binaries, or stars with well-measured properties.

5.2 Broader science wants

Those which may or may not overlap with exoplanet science.

Observing asteroseismic targets In stellar physics, asteroseismology can reveal the interior properties of stars and inform theories of stellar evolution; in exoplanet science, it can provide accurate estimates of stellar parameters such as mass, radius, and age (Chaplin and Miglio [2013] give a broad review). Accurate stellar parameters mean accurate exoplanet parameters. Asteroseismic studies can also sometimes extract projected obliquities of exoplanet systems, as well as orbital eccentricities based on asteroseismic densities (see Huber [2015] for an overview).

Similar to *Kepler*, *TESS* will be able to detect solar-like oscillations for main sequence and red-giant stars. The *TESS* Asteroseismic Consortium (TASC) is compiling a list of asteroseismic targets that will be delivered to *TESS*'s Payload Operations Center[13] The expected data allocation for these targets is ~ 1000 stars at a cadence of 20 seconds and ~ 10000 at a cadence of 2 minutes. Short-cadence observations are essential for realizing *TESS*'s asteroseismic potential since the relevant p-mode oscillation periods are of order minutes for main-sequence stars, and hours for giant stars.

[13] The Payload Operations Center is a subset of the Science Operations Center, and is housed at MIT; the Science Operations Center also houses the Science Processing Operations Center. See Jenkins et al. [2016] for a who-does-what in the *TESS* project.

Campante et al. [2016] (hereafter, C+16) estimate the signal-to-noise ratio of solar-like oscillations in the power spectra of plausible targets to predict *TESS*'s asteroseismic yield. Considering the overlap of *TESS*'s asteroseismic and transit sensitivities, they find that *TESS* should detect solar-like oscillations in a few dozen F dwarfs and subgiants that also have *TESS*-detected transiting planets. They also consider *TESS*'s asteroseismic sensitivity with respect to the population of all known exoplanet-host stars found from transit and RV surveys. *TESS* will observe these targets at 2 minute cadence. For this latter sample, they predict detection of p-modes in over 300 solar type and red-giant planet-hosting stars – a three-fold improvement in the asteroseismic yield of exoplanet-host stars compared to *Kepler*'s.

Subgiants should be readily differentiated from similarly-colored M dwarfs following *Gaia*'s initial data releases [Perryman, 2002]; C+16 thus also advocate for the inclusion of subgiants for purposes of studying asteroseismic oscillations, based on the estimate that $\mathcal{O}(2000)$ subgiants could have detectable asteroseismic modes.

The relevance of all these points to extended *TESS* observations, as always, comes in the form of trade-offs. Firstly, the asteroseismic yield predictions estimated in C+16 are based on a test designed to resolve two important asteroseismic parameters: the frequency of the maximum oscillation amplitude $\nu_{\max}$ and the average splitting $\Delta\nu$ between neighboring overtones of the same spherical degree (l). These two parameters can be used to estimate stellar properties to $\lesssim 10\%$ precision, *e.g.,* [Aguirre et al., 2012], but multi-month datasets enable more precise and accurate measurements of the amplitudes and widths of oscillation-modes in main sequence stars. The extended mission trade-off for asteroseismology can be framed as quality *vs.* quantity: observing a smaller area of sky for a longer duration as in `npole` could enable more robust and varied asteroseismic detections. Repeating the primary mission as in `nhemi` could enable a greater number of weaker detections in bright stars. Covering more sky would also enable access to a broader target sample, for instance including many young open clusters to perform ensemble asteroseismology [Aerts et al., 2013].

All-sky variable targets: pulsating stars, eruptive stars, cataclysmic variables, rotating variables, eclipsing binaries *TESS* can obtain 0.01mag photometry over an hour's integration time for $I_c \lesssim 16$, and can achieve mmag photometry over the same binning for $I_c \lesssim 13$ (cf. Fig. 7). A cornucopia of variable sources can be observed at high precision with these magnitude thresholds. Uninterrupted, high quality *TESS* photometry for the brightest variable targets on the sky could provide new probes into the physical mechanisms of stellar pulsation phenomena, as well as improve the fidelity of standard candles. Szabo et al. [2013] give a compelling overview of the results that came from *Kepler*'s observations of dozens of RR Lyrae and a single Cepheid variable. The essential lesson: probing new regimes of precision brings about the discovery and explanation of new phenomena. The OGLE-III and IV campaigns have identified numerous variables stars in nearby galaxies as well as the in galactic bulge [Soszynski et al., 2009, 2010, 2011]. *TESS* could observe the brightest of these targets with photometry orders of magnitude more precise than has ever been done.

really? could *TESS* see these? theyd be totally blurred over the fat pixels

We recommend specifically for the *TESS* team to solicit experts in the subfield of variable-star astronomy to contribute their knowledge of these targets for *TESS*'s primary mission (perhaps in a working group; at least in Guest Observer proposals).

Beyond periodic variables, *TESS* could observe cataclysmic variables. Likely the most interesting of this class of events would be observing the earliest stages of Type Ia supernovae (SNe). Type Ia SNe are almost certainly thermonuclear explosions of carbon-oxygen white dwarfs, but it is unclear whether their runaway is triggered through accretion of material from another white dwarf, or from a non-degenerate companion. Observations with *Swift* have shown that at least some Ia SNe come from the non-degenerate companion case, but four supernovae observed with *Kepler* showed no signature of such companions [Cao et al., 2015, Olling et al., 2015]. Observations with *TESS* could resolve the question: as noted in pp.43-45 of STScI Science Definition Team [2016], a dedicated search of *TESS*'s full frame images could shift this subfield from having a few observational examples to a much larger population. This could provide inroads towards the decades-old SNe Ia progenitor question: "what rate from each channel?".

Any of the proposed extended mission pointing strategies would enable a SNe Ia search, although they would need to be coupled with ground-based follow-up given the $\gtrsim 1$ month timescales of SNe. For purposes of observing variable stars, the same claim holds: any proposed pointing strategy would work. In all cases, we also note the 'quality vs. quantity' trade-off: if the stars in a field are observed for longer (as in `npole`), the light curves of any given star of interest will have more information in them. However, there will be fewer such stars compared to a scenario that covers more sky in a given year (*e.g.*, `nhemi`). Another practical point is that many of the best-characterized fields for variable-star astronomy, notably the MACHO and OGLE fields, are near the South Ecliptic Pole, which will also have a large overlap with LSST and *Gaia*.

Solar system objects (TNOs, main belt asteroids) The use of space-based photometers for solar-system observations is just being realized. Szabó et al. [2015] noted that it is possible to identify main belt asteroids and sometimes extract their shapes and rotation periods from *K2* data. [Kiss et al., 2016] applied a similar approach to *K2* light curves and constrained the rotation period and asphericity of Nereid, Neptune's third-largest moon. These types of observations may be difficult to generalize for *TESS* because of its larger pixel size. The chief relevance of main-belt asteroids to extended missions in particular is that any fields that observe close to the ecliptic plane will be contaminated by them (along with major planets, and zodiacal background light). Assuming that the event rates are similar to the $\sim 1/2$ of targets that have at least one asteroid event over 90 days of *K2* observing [Szabó et al., 2015], *TESS*'s photometric reduction pipelines will need to take these effects into account.

Light curves from variable AGN Edelson et al. [2013] have an algorithm to identify ~4000 AGN candidates across the sky. Roughly 2% of these candidates (80 of them) could be observed in the 1-year

CVZ data from the primary mission. Any extended mission scenario will provide a reasonably-sized sample of them. That said, `hemis14d` would likely be the worst because of its 14-day window functions.

6 Discussion of risks and opportunities

This section begins to answer the question "what opportunities will extended mission *X* give?". Most of the following points entail considering *TESS* in its broader context, rather than focusing only on what the *TESS* instrument itself is capable of observing as we did in Sec. 5.

6.1 Opportunities

What's best on a >1 year horizon for planet detections? *TESS*'s orbit is stable for more than 1000 years [Gangestad et al., 2013]. While minor mechanical failures should be expected on the timescale of a few years, it is plausible that the spacecraft could outlive both the 2-year primary mission and the 1-year extended mission. It is therefore important to select a 1-year extended mission scenario that offers strong prospects for continued observing.

A simple point is that `nhemi`, `npole`, and `shemiAvoid` can all be inverted to their southern or northern complements for a fourth year of observing. This will yield a comparable number of new planets to what they find in year 3 ($\mathcal{O}(1300)$ with $R_p < 4R_\oplus$). This argues strongly to continue observing the entire sky, rather than focusing on a single ecliptic hemisphere after the primary mission's completion. This would continue *TESS*'s role as a planet-discovery machine, while also addressing the practical matter of refining ephemerides in order to enable detailed characterization with suitable instruments.

The `elong`, `eshort`, and `hemis14d` scenarios are less obviously extensible to multiple years. The main reasons to return to the ecliptic after performing `elong` or `eshort` would be to make *TESS*'s survey truly 'all-sky', and to complete all possible *K2* follow-up observations (see discussion below). Of course, this would need to happen during intervals in which the Moon and Earth were not in the way.

Any of our proposed scenarios could simply be repeated indefinitely (as could their two-year 'all-sky' versions). The main trade-off this presents becomes apparent comparing 2 years of `hemis14d` to repeating the primary mission over 2 years. If we repeat the primary mission over 2 years, the northern and southern CVZs each get 1 year of continuous observation. If we do `hemis14d` for 2 years, the northern and southern 'long viewing zones' each get 2 years of 14-day windowed observations. The latter case allows 2-transit detections of $P \lesssim 1$ year planets over 2% of the sky. The former allows 2-transit detections of $P \lesssim 6$ month planets over 1% of the sky. This simple consideration of course misses that point that data obtained from repeating the primary mission would be less subject aliasing issues and would have fewer period ambiguities. That said, repeating `hemis14d` for two years might be a middle ground between a strategy like "repeat `npole` indefinitely" and "repeat the primary mission indefinitely".

A longer-term question is "when will *TESS* hit the point of diminishing returns?" The 'low-hanging fruit' of small planets transiting bright stars at short orbital periods will eventually be found if *TESS* continues to observe the same sky. The most important qualitative point of this memo, made in Fig. 15, is that after *TESS*'s primary mission there will be many objects remaining for which merely doubling the number of observed transits will enable their detection. Eventually though, the peak of the phase-folded SNR distribution shown in Fig. 15 will shift past the detection threshold, and more observations will only allow us to probe out to longer orbital periods and dimmer stars. No detailed study has yet quantified when *TESS* will reach this inevitability.

However, we can use *Kepler* 's primary mission as a point for comparison: we retrieve all KOIs with a Kepler Disposition of 'CANDIDATE' as reported by NASA's Exoplanet Archive (August 15, 2016), and plot the periods of KOIs as a function of KOI number, coloring each KOI by its radius.

did kepler actually reach this regime? ask J Rowe? maybe want same plot, colored by kep mag too? this & above paragraph maybe cut...

If we take the KOI number as a rough proxy for total observing time of a given *Kepler* object (ignoring short-term sociological trends), if *Kepler* reached the 'point of no more low-hanging fruit', we would expect the later KOI numbers to not have any short-period small planets. Fig. 25 shows that even after 4 years of observing the same field, the *Kepler* team was still announcing short-period small planet detections. Given this result it seems likely that *TESS* could perform a scenario like `nhemi` or `npole` for > 2 years before this became an issue.

Ability to upgrade cadence of targets detected in long-cadence images

How adept will we be at upgrading suspected transiting planet hosts to shorter cadence? This is an issue relevant to both *TESS*'s primary mission as well as the extended mission: if it becomes apparent from the SPOC's processing that a FFI transit-signal in the N^{th} observing

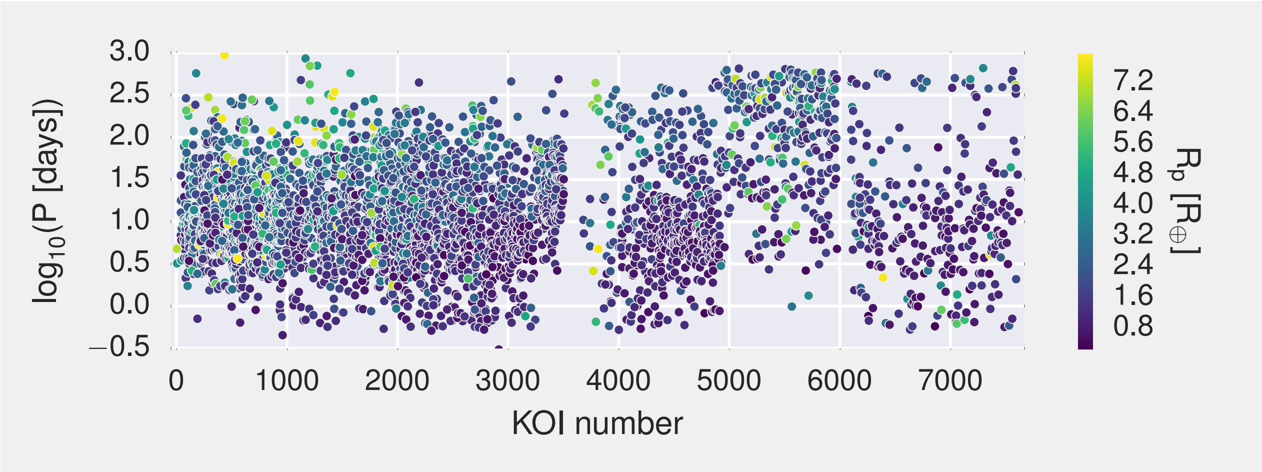

Figure 25: Did *Kepler* reach the point of diminishing returns? The first catalog went up to KOI number 1000. Q6 took us to 2000, Q8 to 2800, Q12 to 4200, Q16 to 5500, and Q17 (DR24) to 7000. The pipelines changed in these times (Q6 pipeline method for single pass detections, multis from BLS, Q8 switch to multiple-pass wavelet, Q12 to community disposition, Q16 to automating disptions, Q17 to robovetting and deep EBs)

sector is likely a planet, it could be observed at short cadence in the $(N+1)^{\rm st}$ observing sector to improve the probability both of detecting a planet, and also of obtaining a detection with precise orbital parameters. Adding such stars will not crowd-out a significant number of stars from the baseline target list provided that a strong enough threshold is set for what becomes labeled a 'promising candidate'. As planned, the SPOC will only compute pixel-level calibrations, and not light curves, from the FFI data [Jenkins et al., 2016]. A 'quick-look' FFI pipeline could be an important tool towards optimizing *TESS*'s science yield based on this point.

so they're not doing ANY planet candidates?

Our simulation ignored this question and assumed that *none* of the planets or planet-candidates found in the primary mission would be observed at upgraded cadence, unless when their star's `Merit` was recomputed for the extended mission, it happened to rank in the top 2×10^5 targets. Another extreme would be to upgrade *every* TOI from the primary mission to 2 minute cadence in an extended mission. If we did this, one major change in our predicted yield would be that Fig. 14 would show nearly all of the extended mission's 'new planets' being detected in postage stamps. More importantly, this strategy would lead to more planet detections by helping build SNR on transiting events with $\lesssim 1$ hr durations, and also potentially help in detecting additional transiting companions.

Modify the cadence for full frame images and target stars; modify allocation of data mass between them. The above question on upgrading the cadence of promising targets ties into a broader question: "what is the optimal cadence and relative weight between postage stamps and full frame images?" To our knowledge, this question has not been studied in depth. By way of preliminary calculation, we ran our yield simulation for the primary mission, but rather than observing 2×10^5 2-min targets and 3.8×10^6 30-min targets, we observed 4×10^5 4-min targets and 3.6×10^6 30-min targets (note both cases that the FFIs are complete for $R_p < 4R_\oplus$). This simple change increases the absolute number of detected planets by $\sim$15%.

The main benefit of short cadence in transit detection is in resolving the shortest transit durations that would otherwise be 'smeared'. 30 minute cadence is sufficient for this purpose on most transit timescales (with the exception being the closest planets to M dwarfs). Auxiliary benefits of shorter cadence include: *(a)* resolving the ingress and egress phases of transits, which helps remove degeneracies during retrieval of a planet's physical and orbital parameters, and *(b)* retrieving precise mid-transit times and ingress/egress times, which helps ephemeris prediction.

While 2 minute cadence may be overkill for simply detecting transits, the benefits that come from fine time-resolution may justify the additional data cost. That said, we may discover in the primary mission (or beforehand, if this question is studied at greater depth) that 2 minute cadence is not worth the additional cost; in that case, we could change these parameters in an extended mission.

Follow-up for TESS : Ground and space-based instruments will reveal essential details of the *TESS* planet sample. Given the impracticality of listing out every such facility, we focus here on the resources that we expect will be most important towards broadly advancing our understanding of *TESS*'s planets.

- *JWST :* Exoplanet observations with *JWST* will encompass transit, occultation, and phase curve measurements. The class of measurement determines the planetary and stellar parameters that are most important in building a large SNR, but for all three classes of observation, many promising targets are already known [Stevenson et al., 2016]. The main contribution of *TESS* will be finding hitherto unknown sub-Neptune radius planets orbiting bright stars.

  The main point for consideration of *TESS* and *JWST*'s overlap is that of sky coverage. *JWST* can observe targets within 5° (10°) [60°] of the North and South Ecliptic Poles for the entire (two thirds of the) [one third of the] year. The feasibility of transit programs that require multiple visits, for instance super-Earth spectroscopy, thus greatly depend on their targets' on-sky locations.

  To assess how much extended *TESS* missions might actually impact this point of overlap, we ask: *(1)* How many new $R_p < 4R_\oplus$ planets does each scenario give in *JWST*'s easily-viewed zones? *(2)* Of those, how many have atmospheres prone to characterization?

We answer these questions in Tables 3 to 5. The glaring point of Table 4 is that there will be very few *TESS*-detected super-Earths in *JWST*'s continuous viewing zones with truly great prospects for transmission spectroscopy. This is a geometric problem (the *JWST* CVZs take up 0.4% of the sky) as well as an abundance problem (most $R_p < 4R_\oplus$ planets have substantially less SNR in transmission than GJ 1214b).

Another important trend from the tables is that while $|\beta| > 80°$ planets show a factor of 4 difference in yield between `eshort` (50) and `hemis14d` (200), if we restrict our interest to $\mathrm{SNR}_{\mathrm{atm}} > \mathrm{SNR}_{\mathrm{GJ\ 1214b}}/5$ planets, there is practically no difference between extended missions; the primary mission detects the most important planets for *JWST* follow-up.

Given that a $R_p < 2R_\oplus$ planet must be observed in-transit for hundreds of hours to yield atmospheric temperatures and abundances of select molecules [Gillon et al., 2016, Barstow and Irwin, 2016], it is likely that only the very best targets will be selected. That said, the main point of Table 5 is that *TESS* will detect the most promising planets for *JWST* follow-up after only a year's observation. This means that *TESS* is not 'bound' to the ecliptic poles in an extended mission to support *JWST*'s target selection. More important for ensuring *JWST*–*TESS* overlap will be the efficient spectroscopic and photometric follow-up of *TESS*'s planets from the ground; by *JWST*'s launch in October 2018, only a few verified *TESS* planets will be known.

In passing, we highlight an important assumption relevant to this topic: our `Merit` statistic is weighted by $\sqrt{N_{\mathrm{obs}}}$, so our density of target stars near the ecliptic poles is roughly $3.5\times$ that nearest to the ecliptic plane. The actual prioritization scheme for *TESS* targets may differ. An additional minor concern is the saturation limits on *JWST*'s instruments – $J \gtrsim 6$ ($J > 11$) for medium (low) resolution NIRSpec spectroscopy, and $J > 8.1$ ($J > 6.9$) for standard (subarray) spectroscopy with NIRISS [Beichman et al., 2014]. Only a small number of *TESS*'s planets reach these limits.

- *CHEOPS:* We refer the interested reader to Berta-Thompson et al. [2016] for an overview of how *TESS* and *CHEOPS* complement each other. Re-stating the main points: *CHEOPS* provides more precise photometry for essentially all stars than *TESS* , and uses a narrow field of view to select individual targets. *CHEOPS*s' visibility is best near the ecliptic, and non-existent near the ecliptic

Table 3: Newly detected sub-Neptune radius planets. $|\beta| > 85°$ can be observed all year by *JWST*; $|\beta| > 80°$ can be observed for $\geq$ two-thirds of the year, $|\beta| > 30°$ for $\geq$ one-third.

	$\|\beta\| > 85°$	$\|\beta\| > 80°$	$\|\beta\| > 30°$	All sky
primary	103	453	2088	2483
`nhemi`	38	170	1024	1284
`npole`	41	176	1419	1419
`shemiAvoid`	24	100	934	1327
`elong`	22	86	667	1169
`eshort`	12	52	857	1216
`hemis14d`	44	192	1130	1433

Table 4: $R_p > 4R_\oplus$ and $\mathrm{SNR}_{\mathrm{atm}} > \mathrm{SNR}_{\mathrm{GJ\ 1214b}}/2$.

	$\|\beta\| > 85°$	$\|\beta\| > 80°$	$\|\beta\| > 30°$	All sky
primary	1	4	71	104
`nhemi`	0	0	7	14
`npole`	0	0	8	8
`shemiAvoid`	0	0	8	24
`elong`	0	0	5	21
`eshort`	0	0	9	23
`hemis14d`	0	0	10	22

Table 5: $R_p > 4R_\oplus$ and $\mathrm{SNR}_{\mathrm{atm}} > \mathrm{SNR}_{\mathrm{GJ\ 1214b}}/5$.

	$\|\beta\| > 85°$	$\|\beta\| > 80°$	$\|\beta\| > 30°$	All sky
primary	21	83	1019	1361
`nhemi`	1	4	242	397
`npole`	1	4	278	278
`shemiAvoid`	1	3	261	523
`elong`	1	3	164	445
`eshort`	0	2	299	530
`hemis14d`	1	6	312	515

poles. *TESS* and *CHEOPS* could together measure TTVs, to both measure planet masses and also search for additional companions. As these systems will be accessible to radial velocities, they will be important keystones for cross-checking RV and TTV mass measurements.

Extended missions that focus exclusively on the ecliptic poles, like `npole`, seriously neglect the complementarity of *TESS* and *CHEOPS*. Those that focus on the ecliptic, including `elong` and `eshort`, provide the largest amount of overlapping coverage.

- *Ground-based follow-up for TESS :* Ground-based spectroscopic and photometric follow-up are essential components of *TESS*'s baseline mission. After rejecting false-positives probabilistically or via imaging and reconnaissance spectroscopy, RV measurements will yield masses and orbital elements, *e.g.,* eccentricities, for many *TESS* planets. Ground-based supporting photometry taken before, during, and after *TESS*'s observations will also help in discovering longer period companions to short-P transiters, and in building SNR on $R_p \gtrsim 4R_\oplus$ planets.

  The primary mission will clarify whether ground-based follow-up resources need to constrain *TESS*'s extended observing. Based on the expected contributors for RV as well as photometry – HARPS, HARPS-N, CARMENES, SPIROU, LCOGT, HAT, KELT, WASP, NGTS, and others – there should be ample resources in both hemispheres for *TESS* to be able to observe anywhere without risking insufficient follow-up.

  That said, a minor bonus for focusing *TESS* observations near the ecliptic as in `elong` or `eshort` is that relatively more ground-based telescopes can follow-up on these targets, rather than only those in Earth's northern or southern hemispheres.

  An additional point to be considered for ground-based follow-up of an extended mission would be to confirm *TESS* planets orbiting rapidly rotating stars through spectroscopic transit measurements of the Rossiter-McLaughlin effect *e.g.*, [Gaudi and Winn, 2007]. Multiplexing spectrographs might enable confirmation (without mass measurements) at a more rapid rate than measuring the orbital velocity of the parent star over a full orbital period.

TESS as a follow-up mission Hundreds of transiting exoplanets have been discovered from the ground[14] and thousands have been found from space. *TESS* will follow-up on these discoveries – the primary mission's target list will include known planet-hosts from transit and RV surveys. While the value-added will be largest for systems that only have ground-based photometric and/or spectroscopic data, many of these systems could yield additional transiting companions along with refined physical and orbital parameters for the known planets. An inspiring example is the WASP-47 system, for which the WASP team found a hot Jupiter, subsequent RV follow-up yielded

[14] Notably surveys that have discovered transiting planets include OGLE [Udalski et al., 2003b,a], HAT [Bakos et al., 2004], TrES using STARE [Alonso et al., 2004], the XO telescope [McCullough et al., 2005], WASP [Pollacco et al., 2006], KELT [Pepper et al., 2007], MEarth [Irwin et al., 2008], TRAPPIST [Jehin et al., 2011], and the Qatar Exoplanet Survey (QES) [Alsubai et al., 2014]. Other transit surveys have recently begun: the APACHE project observes from the Western Italian Alps [Sozzetti et al., 2013]; SPECULOOS will soon begin observing from the Atacama Desert [Gillon et al., 2013]; NGTS is succeeding SuperWASP [Wheatley et al., 2013]

a $P = 2$ year Jupiter-mass outer companion, and further *K2* observations yielded two $R_p < 4R_\oplus$ planets transiting inside and outside of the hot Jupiter's orbit [Hellier et al., 2012, Neveu-VanMalle et al., 2016, Becker et al., 2015, Dai et al., 2015]. Even for the *Kepler* field, which *TESS* will observe with less precision than *Kepler* had, *TESS*'s observations will aid analyses of transit timing variations, secure a small number of long-period transiters, and provide a cross-calibration between the two missions.

We highlight where we expect *TESS* to provide a substantial additional value to already-studied fields and systems:

- *Kepler's field: TESS* will observe the *Kepler* field for an average of $2 \times 26 = 52$ days in 2019. This will also entail observing a few of *Kepler*'s modules for 78 days, and a few for 26 (see Fig. 4). A practical note for extended missions is that `npole` observes the *Kepler* field for an average of $4 \times 26 = 104$ days per year – twice as long as `nhemi`.

  The main reasons to allocate extra pixel weight to the *Kepler* field include: *(a)* detecting transits over a long baseline (*e.g.,* to refine ephemerides); *(b)* measuring transit timing variations; *(c)* confirming few-transit KOI candidates, *e.g.* [Wang et al., 2015, Uehara et al., 2016, Foreman-Mackey et al., 2016], *(d)* calibrating *TESS* against well-studied candidates, *(e)* continue observations of CBPs & multiple star systems, and *(f)* characterize stellar cycles over long timescales through star-spot measurements.

  Sullivan [2013] explored *TESS*'s performance on KOIs in some detail. He found that even with *TESS*'s reduced sensitivity to *Kepler*'s dim stars, it should detect $5 - 10\%$ of the KOIs at $\geq 3\sigma$ significance per transit. A few dozen of these planets have $R_p < 4R_\oplus$, and $\sim$50 reside in multi-planet systems and are likely to give interesting TTV measurements. We note that Sullivan [2013] used October 2013's KOI list, which has since at least doubled in length.

- *Ground-based surveys: TESS*'s photometric precision provides the greatest relative benefit for planets that have never been observed from space. WASP and HAT have detected the largest number of transiting systems from the ground, in both the northern and southern celestial hemispheres. These targets, and even those from RV surveys, are promising candidates for detailed study in *TESS*'s data. At the very least, *TESS* data for known transiters will yield improvements on uncertainties in planetary radii, and will also lead to discovery of many new transiting companions. Beyond transit science, the discovery of short-period non-transiting planets through phase curve measurements is also worth pursuing [Millholland et al., 2016].

Will the desire to follow up ground-based surveys impact *TESS*'s extended mission? Likely not; the north and south skies have similar numbers of known transiting and RV-detected planets. As long as the extended mission continues to observe both hemispheres (rather than focusing on a single one in perpetuity), the value-added to known transiting and even RV planets from the primary mission will only improve in an extended mission.

- *K2: K2* observes $\pm 6°$ about the ecliptic for $\sim$80 days per field, and is expected to discover anywhere from 500-1000 planets over its total mission lifetime [Howell et al., 2014, Crossfield et al., 2016]. In a sense, *K2* is a stepping stone between *Kepler* and *TESS*: *Kepler* observed a single field over a long baseline, *K2* observes many fields over mid-length baseline, and *TESS* will observe the majority of the sky for a short baseline.

  If everything works, in early 2020 *TESS* will begin its extended mission and *K2*'s on-board fuel supply will be either almost or entirely depleted. *K2* will have covered $\gtrsim$ 60% of the area in the $|\beta| < 6°$ band about the ecliptic – the exact band that *TESS* misses during its primary mission. Hundreds more *K2* planets will be confirmed and vetted beyond those that already have been from early campaigns [Foreman-Mackey et al., 2015, Vanderburg et al., 2016, Crossfield et al., 2016].

  Our presentation of 'newly detected planets' for both `elong` and `eshort` assumed no knowledge from *K2*. This is quite unrealistic – a large fraction of the planets that *TESS* will be capable of detecting near the ecliptic will already either exist as candidates in *K2*'s data or have been discovered. Once processed, *K2*'s precision is within a factor of 2 or 3 of *Kepler*'s; this is comparable to or better than *TESS* for most stars. The median *K2* candidate magnitude is 2 *Kepler* magnitudes brighter than that of KOIs[15] – *TESS* would want to observe many of the same targets that are already being selected from the Ecliptic Plane Input Catalog [Huber et al., 2016]. For a scenario like `elong`, the average *TESS* coverage per star over the extended mission in the $\pm 12°$ band would be $\sim$7 spacecraft orbits, or $\sim$91 days of near-continuous observing.

Summarizing then what we find to be the most compelling reasons to observe the ecliptic in an extended *TESS* mission: *(a)* catch 'holes' in the $|\beta| < 12°$ band that *K2* missed, completing the all-sky search for small planets transiting the brightest stars; *(b)* observe targets in *K2* fields that simply were not selected in *K2*'s $\sim$20000 per campaign. For instance, *TESS*'s bandpass allows probing down to cooler M dwarfs than *Kepler*'s; *(c)* double the *K2* observing baseline for most targets. In turn, confirm low-SNR

[15] $K = 12.8$ to $K = 14.6$, based on data from NASA's Exoplanet Archive, August 21 2016

candidates, and detect extra transits for a relatively large number of $20 < P < 40$ day planets; *(d)* measure TTVs for targets over baselines up to 5-years. *(e)* confirm a small but significant number of $P > 40$ day planets (even single transiters, *e.g.,* [Osborn et al., 2016]).

TESS's value-added for the *K2* targets is closer to that for ground-based targets than for *Kepler* . Given the huge role that combining *TESS* and *K2* data would necessarily play if *TESS* were to observe the ecliptic, and given our non-treatment of this question in our yield simulations, we recommend that a detailed study of *K2* and *TESS*'s combined potential be carried out before ruling for or against `elong` or `eshort`.

- *CoRoT & MOST :* We also comment briefly on the overlap of *TESS* with two other space-missions: CNES and ESA's *CoRoT* [Auvergne et al., 2009] as well the Canadian *MOST* satellite [Walker et al., 2003]. *CoRoT*'s two 'eyes' are each roughly 10° in diameter, are approximately centered at $(\lambda, \beta) = (286^\circ, 23^\circ)$ and $(106^\circ, -23^\circ)$, and thus are near the galactic plane [Deleuil et al., 2009]. *TESS*'s images of these fields will be heavily contaminated by background stars, but could contribute additional information to the $\sim$30 confirmed *CoRoT* planets. *MOST*'s continuous viewing zone spanned -19° to 36° in declination, which means its targets fell between $\pm 40^\circ$ in ecliptic latitude[16].

  In *TESS*'s extended mission, both the *CoRoT* and *MOST* fields are neglected in scenarios that focus exclusively on the ecliptic poles, *i.e.,* `npole`. Some groups may take up the challenge of combining data from these earlier missions with that from *TESS*'s primary mission. If these efforts show promise, the argument for continuing observations of these fields would be strengthened.

[16] Retrieved MOST targets from Canadian Astronomy Data Center, August 21 2016.

Guest Investigator program In *TESS*'s first two years, its Guest Investigator (GI) office will solicit proposals for new research using 10^4 short cadence targets per year in addition to the full frame images. The GI office's task is to generate and maintain involvement from the greater scientific community, and for a simple reason: many of the highlights of previous space telescopes stem from competitive community proposal calls, rather than just from the science teams! By serving as a bridge between the science team and the broader community, the GI program thus plays an important role in maximizing *TESS*'s science return.

Although its role in the extended mission has yet to be defined, the historic lesson is that *TESS*'s GI office or science team should solicit community feedback during the process of defining the extended mission. This may entail a call for white papers, comments on this particular work, or direct proposals to the GI office. As exemplified in NASA's 2016 Astrophysics Senior Review [Donahue et al., 2016], everyone benefits from the discussion generated by such community feedback.

6.2 Risks

Risk that planet detection simulation gets yield wrong: What is the risk that we over or under-estimated *TESS*'s planet yield, either in the primary mission, or in any given extended mission? We summarized the assumptions that went into our yield calculations in Sec. 3.7. We made them believing that they were all good enough for estimating *TESS*'s absolute planet yield to perhaps a factor of two.

Highlighting a few of these assumptions in order of decreasing egregiousness:

1.) *We assume no knowledge of what observations other telescopes* have performed on the stars we observe. As indicated in the text, this assumption is worst for the `elong` and `eshort` scenarios, for which *K2* and *TESS*'s overlap will be important. Estimating the magnitude of our error, assume *K2* will have observed 70% of the sky in the $|\beta| < 6°$ band about the ecliptic by 2019. Of the 1169 'new' $R_p < 4R_\oplus$ planets that *TESS* detects in `elong`, 502 of them are within $|\beta| < 12°$ of the ecliptic. Assuming that all of these detections are uniformly distributed over the $|\beta| < 12°$ band, this means that 35% (the ratio of the annuli) of *TESS*'s new planets will already have been detected in *K2* data. This simple estimate quantifies our global error in reporting 'new' planets near the ecliptic, but avoids the issue of merging the two datasets to discover long period planets. This latter opportunity could be an important reason to actually do `elong` or `eshort` and thus demands detailed study, which we recommend below.

2.) *The difference in* $1.25R_\oplus < R_p < 2R_\oplus$ *planet yield from S+15.* We discussed this point in Sec. 4.1. S+15 claim that *TESS* detects roughly 900 super-Earths in full frame images, and 500 in postage stamps. We claim that *TESS* detects roughly 10 super-Earths in full frame images, and 400 in postage stamps. This is a discrepancy of a factor of 4 in one of *TESS*'s most significant data products. We do not understand the origin of the difference between our method and S+15's. That said, based on *(a)* raw output data generated by the author of S+15 and dated in May 2015 (3 months after initial ApJ submission, 1 month before acceptance); *(b)* the data we generated from the earliest available version of S+15's code, dated in October 2015 (before any of our methodological changes); *(c)* the analytic estimates of Winn [2013] which predict $\sim$ 300 super-Earth detections; and *(d)* a plausibility argument presented in Sec. 4.1 that showed S+15's results implied a detection efficiency biased sub-linearly in R_p, whilst ours implies a bias between linear and quadratic in R_p, we think that we are closer to what *TESS* will actually see.

3.) *We use a SNR threshold of 7.3.* This number was computed in S+15 based on the argument that it would be a sufficient threshold to give one false positive per 2×10^5 light curves. This criterion is a self-consistent ad-hoc choice that we made for target stars. Applying the same criterion to full frame images would lead to more than one false positive, since full frame images come from a much larger sample of stars. Any pipeline that is written to work with *TESS* data will confront this problem: processing 10^8 vs. 4×10^6 vs. 2×10^5 stars requires different false positive thresholds. Extrapolating from S+15's Fig 15, a threshold sufficient to give 0.05 false positives per 2×10^5 light curves, or 1 false positive per 4×10^6 light curves (as from our full frame images), is roughly 7.5. Making the same ad-hoc estimate that S+15 did and multiplying by 1.03 for the expected drop in SNR from cosmic ray noise gives a SNR threshold of 7.7 for full frame images. Considering our Fig. 15 (and noting the black line is for the sum of postage stamp and full frame image detections), adopting a SNR threshold of 7.7 for FFIs would mean a loss of $\sim 30 \times 4 = 120$ planets over two years, or 60 of what we claim are 'detected planets' from full frame images in 1 year's extended mission.

4.) *We use synthetic stars from a single galactic model (TRILEGAL).* One check on the robustness of this model would be to compare with other galactic models like GALAXIA [Sharma et al., 2011] or a Besaçon model [Robin et al., 2003]. We have already done this using a simple analytic model in Winn [2013], which agrees with our work to factors of a few. We might eventually use the real star catalog that *TESS*'s Target Selection Working Group is assembling, but this would come with at-present large uncertainties on stellar radii and effective temperatures.

While we recommend that these broader checks be performed in future *TESS* yield calculations, they are excessive for the purposes of this report given that we only used the nearest, brightest, stars ($d \lesssim$ 1kpc, $I_c \lesssim 16$) with a simple prescription for background contamination in evaluating *TESS*'s $R_p < 4R_\oplus$ detections. The relative uncertainties become much greater if we try to estimate detections of giant planets and false positives throughout the galactic disk. That said, we take S+15's cross-checks (cf Fig. 5 of that paper) against actual surveys of the local stellar population as indicative that we probably have the number of nearby stars, as well as their properties, correct to our desired factor of 2.

5.) At least 2 transits for detection: recall Figs. 16 and 17. If we were to use a more stringent criteria, for instance at least 3 transits for detection as the *Kepler* pipeline currently does, we would lose $\mathcal{O}(200)$ of the planets detected in the primary mission, and $\mathcal{O}(100)$ from the extended missions. This assumption disproportionately affects long-period planets.

6.) No instrument aging, no spacecraft systematics, etc. To our best knowledge detailed models do not currently exist for how *TESS*'s optics and CCDs will degrade with time. We are also assuming that, as with *K2* , time-correlated spacecraft level systematics can be removed in post-processing. These assumptions are reasonable at our current state of pre-flight knowledge, and will need to be changed accordingly as the mission progresses. If we were to assume a gradual decline in photometric performance, for instance from an increased number of dead or 'hot' pixels, the relative extended-mission-to-extended-mission comparisons would remain identical. The absolute extended-mission-to-primary-mission yields would decrease.

7.) Non-consideration of efficacy of processing pipeline. For instance, `hemis14d` will come with period ambiguities and aliasing problems imposed by its 14 day sampling at the 'continuous' viewing zones. Similar issues are generic across extended missions for which we detect a small number of transits in the primary mission, and then a small number of transits in the extended mission.

A robust way to approach this problem would be to generate a synthetic simulated *TESS* dataset, *i.e.*, at the image-level, rather than at the idealized phase-folded SNR level from this work, for each extended mission's observations. Then actually perform astrometry on injected stars, extract light curves, de-trend them, and find their transits. This exercise would likely also be a useful way to prepare the SPOC and broader community for what we expect the era of *TESS* photometry to entail in terms of data quality.

Given these assumptions in which we are most-wrong, we ask: are we fooling ourselves? How accurate can we hope our $R_p < 4R_\oplus$ yield calculations to be? Assuming that our most important assumption – the in-flight photometric performance – holds, and qualifying our global uncertainty as greater for ecliptic vs. non-ecliptic focused scenarios because of *K2*, we hope to be no more wrong than a factor of two.

Miscellaneous risks To be considered as knowledge of *TESS*'s in-flight performance improves:

- What is the risk of not meeting 'threshold' science – essentially whatever goals the science team decides will be the main drivers for an extended mission?
- Is there a risk of excessive false positives, for instance from field crowding, from any particular extended mission? This is primarily an issue for fields near the galactic plane and bulge.
- Would any expected partial instrument failures make a certain observing scenario infeasible? (à la *K2*, for instance)

7 *Concluding remarks and recommendations*

This trade-study laid out technical requirements, science goals, opportunities, and risks relevant towards observing with *TESS* after its first two years. The baseline science requirements for *TESS*'s primary mission are defined [Ricker et al., 2014], and an extended mission offers a chance to re-prioritize. Is securing *TESS*'s ephemerides more important than probing out to the longest period planets? Are the variations in absolute new planet yields, at $\lesssim 30\%$ between all the extended missions, more valuable than other desires and opportunities?

7.1 *Recommendations*

Analyze target prioritization problem and decide whether or not to optimize target selection based on results. Planet occurrence rates are functionally dependent on a star's properties – should this affect which stars we give upgraded cadence? Is our proposed `Merit` statistic (Eq. 1) how we want to prioritize targets?

Optimize cadence: 200k at 2min vs. 400k at 4min, & related trade-offs.

Take steps to address the 'upgrading cadence' problem: if there is a likely transiting planet in full frame image data, upgrading the planet to short cadence in future observing sectors improves the probability and fidelity of detection.

Guest Investigator Office / TESS Science Office: solicit advice from experts in asteroseismology and variable-sky astronomy to understand how extended missions affect their science cases (*e.g.*, data throughput rates are particularly important for time-sensitive supernovae observations). More broadly, solicit community feedback during the process of defining the extended mission. This may entail a call for white papers, comments on this report, or direct proposals to the GI office. As exemplified in NASA's 2016 Astrophysics Senior Review, everyone benefits from the discussions generated by such community feedback [Donahue et al., 2016].

Decide (explicitly or implicitly) on weights between our proposed metrics. Perhaps also brainstorm others – Sec. 3.3 gives a summarized list. Are the $\lesssim 30\%$ variations in absolute new planet yields more valuable than other desires or opportunities?

Simulate combining TESS and K2 data from `elong` *and* `eshort`. This is perhaps the most important qualitative difference between observing towards and away from the ecliptic. Would *TESS*+*K2* enable more discoveries out at long periods than alternatives? How many of the new planets that *TESS* detects on the ecliptic will actually be detected by *K2* ? Is the value-added of combining datasets a compelling case compared with discovery?

Further topics for study: 1.) Would observing `npole` for 2 years hit the 'low-hanging fruit' barrier? How much dimmer would the host stars of new planets be in such a scenario? Would the planets tend to be smaller? Would there be fewer of them? *2.)* Study the limiting case of `hemis14d` for 2 years, vs primary mission repeat for 2 years, vs `npole`×2 for 2 years. The most interesting aspect here is the continuous viewing zones: 2 CVZs at 14-day sampling, vs. 2 CVZs at continuous sampling for one-year each, vs. 1 CVZ for full sampling over two years.[17]

[17] Our simplified perfect period extraction would miss challenges from the data processing.

Acknowledgements

We are grateful to Peter Sullivan, who wrote most of the planet detection simulation that we adapted for the purposes of this trade-study. We thank him for explaining his work and for his helpful comments on our results. We thank Jack Lissauer for his input regarding the value of observing *Kepler*'s field with *TESS*. And finally we are indebted to Ed Morgan, Isaac Meister, Kenton Philips, and the *TESS* project for providing the computing resources used in this work.

Facility: *TESS*

Software: Matplotlib [Hunter, 2007], Numpy [Walt et al., 2011], Scipy [Jones et al., 2001], JPL NAIF's SPICE library [Acton, 1996], and the IDL Astronomy User's Library [Landsman, 1995].

Resources: This research has made use of the NASA Astrophysics Data System and the NASA Exoplanet Archive. The NASA Exoplanet Archive is operated by the California Institute of Technology, under contract with the National Aeronautics and Space Administration under the Exoplanet Exploration Program. This paper also makes use of data collected by the Kepler mission. Funding for the Kepler mission is provided by the NASA Science Mission directorate.

Appendices

A Models relevant to Earth-Moon crossings

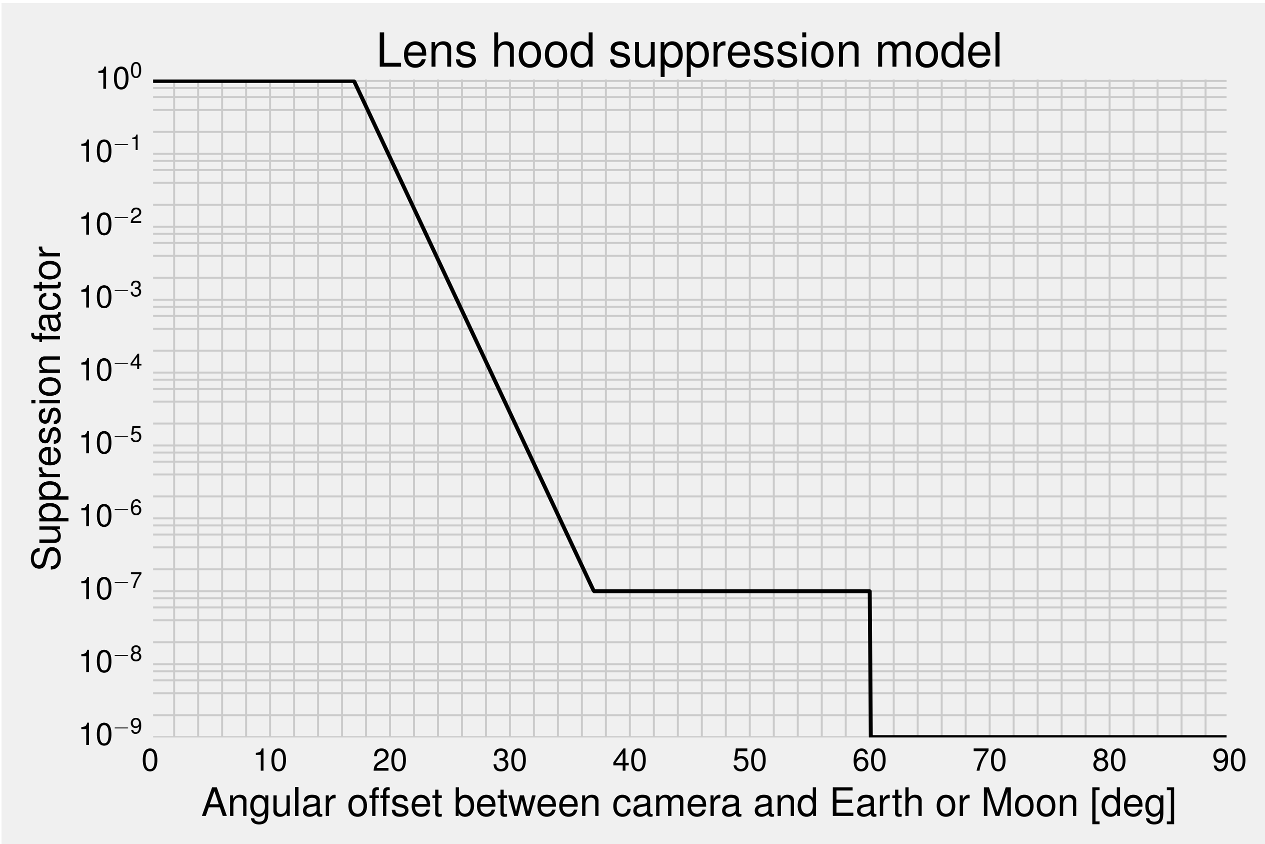

Figure 26: Lens hood suppression plotted against the angular offset to the Earth or Moon. This suppression factor is defined as the fraction of incident flux that is blocked by the spacecraft, sunshade, lens hood, or combinations thereof.

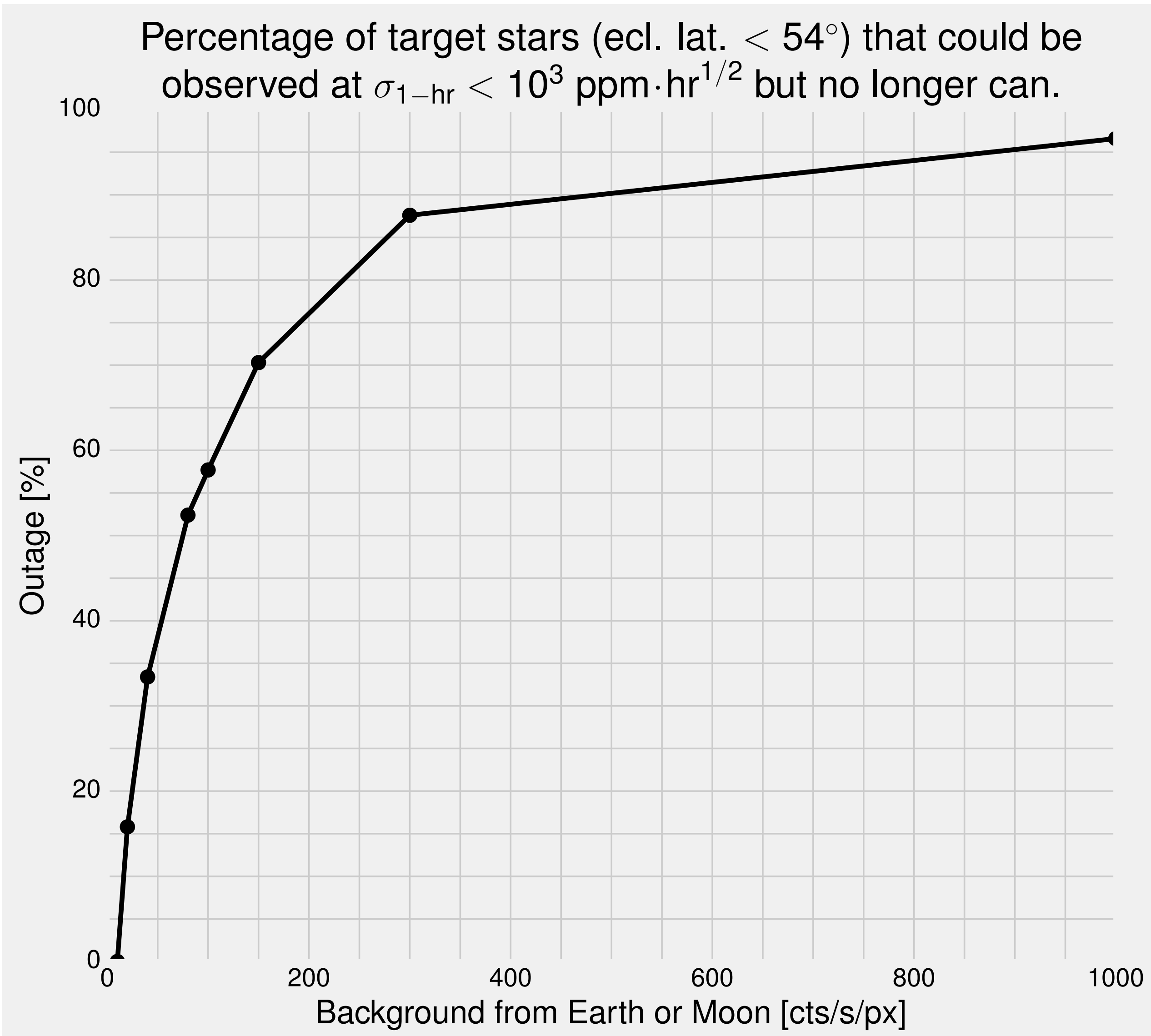

Figure 27: The procedure described in Sec. 3.6 drops fields in which $\sim$90% of the target stars (in the lower two camera fields) cannot be observed.

B Changes from Sullivan et al. [2015]

On the angular dependence of TESS's pixel response function: In our SNR calculation, we do not keep track of individual times for every transit. How then do we assign PSFs to different transits from the same object that fall on different regions of the CCDs, and thus should have slightly better or degraded PSFs? (Largest cumulative flux fraction at the CCD's center, smallest at the corners).

S+15 dealt with this by computing the mean of all the field angles (distance from the center of the CCD axis), and then passing this mean into a look-up table for PSFs based on four PSFs that had been computed from a ray-tracing model at four different field angles. S+15 then 'observes' each eclipsing object with a single class of PSF. This leads to the implausible phenomenon that extra observations can actually *lower* the SNR of an eclipsing object if they are taken with an unfavorable field angle/PSF. This effect is largely off-set by the extra pointing increasing the SNR, but for extended missions (coming back to the same objects at potentially very different field angles) it winds up reducing observed SNR for $\sim$3% of detected objects.

In extended missions (as well as in the primary mission) we expect stars to land on very different regions of the CCD over the course of being observed. We simplify this in our work by assuming that all stars land on the center of the *TESS* CCDs (the green curve of S+15 Fig. 13). This assumption is justified because our chief point of quantitative comparison is the ability of different pointing strategies to impact *TESS*'s planet yield in extended missions, and there is little *a priori* reason to assume that any one pointing scenario should be biased for an extra amount of stars to land on the 'bad regions' of *TESS*'s CCDs.

References

C. H. Acton. Planetary data system: Ancillary data services of NASA's Navigation and Ancillary Information Facility. *Planetary and Space Science*, 44(1):65–70, Jan. 1996. ISSN 0032-0633. DOI: 10.1016/0032-0633(95)00107-7. URL `http://www.sciencedirect.com/science/article/pii/0032063395001077`.

C. Aerts, K. Zwintz, P. Marcos-Arenal, E. Moravveji, P. Degroote, P. Pápics, A. Tkachenko, J. De Ridder, M. Briquet, A. Thoul, and others. Ensemble Asteroseismology of the Young Open Cluster NGC 2244. *arXiv preprint arXiv:1309.3042*, 2013. URL `http://arxiv.org/abs/1309.3042`.

E. Agol, J. Steffen, R. Sari, and W. Clarkson. On detecting terrestrial planets with timing of giant planet transits. *Monthly Notices of the Royal Astronomical Society*, 359(2):567–579, May 2005. ISSN 0035-8711, 1365-2966. DOI: 10.1111/j.1365-2966.2005.08922.x.

V. S. Aguirre, L. Casagrande, S. Basu, T. L. Campante, W. J. Chaplin, D. Huber, A. Miglio, A. M. Serenelli, J. Ballot, T. R. Bedding, J. Christensen-Dalsgaard, O. L. Creevey, Y. Elsworth, R. A. García, R. L. Gilliland, S. Hekker, H. Kjeldsen, S. Mathur, T. S. Metcalfe, M. J. P. F. G. Monteiro, B. Mosser, M. H. Pinsonneault, D. Stello, A. Weiss, P. Tenenbaum, J. D. Twicken, and K. Uddin. Verifying Asteroseismically Determined Parameters of Kepler Stars Using Hipparcos Parallaxes: Self-consistent Stellar Properties and Distances. *The Astrophysical Journal*, 757(1):99, 2012. ISSN 0004-637X. DOI: 10.1088/0004-637X/757/1/99. URL `http://stacks.iop.org/0004-637X/757/i=1/a=99`.

R. Alonso, T. M. Brown, G. Torres, D. W. Latham, A. Sozzetti, Georgi Mandushev, J. A. Belmonte, D. Charbonneau, H. J. Deeg, E. W. Dunham, F. T. O'Donovan, and R. P. Stefanik. TrES-1: The Transiting Planet of a Bright K0 V Star. *The Astrophysical Journal Letters*, 613(2):L153, 2004. ISSN 1538-4357. DOI: 10.1086/425256. URL `http://stacks.iop.org/1538-4357/613/i=2/a=L153`.

K. A. Alsubai, N. R. Parley, D. M. Bramich, K. Horne, A. C. Cameron, R. G. West, P. M. Sorensen, D. Pollacco, J. C. Smith, and O. Fors. The Qatar Exoplanet Survey. *arXiv:1401.1984 [astro-ph]*, Jan. 2014. URL `http://arxiv.org/abs/1401.1984`. arXiv: 1401.1984.

D. J. Armstrong, H. P. Osborn, D. J. A. Brown, F. Faedi, Y. Gomez Maqueo Chew, D. V. Martin, D. Pollacco, and S. Udry. On the abundance of circumbinary planets. *Monthly Notices of the Royal Astronomical Society*, 444(2):1873–1883, Sept. 2014. ISSN 0035-8711, 1365-2966. DOI: 10.1093/mnras/stu1570. URL http://mnras.oxfordjournals.org/cgi/doi/10.1093/mnras/stu1570.

M. Auvergne et al. The CoRoT satellite in flight: description and performance. *Astronomy and Astrophysics*, 506:411–424, Oct. 2009. ISSN 0004-6361. DOI: 10.1051/0004-6361/200810860.

G. Bakos, R. W. Noyes, G. Kovács, K. Z. Stanek, D. D. Sasselov, and I. Domsa. Wide-Field Millimagnitude Photometry with the HAT: A Tool for Extrasolar Planet Detection. *Publications of the Astronomical Society of the Pacific*, 116(817):266, 2004. ISSN 1538-3873. DOI: 10.1086/382735. URL http://stacks.iop.org/1538-3873/116/i=817/a=266.

I. Baraffe and G. Chabrier. Mass–Spectral Class Relationship for M Dwarfs. *The Astrophysical Journal*, 461(1), Apr. 1996. ISSN 0004637X. DOI: 10.1086/309988. URL http://stacks.iop.org/1538-4357/461/i=1/a=L51.

J. K. Barstow and P. G. J. Irwin. Habitable worlds with JWST: transit spectroscopy of the TRAPPIST-1 system? *Monthly Notices of the Royal Astronomical Society: Letters*, page slw109, May 2016. ISSN 1745-3925, 1745-3933. DOI: 10.1093/mnrasl/slw109. URL http://arxiv.org/abs/1605.07352. arXiv: 1605.07352.

G. Basri, L. M. Walkowicz, and A. Reiners. Comparison of Kepler Photometric Variability with the Sun on Different Timescales. *The Astrophysical Journal*, 769(1):37, 2013. ISSN 0004-637X. DOI: 10.1088/0004-637X/769/1/37. URL http://stacks.iop.org/0004-637X/769/i=1/a=37.

J. C. Becker, A. Vanderburg, F. C. Adams, S. A. Rappaport, and H. M. Schwengeler. WASP-47: A Hot Jupiter System with Two Additional Planets Discovered by K2. *arXiv preprint arXiv:1508.02411*, 2015. URL http://arxiv.org/abs/1508.02411.

C. Beichman, B. Benneke, H. Knutson, R. Smith, P.-O. Lagage, C. Dressing, D. Latham, J. Lunine, S. Birkmann, P. Ferruit, G. Giardino, E. Kempton, S. Carey, J. Krick, P. D. Deroo, A. Mandell, M. E. Ressler, A. Shporer, M. Swain, G. Vasisht, G. Ricker, J. Bouwman, I. Crossfield, T. Greene, S. Howell, J. Christiansen, D. Ciardi, M. Clampin, M. Greenhouse, A. Sozzetti, P. Goudfrooij, D. Hines, T. Keyes, J. Lee, P. McCullough, M. Robberto, J. Stansberry, J. Valenti, M. Rieke, G. Rieke, J. Fortney, J. Bean, L. Kreidberg, D. Ehrenreich, D. Deming, L. Albert, R. Doyon, and D. Sing. Observations of Transiting Exoplanets with the James Webb Space Telescope (JWST). *Publications of the Astronomical Society of the Pacific*, 126:1134–1173, Dec. 2014. DOI: 10.1086/679566.

Z. Berta-Thompson, I. Ribas, S. Seager, and L. Bouma. Projects for a TESS and CHEOPS Collaboration. TESS Internal Report, MIT, June 2016.

C. J. Burke, S. T. Bryson, F. Mullally, J. F. Rowe, J. L. Christiansen, S. E. Thompson, J. L. Coughlin, M. R. Haas, N. M. Batalha, D. A. Caldwell, J. M. Jenkins, M. Still, T. Barclay, W. J. Borucki, W. J. Chaplin, D. R. Ciardi, B. D. Clarke, W. D. Cochran, B.-O. Demory, G. A. Esquerdo, I. Thomas N. Gautier, R. L. Gilliland, F. R. Girouard, M. Havel, C. E. Henze, S. B. Howell, D. Huber, D. W. Latham, J. Li, R. C. Morehead, T. D. Morton, J. Pepper, E. Quintana, Darin Ragozzine, S. E. Seader, Y. Shah, A. Shporer, P. Tenenbaum, J. D. Twicken, and A. Wolfgang. Planetary Candidates Observed by Kepler IV: Planet Sample from Q1-Q8 (22 Months). *The Astrophysical Journal Supplement Series*, 210(2):19, 2014. ISSN 0067-0049. DOI: 10.1088/0067-0049/210/2/19. URL http://stacks.iop.org/0067-0049/210/i=2/a=19.

T. L. Campante, M. Schofield, J. S. Kuszlewicz, L. Bouma, W. J. Chaplin, D. Huber, J. Christensen-Dalsgaard, H. Kjeldsen, D. Bossini, T. S. H. North, T. Appourchaux, D. W. Latham, J. Pepper, G. R. Ricker, K. G. Stassun, R. Vanderspek, and J. N. Winn. The asteroseismic potential of TESS: exoplanet-host stars. *arXiv:1608.01138 [astro-ph]*, Aug. 2016. URL http://arxiv.org/abs/1608.01138. arXiv: 1608.01138.

Y. Cao, S. R. Kulkarni, D. A. Howell, A. Gal-Yam, M. M. Kasliwal, S. Valenti, J. Johansson, R. Amanullah, A. Goobar, J. Sollerman, F. Taddia, A. Horesh, I. Sagiv, S. B. Cenko, P. E. Nugent, I. Arcavi, J. Surace, P. R. Woźniak, D. I. Moody, U. D. Rebbapragada, B. D. Bue, and N. Gehrels. A strong ultraviolet pulse from a newborn type Ia supernova. *Nature*, 521(7552):328–331, May 2015. ISSN 0028-0836. DOI: 10.1038/nature14440. URL http://www.nature.com/nature/journal/v521/n7552/full/nature14440.html.

J. A. Carter, J. C. Yee, J. Eastman, B. S. Gaudi, and J. N. Winn. Analytic approximations for transit light-curve observables, uncertainties, and covariances. *The Astrophysical Journal*, 689(1):499, 2008. URL http://iopscience.iop.org/0004-637X/689/1/499.

W. J. Chaplin and A. Miglio. Asteroseismology of Solar-Type and Red-Giant Stars. *Annual Review of Astronomy and Astrophysics*, 51(1):353–392, 2013. DOI: 10.1146/annurev-astro-082812-140938. URL http://dx.doi.org/10.1146/annurev-astro-082812-140938.

D. Charbonneau, Z. K. Berta, J. Irwin, C. J. Burke, P. Nutzman, L. A. Buchhave, C. Lovis, X. Bonfils, D. W. Latham, S. Udry, R. A.

Murray-Clay, M. J. Holman, E. E. Falco, J. N. Winn, D. Queloz, F. Pepe, M. Mayor, X. Delfosse, and T. Forveille. A super-Earth transiting a nearby low-mass star. *Nature*, 462(7275):891–894, Dec. 2009. ISSN 0028-0836, 1476-4687. DOI: 10.1038/nature08679.

I. J. M. Crossfield, D. R. Ciardi, E. A. Petigura, E. Sinukoff, J. E. Schlieder, A. W. Howard, C. A. Beichman, H. Isaacson, C. D. Dressing, J. L. Christiansen, B. J. Fulton, S. Lépine, L. Weiss, L. Hirsch, J. Livingston, C. Baranec, N. M. Law, R. Riddle, C. Ziegler, S. B. Howell, E. Horch, M. Everett, J. Teske, A. O. Martinez, C. Obermeier, B. Benneke, N. Scott, N. Deacon, K. M. Aller, B. M. S. Hansen, L. Mancini, S. Ciceri, R. Brahm, A. Jordán, H. A. Knutson, T. Henning, M. Bonnefoy, M. C. Liu, J. R. Crepp, J. Lothringer, P. Hinz, V. Bailey, A. Skemer, and D. Defrere. 197 Candidates and 104 Validated Planets in K2's First Five Fields. *arXiv:1607.05263 [astro-ph]*, July 2016. URL `http://arxiv.org/abs/1607.05263`. arXiv: 1607.05263.

F. Dai, J. N. Winn, P. Arriagada, R. P. Butler, J. D. Crane, J. A. Johnson, S. A. Shectman, J. K. Teske, I. B. Thompson, A. Vanderburg, and R. A. Wittenmyer. Doppler Monitoring of the WASP-47 Multiplanet System. *The Astrophysical Journal*, 813(1):L9, Oct. 2015. ISSN 2041-8213. DOI: 10.1088/2041-8205/813/1/L9. URL `http://arxiv.org/abs/1510.03811`. arXiv: 1510.03811.

M. Deleuil, J. C. Meunier, C. Moutou, C. Surace, H. J. Deeg, M. Barbieri, J. Debosscher, J. M. Almenara, F. Agneray, Y. Granet, P. Guterman, and S. Hodgkin. *EXO-DAT* : AN INFORMATION SYSTEM IN SUPPORT OF THE *CoRoT* /EXOPLANET SCIENCE. *The Astronomical Journal*, 138(2):649–663, Aug. 2009. ISSN 0004-6256, 1538-3881. DOI: 10.1088/0004-6256/138/2/649. URL `http://stacks.iop.org/1538-3881/138/i=2/a=649?key=crossref.840f61ed35675d7e4c8eb26b751115fb`.

D. Deming, S. Seager, J. Winn, E. Miller-Ricci, M. Clampin, D. Lindler, T. Greene, D. Charbonneau, G. Laughlin, G. Ricker, D. Latham, and K. Ennico. Discovery and Characterization of Transiting Super Earths Using an All-Sky Transit Survey and Follow-up by the James Webb Space Telescope. *Publications of the Astronomical Society of the Pacific*, 121(883):952, 2009. ISSN 1538-3873. DOI: 10.1086/605913. URL `http://stacks.iop.org/1538-3873/121/i=883/a=952`.

M. Donahue, M. Bautz, R. Green, G. Hasinger, L. Kaltenegger, H. Krawczynski, A. MacFayden, D. McCammon, R. Oppenheimer, P. Szkody, and D. Zaritsky. 2016 NASA Astrophysics

Senior Review. Technical report, NASA, Feb. 2016. URL http://science.nasa.gov/media/medialibrary/2016/06/09/Main_Panel_SR2016_Report_FinalTAGGED.pdf.

C. D. Dressing and D. Charbonneau. The Occurrence of Potentially Habitable Planets Orbiting M Dwarfs Estimated from the Full Kepler Dataset and an Empirical Measurement of the Detection Sensitivity. *arXiv preprint arXiv:1501.01623*, 2015. URL http://arxiv.org/abs/1501.01623.

R. Edelson, R. Mushotzky, M. Malkan, S. Vaughan, and K. Horne. AGN variability studies with the repurposed Kepler mission. 2013. URL http://keplerscience.arc.nasa.gov/K2/docs/WhitePapers/edelson%20white%20paper.pdf.

D. C. Fabrycky, E. B. Ford, M. J. Payne, J. Steffen, D. Ragozzine, T. Mazeh, J. J. Lissauer, and W. Welsh. A Habitable Zone Census via Transit Timing and the Imperative for Continuing to Observe the Kepler Field. *arXiv:1309.1177 [astro-ph]*, Sept. 2013. URL http://arxiv.org/abs/1309.1177. arXiv: 1309.1177.

D. Foreman-Mackey, B. T. Montet, D. W. Hogg, T. D. Morton, D. Wang, and B. Schölkopf. A systematic search for transiting planets in the K2 data. *arXiv:1502.04715 [astro-ph]*, Feb. 2015. URL http://arxiv.org/abs/1502.04715. arXiv: 1502.04715.

D. Foreman-Mackey, T. D. Morton, D. W. Hogg, E. Agol, and B. Schölkopf. The population of long-period transiting exoplanets. *arXiv:1607.08237 [astro-ph]*, July 2016. URL http://arxiv.org/abs/1607.08237. arXiv: 1607.08237.

F. Fressin, G. Torres, D. Charbonneau, S. T. Bryson, J. Christiansen, C. D. Dressing, J. M. Jenkins, L. M. Walkowicz, and N. M. Batalha. THE FALSE POSITIVE RATE OF *KEPLER* AND THE OCCURRENCE OF PLANETS. *The Astrophysical Journal*, 766(2): 81, Apr. 2013. ISSN 0004-637X, 1538-4357. DOI: 10.1088/0004-637X/766/2/81.

J. W. Gangestad, G. A. Henning, R. R. Persinger, and G. R. Ricker. A high Earth, lunar resonant orbit for lower cost space science missions. *arXiv preprint arXiv:1306.5333*, 2013. URL http://arxiv.org/abs/1306.5333.

B. S. Gaudi and J. N. Winn. Prospects for the Characterization and Confirmation of Transiting Exoplanets via the Rossiter-McLaughlin Effect. *The Astrophysical Journal*, 655(1):550, 2007. ISSN 0004-637X. DOI: 10.1086/509910. URL http://stacks.iop.org/0004-637X/655/i=1/a=550.

M. Gillon, E. Jehin, L. Delrez, P. Magain, C. Opitom, and S. Sohy. SPECULOOS: Search for habitable Planets EClipsing ULtra-cOOl Stars. July 2013. URL http://orbi.ulg.ac.be/handle/2268/159868.

M. Gillon, E. Jehin, S. M. Lederer, L. Delrez, J. de Wit, A. Burdanov, V. Van Grootel, A. J. Burgasser, A. H. M. J. Triaud, C. Opitom, B.-O. Demory, D. K. Sahu, D. Bardalez Gagliuffi, P. Magain, and D. Queloz. Temperate Earth-sized planets transiting a nearby ultracool dwarf star. *Nature*, 533(7602):221–224, May 2016. ISSN 0028-0836, 1476-4687. DOI: 10.1038/nature17448. URL http://www.nature.com/doifinder/10.1038/nature17448.

L. Girardi, M. A. T. Groenewegen, E. Hatziminaoglou, and L. da Costa. Star counts in the Galaxy: Simulating from very deep to very shallow photometric surveys with the TRILEGAL code. *Astronomy and Astrophysics*, 436(3):895–915, June 2005. ISSN 0004-6361, 1432-0756. DOI: 10.1051/0004-6361:20042352. URL http://www.edpsciences.org/10.1051/0004-6361:20042352.

G. M. H. J. Habets and J. R. W. Heintze. Empirical bolometric corrections for the main-sequence. *Astronomy and Astrophysics Supplement Series*, 46:193–237, Nov. 1981. ISSN 0365-0138.

C. Hellier, D. R. Anderson, A. C. Cameron, A. P. Doyle, A. Fumel, M. Gillon, E. Jehin, M. Lendl, P. F. L. Maxted, F. Pepe, D. Pollacco, D. Queloz, D. Ségransan, B. Smalley, A. M. S. Smith, J. Southworth, A. H. M. J. Triaud, S. Udry, and R. G. West. Seven transiting hot Jupiters from WASP-South, Euler and TRAPPIST: WASP-47b, WASP-55b, WASP-61b, WASP-62b, WASP-63b, WASP-66b and WASP-67b. *Monthly Notices of the Royal Astronomical Society*, 426(1): 739–750, Oct. 2012. ISSN 0035-8711, 1365-2966. DOI: 10.1111/j.1365-2966.2012.21780.x. URL http://mnras.oxfordjournals.org/content/426/1/739.

T. J. Henry, W.-C. Jao, J. P. Subasavage, T. D. Beaulieu, P. A. Ianna, E. Costa, and R. A. Méndez. The solar neighborhood. XVII. Parallax results from the CTIOPI 0.9 m program: 20 new members of the RECONS 10 parsec sample. *The Astronomical Journal*, 132(6):2360, 2006. URL http://iopscience.iop.org/1538-3881/132/6/2360/205485.web.ps.gz.

S. B. Howell, C. Sobeck, M. Haas, M. Still, T. Barclay, F. Mullally, John Troeltzsch, S. Aigrain, S. T. Bryson, D. Caldwell, W. J. Chaplin, W. D. Cochran, D. Huber, G. W. Marcy, A. Miglio, J. R. Najita, M. Smith, J. D. Twicken, and J. J. Fortney. The K2 Mission: Characterization and Early Results. *Publications of the Astronomical Society of* *the Pacific*, 126(938):398, 2014. ISSN 1538-3873. DOI: 10.1086/676406. URL http://stacks.iop.org/1538-3873/126/i=938/a=398.

D. Huber. Asteroseismology of Exoplanet Host Stars. *arXiv:1511.07441 [astro-ph]*, Nov. 2015. URL http://arxiv.org/abs/1511.07441. arXiv: 1511.07441.

D. Huber, S. T. Bryson, M. R. Haas, T. Barclay, G. Barentsen, S. B. Howell, S. Sharma, D. Stello, and S. E. Thompson. THE *K2* ECLIPTIC PLANE INPUT CATALOG (EPIC) AND STELLAR CLASSIFICATIONS OF 138,600 TARGETS IN CAMPAIGNS 1–8. *The Astrophysical Journal Supplement Series*, 224(1):2, May 2016. ISSN 1538-4365. DOI: 10.3847/0067-0049/224/1/2. URL http://stacks.iop.org/0067-0049/224/i=1/a=2?key=crossref.5ad035712fa408a531ce851b0b7783f0.

J. D. Hunter. Matplotlib: A 2d Graphics Environment. *Computing in Science & Engineering*, 9(3):90–95, 2007. ISSN 1521-9615. DOI: 10.1109/MCSE.2007.55. URL http://ieeexplore.ieee.org/lpdocs/epic03/wrapper.htm?arnumber=4160265.

J. Irwin, D. Charbonneau, P. Nutzman, and E. Falco. The MEarth project: searching for transiting habitable super-Earths around nearby M dwarfs. In *Transiting Planets*, volume 4 of *Proceedings of the International Astronomical Union*, pages 37–43, May 2008. DOI: 10.1017/S1743921308026215. URL http://journals.cambridge.org/article_S1743921308026215.

E. Jehin, M. Gillon, D. Queloz, P. Magain, J. Manfroid, V. Chantry, M. Lendl, D. Hutsemékers, and S. Udry. TRAPPIST: TRAnsiting Planets and PlanetesImals Small Telescope. *The Messenger*, 145:2–6, Sept. 2011. ISSN 0722-6691. URL http://adsabs.harvard.edu/abs/2011Msngr.145....2J.

J. M. Jenkins, J. D. Twicken, S. McCauliff, J. Campbell, D. Sanderfer, D. Lung, M. Mansouri-Samani, F. Girouard, P. Tenenbaum, T. Klaus, J. C. Smith, D. A. Caldwell, A. D. Chacon, C. Henze, C. Heiges, D. W. Latham, E. Morgan, D. Swade, S. Rinehart, and R. Vanderspek. The TESS science processing operations center. volume 9913, pages 99133E–99133E–20, 2016. DOI: 10.1117/12.2233418. URL http://dx.doi.org/10.1117/12.2233418.

E. Jones, T. Oliphant, P. Peterson, et al. Open source scientific tools for python, 2001.

C. H. Kepner and B. B. Tregoe. Rational Manager. 1965. URL http://agris.fao.org/agris-search/search.do?recordID=US201300461852.

D. M. Kipping and C. Lam. Transit Clairvoyance: Enhancing TESS follow-up using artificial neural networks. Private communication, June 2016.

B. Kirk, K. Conroy, A. Prša, M. Abdul-Masih, A. Kochoska, G. Matijevič, K. Hambleton, T. Barclay, S. Bloemen, T. Boyajian, L. R. Doyle, B. J. Fulton, A. J. Hoekstra, K. Jek, S. R. Kane, V. Kostov, D. Latham, T. Mazeh, J. A. Orosz, J. Pepper, B. Quarles, D. Ragozzine, A. Shporer, J. Southworth, K. Stassun, S. E. Thompson, W. F. Welsh, E. Agol, A. Derekas, J. Devor, D. Fischer, G. Green, J. Gropp, T. Jacobs, C. Johnston, D. M. LaCourse, K. Saetre, H. Schwengeler, J. Toczyski, G. Werner, M. Garrett, J. Gore, A. O. Martinez, I. Spitzer, J. Stevick, P. C. Thomadis, E. H. Vrijmoet, M. Yenawine, N. Batalha, and W. Borucki. Kepler Eclipsing Binary Stars. VII. The Catalog of Eclipsing Binaries Found in the Entire Kepler Data Set. *The Astronomical Journal*, 151, Mar. 2016. ISSN 0004-6256. DOI: 10.3847/0004-6256/151/3/68.

C. Kiss, A. Pál, A. I. Farkas-Takács, G. M. Szabó, R. Szabó, L. L. Kiss, L. Molnár, K. Sárneczky, T. G. Müller, M. Mommert, and J. Stansberry. Nereid from space: rotation, size and shape analysis from K2, Herschel and Spitzer observations. *Monthly Notices of the Royal Astronomical Society*, 457(3):2908–2917, Apr. 2016. ISSN 0035-8711, 1365-2966. DOI: 10.1093/mnras/stw081. URL http://mnras.oxfordjournals.org/content/457/3/2908.

R. k. Kopparapu, R. Ramirez, J. F. Kasting, V. Eymet, T. D. Robinson, S. Mahadevan, R. C. Terrien, S. Domagal-Goldman, V. Meadows, and R. Deshpande. Habitable Zones Around Main-Sequence Stars: New Estimates. *The Astrophysical Journal*, 765(2):131, Mar. 2013. ISSN 0004-637X, 1538-4357. DOI: 10.1088/0004-637X/765/2/131. arXiv: 1301.6674.

V. B. Kostov, J. A. Orosz, W. F. Welsh, L. R. Doyle, D. C. Fabrycky, N. Haghighipour, B. Quarles, D. R. Short, W. D. Cochran, M. Endl, E. B. Ford, J. Gregorio, T. C. Hinse, H. Isaacson, J. M. Jenkins, E. L. N. Jensen, S. Kane, I. Kull, D. W. Latham, J. J. Lissauer, G. W. Marcy, T. Mazeh, T. W. A. Muller, J. Pepper, S. N. Quinn, D. Ragozzine, A. Shporer, J. H. Steffen, G. Torres, G. Windmiller, and W. J. Borucki. Kepler-1647b: the largest and longest-period Kepler transiting circumbinary planet. *arXiv:1512.00189 [astro-ph]*, Dec. 2015. URL http://arxiv.org/abs/1512.00189. arXiv: 1512.00189.

W. B. Landsman. The IDL Astronomy User's Library. volume 77, page 437, 1995. URL http://adsabs.harvard.edu/abs/1995ASPC...77..437L.

L. Lyons. *A Practical Guide to Data Analysis for Physical Science Students*. Cambridge University Press, Nov. 1991. ISBN 978-0-521-42463-9. 1996 paperback reprinting.

D. V. Martin and A. H. M. J. Triaud. Planets transiting non-eclipsing binaries. *Astronomy & Astrophysics*, 570:A91, Oct. 2014a. ISSN 0004-6361, 1432-0746. DOI: 10.1051/0004-6361/201323112. URL http://www.aanda.org/10.1051/0004-6361/201323112.

D. V. Martin and A. H. M. J. Triaud. Planets transiting non-eclipsing binaries. *Astronomy & Astrophysics*, 570:A91, Oct. 2014b. ISSN 0004-6361, 1432-0746. DOI: 10.1051/0004-6361/201323112. URL http://www.aanda.org/10.1051/0004-6361/201323112.

D. V. Martin, T. Mazeh, and D. C. Fabrycky. No circumbinary planets transiting the tightest Kepler binaries-a fingerprint of a third star. *arXiv preprint arXiv:1505.05749*, 2015. URL http://arxiv.org/abs/1505.05749.

T. Mazeh, T. Holczer, and S. Faigler. Dearth of short-period Neptunian exoplanets - a desert in period-mass and period-radius planes. *Astronomy & Astrophysics*, 589:A75, May 2016. ISSN 0004-6361, 1432-0746. DOI: 10.1051/0004-6361/201528065. URL http://arxiv.org/abs/1602.07843. arXiv: 1602.07843.

P. R. McCullough, J. E. Stys, J. A. Valenti, S. W. Fleming, K. A. Janes, and J. N. Heasley. The XO Project: Searching for Transiting Extrasolar Planet Candidates. *Publications of the Astronomical Society of the Pacific*, 117(834):783, 2005. ISSN 1538-3873. DOI: 10.1086/432024. URL http://stacks.iop.org/1538-3873/117/i=834/a=783.

S. Meibom, G. Torres, F. Fressin, D. W. Latham, J. F. Rowe, D. R. Ciardi, S. T. Bryson, L. A. Rogers, C. E. Henze, K. Janes, S. A. Barnes, G. W. Marcy, H. Isaacson, D. A. Fischer, S. B. Howell, E. P. Horch, J. M. Jenkins, S. C. Schuler, and J. Crepp. The same frequency of planets inside and outside open clusters of stars. *Nature*, 499(7456): 55–58, June 2013. ISSN 0028-0836, 1476-4687. DOI: 10.1038/nature12279. URL http://www.nature.com/doifinder/10.1038/nature12279.

S. Millholland, S. Wang, and G. Laughlin. On the Detection of Non-Transiting Hot Jupiters in Multiple-Planet Systems. *The Astrophysical Journal*, 823(1):L7, May 2016. ISSN 2041-8213. DOI: 10.3847/2041-8205/823/1/L7. arXiv: 1602.05674.

S. M. Mills, D. C. Fabrycky, C. Migaszewski, E. B. Ford, E. Petigura, and H. Isaacson. A resonant chain of four transiting, sub-Neptune planets. *Nature*, 533(7604):509–512, May 2016. ISSN 0028-0836.

DOI: 10.1038/nature17445. URL http://www.nature.com/nature/journal/v533/n7604/full/nature17445.html.

M. Neveu-VanMalle, D. Queloz, D. R. Anderson, D. J. A. Brown, A. Collier Cameron, L. Delrez, R. F. Díaz, M. Gillon, C. Hellier, E. Jehin, T. Lister, F. Pepe, P. Rojo, D. Ségransan, A. H. M. J. Triaud, O. D. Turner, and S. Udry. Hot Jupiters with relatives: discovery of additional planets in orbit around WASP-41 and WASP-47. *Astronomy & Astrophysics*, 586:A93, Feb. 2016. ISSN 0004-6361, 1432-0746. DOI: 10.1051/0004-6361/201526965. URL http://www.aanda.org/10.1051/0004-6361/201526965.

H. Ngo, H. A. Knutson, S. Hinkley, M. Bryan, J. R. Crepp, K. Batygin, I. Crossfield, B. Hansen, A. W. Howard, J. A. Johnson, D. Mawet, T. D. Morton, P. S. Muirhead, and J. Wang. Friends of Hot Jupiters. IV. Stellar companions beyond 50 AU might facilitate giant planet formation, but most are unlikely to cause Kozai-Lidov migration. *arXiv:1606.07102 [astro-ph]*, June 2016. URL http://arxiv.org/abs/1606.07102.

R. P. Olling, R. Mushotzky, E. J. Shaya, A. Rest, P. M. Garnavich, B. E. Tucker, D. Kasen, S. Margheim, and A. V. Filippenko. No signature of ejecta interaction with a stellar companion in three type Ia supernovae. *Nature*, 521(7552):332–335, May 2015. ISSN 0028-0836. DOI: 10.1038/nature14455. URL http://www.nature.com/nature/journal/v521/n7552/full/nature14455.html.

H. P. Osborn, D. J. Armstrong, D. J. A. Brown, J. McCormac, A. P. Doyle, T. M. Louden, J. Kirk, J. J. Spake, K. W. F. Lam, S. R. Walker, F. Faedi, and D. L. Pollacco. Single transit candidates from K2: detection and period estimation. *Monthly Notices of the Royal Astronomical Society*, 457(3):2273–2286, Apr. 2016. ISSN 0035-8711, 1365-2966. DOI: 10.1093/mnras/stw137. URL http://mnras.oxfordjournals.org/lookup/doi/10.1093/mnras/stw137.

J. Pepper, R. W. Pogge, D. L. DePoy, J. L. Marshall, K. Z. Stanek, A. M. Stutz, Shawn Poindexter, R. Siverd, T. P. O'Brien, M. Trueblood, and P. Trueblood. The Kilodegree Extremely Little Telescope (KELT): A Small Robotic Telescope for Large-Area Synoptic Surveys. *Publications of the Astronomical Society of the Pacific*, 119(858):923, 2007. ISSN 1538-3873. DOI: 10.1086/521836. URL http://stacks.iop.org/1538-3873/119/i=858/a=923.

M. a. C. Perryman. GAIA: An Astrometric and Photometric Survey of our Galaxy. In V. Vansevicius, A. Kucinskas, and J. Sudzius, editors, *Census of the Galaxy: Challenges for Photometry and Spectrometry with GAIA*, pages 1–10. Springer Netherlands,

2002. ISBN 978-94-010-3911-6 978-94-010-0361-2. URL http://link.springer.com/chapter/10.1007/978-94-010-0361-2_1. DOI: 10.1007/978-94-010-0361-2_1.

M. A. C. Perryman, L. Lindegren, J. Kovalevsky, E. Hoeg, U. Bastian, P. L. Bernacca, M. Crézé, F. Donati, M. Grenon, M. Grewing, F. van Leeuwen, H. van der Marel, F. Mignard, C. A. Murray, R. S. Le Poole, H. Schrijver, C. Turon, F. Arenou, M. Froeschlé, and C. S. Petersen. The HIPPARCOS Catalogue. *Astronomy and Astrophysics*, 323, July 1997. ISSN 0004-6361.

D. L. Pollacco, I. Skillen, A. C. Cameron, D. J. Christian, C. Hellier, J. Irwin, T. A. Lister, R. A. Street, R. G. West, D. Anderson, W. I. Clarkson, H. Deeg, B. Enoch, A. Evans, A. Fitzsimmons, C. A. Haswell, S. Hodgkin, K. Horne, S. R. Kane, F. P. Keenan, P. F. L. Maxted, A. J. Norton, J. Osborne, N. R. Parley, R. S. I. Ryans, B. Smalley, P. J. Wheatley, and D. M. Wilson. The WASP Project and the SuperWASP Cameras. *Publications of the Astronomical Society of the Pacific*, 118(848):1407, 2006. ISSN 1538-3873. DOI: 10.1086/508556. URL http://stacks.iop.org/1538-3873/118/i=848/a=1407.

E. M. Price and L. A. Rogers. Transit Light Curves with Finite Integration Time: Fisher Information Analysis. *The Astrophysical Journal*, 794(1):92, Sept. 2014. ISSN 1538-4357. DOI: 10.1088/0004-637X/794/1/92. URL http://arxiv.org/abs/1408.4124. arXiv: 1408.4124.

G. R. Ricker, J. N. Winn, and R. Vanderspek. Transiting Exoplanet Survey Satellite. *Journal of Astronomical Telescopes, Instruments, and Systems*, 1(1):014003, Oct. 2014. ISSN 2329-4124. DOI: 10.1117/1.JATIS.1.1.014003. URL http://astronomicaltelescopes.spiedigitallibrary.org/article.aspx?doi=10.1117/1.JATIS.1.1.014003.

A. C. Robin, C. Reylé, S. Derrière, and S. Picaud. A synthetic view on structure and evolution of the milky way. *Astronomy & Astrophysics*, 409(2):523–540, 2003.

S. Sharma, J. Bland-Hawthorn, K. V. Johnston, and J. Binney. Galaxia: a code to generate a synthetic survey of the Milky Way. *The Astrophysical Journal*, 730(1):3, Mar. 2011. ISSN 0004-637X, 1538-4357. DOI: 10.1088/0004-637X/730/1/3. URL http://arxiv.org/abs/1101.3561. arXiv: 1101.3561.

I. Soszynski, A. Udalski, M. K. Szymanski, M. Kubiak, G. Pietrzynski, L. Wyrzykowski, O. Szewczyk, K. Ulaczyk, and R. Poleski.

The Optical Gravitational Lensing Experiment. The OGLE-III Catalog of Variable Stars. III. RR Lyrae Stars in the Large Magellanic Cloud. *arXiv:0903.2482 [astro-ph]*, Mar. 2009. URL http://arxiv.org/abs/0903.2482. arXiv: 0903.2482.

I. Soszynski, A. Udalski, M. K. Szymanski, M. Kubiak, G. Pietrzynski, L. Wyrzykowski, K. Ulaczyk, and R. Poleski. The Optical Gravitational Lensing Experiment. The OGLE-III Catalog of Variable Stars. IX. RR Lyrae Stars in the Small Magellanic Cloud. *arXiv:1009.0528 [astro-ph]*, Sept. 2010. URL http://arxiv.org/abs/1009.0528. arXiv: 1009.0528.

I. Soszynski, W. A. Dziembowski, A. Udalski, R. Poleski, M. K. Szymanski, M. Kubiak, G. Pietrzynski, L. Wyrzykowski, K. Ulaczyk, S. Kozlowski, and P. Pietrukowicz. The Optical Gravitational Lensing Experiment. The OGLE-III Catalog of Variable Stars. XI. RR Lyrae Stars in the Galactic Bulge. *arXiv:1105.6126 [astro-ph]*, May 2011. URL http://arxiv.org/abs/1105.6126. arXiv: 1105.6126.

A. Sozzetti, A. Bernagozzi, E. Bertolini, P. Calcidese, A. Carbognani, D. Cenadelli, J.-M. Christille, M. Damasso, P. Giacobbe, L. Lanteri, M. Lattanzi, and R. Smart. The APACHE Project. *EPJ Web of Conferences*, 47:03006, 2013. ISSN 2100-014X. DOI: 10.1051/epjconf/20134703006. URL http://www.epj-conferences.org/10.1051/epjconf/20134703006.

K. B. Stevenson et al. Transiting Exoplanet Studies and Community Targets for JWST's Early Release Science Program. *Publications of the Astronomical Society of the Pacific*, 128(967):094401, Sept. 2016. ISSN 0004-6280, 1538-3873. DOI: 10.1088/1538-3873/128/967/094401. arXiv: 1602.08389.

STScI Science Definition Team. Big Data at STScI: Enhancing STScI's Astronomical Data Science Capabilities over the Next Five Years. Technical report, Mar. 2016. URL http://archive.stsci.edu/reports/BigDataSDTReport_Final.pdf.

P. Sullivan. TESS's Performance on the Kepler Objects of Interest. Technical Report No. 8, MIT, Oct. 2013.

P. W. Sullivan, J. N. Winn, Z. K. Berta-Thompson, D. Charbonneau, D. Deming, C. D. Dressing, D. W. Latham, A. M. Levine, P. R. McCullough, T. Morton, G. R. Ricker, R. Vanderspek, and D. Woods. THE TRANSITING EXOPLANET SURVEY SATELLITE: SIMULATIONS OF PLANET DETECTIONS AND ASTROPHYSICAL FALSE POSITIVES. *ApJ*, 809(1):77, aug 2015. DOI: 10.1088/0004-637x/809/1/77. URL http://dx.doi.org/10.1088/0004-637X/809/1/77.

R. Szabo, L. Molnar, Z. Kolaczkowski, P. Moskalik, Z. Ivezic, A. Udalski, L. Szabados, C. Kuehn, R. Smolec, A. Pigulski, and others. The Kepler-SEP Mission: Harvesting the South Ecliptic Pole large-amplitude variables with Kepler. *arXiv preprint arXiv:1309.0741*, 2013. URL `http://arxiv.org/abs/1309.0741`.

R. Szabó, K. Sárneczky, G. M. Szabó, A. Pál, C. P. Kiss, B. Csák, L. Illés, G. Rácz, and L. L. Kiss. Main-Belt Asteroids in the K2 Engineering Field of View. *The Astronomical Journal*, 149(3):112, Feb. 2015. ISSN 1538-3881. DOI: 10.1088/0004-6256/149/3/112. URL `http://arxiv.org/abs/1501.05967`. arXiv: 1501.05967.

A. Udalski, G. Pietrzynski, M. Szymanski, M. Kubiak, K. Zebrun, I. Soszynski, O. Szewczyk, and L. Wyrzykowski. The Optical Gravitational Lensing Experiment. Additional Planetary and Low-Luminosity Object Transits from the OGLE 2001 and 2002 Observational Campaigns. *arXiv:astro-ph/0306444*, June 2003a. URL `http://arxiv.org/abs/astro-ph/0306444`. arXiv: astro-ph/0306444.

A. Udalski, O. Szewczyk, K. Zebrun, G. Pietrzynski, M. Szymanski, M. Kubiak, I. Soszynski, and L. Wyrzykowski. The Optical Gravitational Lensing Experiment. Planetary and Low-Luminosity Object Transits in the Carina Fields of the Galactic Disk. *arXiv:astro-ph/0301210*, Jan. 2003b. URL `http://arxiv.org/abs/astro-ph/0301210`. arXiv: astro-ph/0301210.

S. Uehara, H. Kawahara, K. Masuda, S. Yamada, and M. Aizawa. Transiting Planet Candidates Beyond the Snow Line Detected by Visual Inspection of 7557 Kepler Objects of Interest. *arXiv preprint arXiv:1602.07848*, 2016. URL `http://arxiv.org/abs/1602.07848`.

van Leeuwen and F. v. Leeuwen. Validation of the new Hipparcos reduction. *Astronomy & Astrophysics*, 474(2):12, 2007. DOI: 10.1051/0004-6361:20078357.

A. Vanderburg, J. A. Johnson, S. Rappaport, A. Bieryla, J. Irwin, J. A. Lewis, D. Kipping, W. R. Brown, P. Dufour, D. R. Ciardi, R. Angus, L. Schaefer, D. W. Latham, D. Charbonneau, C. Beichman, J. Eastman, N. McCrady, R. A. Wittenmyer, and J. T. Wright. A disintegrating minor planet transiting a white dwarf. *Nature*, 526(7574): 546–549, Oct. 2015. ISSN 0028-0836, 1476-4687. DOI: 10.1038/nature15527.

A. Vanderburg, D. W. Latham, L. A. Buchhave, A. Bieryla, P. Berlind, M. L. Calkins, G. A. Esquerdo, S. Welsh, and J. A. Johnson. Planetary Candidates from the First Year of the K2

Mission. *The Astrophysical Journal Supplement Series*, 222:14, Jan. 2016. ISSN 0067-0049. DOI: 10.3847/0067-0049/222/1/14. URL http://adsabs.harvard.edu/abs/2016ApJS..222...14V.

D. Veras. Post-main-sequence planetary system evolution. *arXiv preprint arXiv:1601.05419*, 2016. URL http://arxiv.org/abs/1601.05419.

G. Walker, J. Matthews, R. Kuschnig, R. Johnson, S. Rucinski, J. Pazder, G. Burley, A. Walker, K. Skaret, R. Zee, S. Grocott, K. Carroll, P. Sinclair, D. Sturgeon, and J. Harron. The *MOST* Asteroseismology Mission: Ultraprecise Photometry from Space. *Publications of the Astronomical Society of the Pacific*, 115(811):1023–1035, Sept. 2003. ISSN 0004-6280, 1538-3873. DOI: 10.1086/377358. URL http://iopscience.iop.org/article/10.1086/377358.

S. v. d. Walt, S. C. Colbert, and G. Varoquaux. The NumPy Array: A Structure for Efficient Numerical Computation. *Computing in Science & Engineering*, 13(2):22–30, Mar. 2011. ISSN 1521-9615. DOI: 10.1109/MCSE.2011.37. URL http://scitation.aip.org/content/aip/journal/cise/13/2/10.1109/MCSE.2011.37.

J. Wang, D. A. Fischer, T. Barclay, A. Picard, B. Ma, B. P. Bowler, J. R. Schmitt, T. S. Boyajian, K. J. Jek, D. LaCourse, C. Baranec, R. Riddle, N. M. Law, C. Lintott, K. Schawinski, D. J. Simister, B. Gregoire, S. P. Babin, T. Poile, T. L. Jacobs, T. Jebson, M. R. Omohundro, H. M. Schwengeler, J. Sejpka, I. A. Terentev, R. Gagliano, J.-P. Paakkonen, H. K. O. Berge, T. Winarski, G. R. Green, A. R. Schmitt, M. H. Kristiansen, and A. Hoekstra. Planet Hunters. VIII. Characterization of 41 Long-Period Exoplanet Candidates from Kepler Archival Data. *The Astrophysical Journal*, 815(2):127, Dec. 2015. ISSN 1538-4357. DOI: 10.1088/0004-637X/815/2/127. URL http://arxiv.org/abs/1512.02559. arXiv: 1512.02559.

P. J. Wheatley, D. L. Pollacco, D. Queloz, H. Rauer, C. A. Watson, R. G. West, B. Chazelas, T. M. Louden, S. Walker, N. Bannister, J. Bento, M. Burleigh, J. Cabrera, P. Eigmüller, A. Erikson, L. Genolet, M. Goad, A. Grange, A. Jordán, K. Lawrie, J. McCormac, and M. Neveu. The Next Generation Transit Survey (NGTS). *EPJ Web of Conferences*, 47:13002, 2013. ISSN 2100-014X. DOI: 10.1051/epjconf/20134713002. URL http://www.epj-conferences.org/10.1051/epjconf/20134713002.

J. N. Winn. Number of Searchable Stars. *TESS Science Memo No. 5, Version 1. Available upon request.*, 2013.